DEVELOPMENT, TESTING, AND EVALUATION OF NDOR'S TL-5 AESTHETIC OPEN CONCRETE BRIDGE RAIL

Submitted by

Karla A. Polivka, M.S.M.E., E.I.T.
Research Associate Engineer

Ronald K. Faller, Ph.D., P.E.
Research Assistant Professor

James C. Holloway, M.S.C.E., E.I.T.
Research Manager

John R. Rohde, Ph.D., P.E.
Associate Professor

Dean L. Sicking, Ph.D., P.E.
Professor and MwRSF Director

MIDWEST ROADSIDE SAFETY FACILITY
University of Nebraska-Lincoln
527 Nebraska Hall
Lincoln, Nebraska 68588-0529
(402) 472-6864

Technical Report Documentation Page

1. Report No. TRP-03-148-05	2.	3. Recipient's Accession No.

4. Title and Subtitle Development, Testing, and Evaluation of NDOR's TL-5 Aesthetic Open Concrete Bridge Rail	5. Report Date December 1, 2005
	6.

7. Author(s) Polivka, K.A., Faller, R.K., Holloway, J.C., Rohde, J.R., and Sicking, D.L.	8. Performing Organization Report No. TRP-03-148-05

9. Performing Organization Name and Address Midwest Roadside Safety Facility (MwRSF) University of Nebraska-Lincoln 527 Nebraska Hall Lincoln, NE 68588-0529	10. Project/Task/Work Unit No.
	11. Contract © or Grant (G) No.

12. Sponsoring Organization Name and Address Nebraska Department of Roads 1500 Nebraska Highway 2 Lincoln, Nebraska 68509-4759	13. Type of Report and Period Covered Final Report 2003-2005
	14. Sponsoring Agency Code

15. Supplementary Notes

Prepared in cooperation with U.S. Department of Transportation, Federal Highway Administration

16. Abstract (Limit: 200 words)

A new Test Level (TL-5) aesthetic open concrete bridge railing system was developed, crash tested, and evaluated for use with reinforced concrete bridge decks. The 1,067-mm (42-in.) high bridge rail was constructed 37.03-m (121-ft 6-in.) long with fifteen bridge posts, each measuring 267-mm (10.5-in.) wide x 762-mm (30-in.) long x 305-mm (12-in.) high. Post spacings were 2,591 mm (8 ft-6 in.) on centers.

One full-scale crash test, using a 35,822-kg (78,975-lb) tractor/trailer vehicle impacting at a speed of 79.6 km/h (49.4 mph) and at an angle of 16.3 degrees, was conducted and reported in accordance with the requirements specified in the National Cooperative Highway Research Program (NCHRP) Report No. 350, *Recommended Procedures for the Safety Performance Evaluation of Highway Features*. The safety performance of the aesthetic open concrete bridge rail was determined to be acceptable according to the TL-5 evaluation criteria specified in NCHRP Report No. 350.

The research study also included additional structural analysis and design on several variations of the aesthetic bridge rail. The design variations included: (1) a TL-5 closed bridge railing; (2) a TL-5 closed median barrier; (3) a TL-4 closed bridge railing; and (4) a TL-4 open concrete bridge railing.

17. Document Analysis/Descriptors Highway Safety, Aesthetic Barrier, Bridge Rail, Concrete Parapet, Roadside Appurtenances, Crash Test, Compliance Test	18. Availability Statement No restrictions. Document available from: National Technical Information Services, Springfield, Virginia 22161

19. Security Class (this report) Unclassified	20. Security Class (this page) Unclassified	21. No. of Pages 154	22. Price

DISCLAIMER STATEMENT

The contents of this report reflect the views of the authors who are responsible for the facts and the accuracy of the data presented herein. The contents do not necessarily reflect the official views nor policies of the Nebraska Department of Roads nor the Federal Highway Administration. This report does not constitute a standard, specification, or regulation.

ACKNOWLEDGMENTS

TABLE OF CONTENTS

List of Figures

List of Tables

1 INTRODUCTION

1.1 Problem Statement

Over the last 30 years, several bridge railing and median barrier systems have been developed for safely redirecting heavy tractor-trailer vehicles. For all of those systems, the lower portion of the reinforced concrete parapets consisted of a solid barrier with either a vertical or sloped front-face geometry. As such, none of these barrier systems were purely configured as a beam and post system. For years, beam and post railing systems (i.e., open concrete bridge railings) have been used throughout the United States (U.S.) for several reasons. First, these open railing systems readily allow for water to drain over the deck edge. Second, these railing systems reduce the propensity for snow accumulation adjacent to the parapet's base during high-wind situations as well as during snow removal operations. Finally, these railing systems provide improved aesthetics through the use of an open rail configuration, often an open concrete rail. Consequently, the existing open concrete bridge railings were developed to redirect small cars, sedans, light trucks, and single-unit trucks but not heavy, tractor-trailer vehicles.

In 2002, the Nebraska Department of Roads (NDOR) determined that there existed a need for a new bridge railing system that would: (1) redirect heavy, tractor-trailer vehicles; (2) provide increased motorist safety by using a more vertical front-face geometry; (3) provide adequate hydraulic water runoff and reduced propensity for snow accumulation; and (4) exhibit improved aesthetic qualities. As such, NDOR partnered with the Midwest Roadside Safety Facility (MwRSF) of the University of Nebraska-Lincoln in order to develop a new, high-performance, aesthetic, open concrete bridge railing for attachment to reinforced concrete bridge decks.

1

1.2 Objective

The objective of the research project was to design an aesthetic open concrete bridge railing system and evaluate its safety performance through full-scale crash testing. The bridge rail system was to be evaluated according to the Test Level 5 (TL-5) safety performance criteria set forth in the National Cooperative Highway Research Program (NCHRP) Report No. 350, *Recommended Procedures for the Safety Performance Evaluation of Highway Features* (1).

1.3 Scope

The research objective was achieved by performing several tasks. First, a literature review was conducted on previously crash tested bridge rails and median barriers using tractor-trailer vehicles. Next, a conceptual development and design phase was undertaken to determine the appearance, geometry, and general configuration of the barrier system. After the final design was completed, the bridge rail system was fabricated and constructed at the MwRSF's outdoor test facility. Following the fabrication of the bridge system, one full-scale vehicle crash test was performed using a tractor/van trailer, weighing approximately 36,000 kg (79,366 lbs), with a target impact speed and an angle of 80.0 km/h (49.7 mph) and 15 degrees, respectively. Finally, the test results were analyzed, evaluated, and documented. Additional structural analysis and design for several variations of the original TL-5 aesthetic open concrete bridge rail was also performed. These design variations will be contained in an alternative publication. Conclusions and recommendations were then made that pertain to the safety performance of the aesthetic concrete bridge railing system.

2 LITERATURE REVIEW AND BARRIER INVESTIGATION

For this study, a literature review was performed in order to acquire information on the testing of barrier systems capable of redirecting heavy, tractor-trailer vehicles. The information garnered from this review was used to provide insight into the actual design lateral impact load as well as the minimum barrier configuration (i.e., reinforcement, size, thickness, structural capacity, anchorage, etc.) deemed necessary to redirect heavy vehicles. For this study, results from previous crash tests conducted into rigid barrier systems were deemed more appropriate for consideration and further evaluation, thus resulting in the selection of eleven tractor-trailer vehicle crash tests with gross vehicle weights ranging approximately between 22,680 kg (50,000 lbs) and 36,287 kg (80,000 lbs). These eleven tests were conducted on rigid bridge railings and median barriers in the 1980's through the 1990's in the U.S. (2-11). All of these referenced crash tests were performed by the Texas Transportation Institute (TTI) of Texas A&M University.

Tables 1 and 2 contain a summary of the test information and parameters for the tractor-trailer barrier impacts identified above. Table 3 contains a summary of the test conditions and results for the tractor-trailer barrier impacts identified previously. Finally, barrier displacements and calculated barrier capacities for selected barrier configurations chosen from these crash tests is provided in Table 4.

As previously mentioned, a barrier's redirective capacity, R_W, can be determined using the yield-line analysis and strength design procedure presented in References (12) and (13). For this procedure, a barrier's redirective capacity is largely based on the moment capacity of the wall, M_W, the cantilever capacity between the parapet and the foundation, M_C, the capacity of additional beams located near the top of the parapet, M_B, and the height of the parapet, H. In addition, R_W is

3

Table 1. Summary of Test Information and Parameters for Selected Heavy, Tractor-Trailer Vehicle Crash Tests

Test No.	Test Date	Test Agency	Reference No.	Vehicle		Barrier Description	Barrier Height (in.)
				Trailer Type	Cab Type		
7046-3	4/7/87	TTI	4	Van	Cab-Over	Vertical Instrumented Tall Wall	90
7046-4	5/8/87	TTI	4	Tanker	Conventional	Vertical Instrumented Tall Wall	90
7046-9	5/27/88	TTI	4	Van	Conventional	Vertical Instrumented Tall Wall	90
7069-13	7/11/88	TTI	8-9	Van	Conventional	Vertical Concrete Bridge Railing	42
7069-10	3/3/88	TTI	8-9	Van	Conventional	F-Shape Concrete Bridge Railing	42
4798-13	5/26/83	TTI	3	Van	Cab-Over	Reinforced Concrete Median Barrier w/ Asphalt	42
7162-1	8/9/90	TTI	2	Van	Conventional	Ontario Un-Reinforced Concrete Median Barrier w/ Asphalt	42
1	NA	TTI	5-6	Tanker	Conventional	Texas T5 Modified Concrete Bridge Railing w/ Extended NJ Shape	90
2416-1	9/18/84	TTI	7	Van	Conventional	Texas T5 HT Modified Concrete Bridge Railing w/ Texas C4 Metal Rail w/ 32-In. NJ Shape	50
6	NA	TTI	10	Van	Conventional	Texas C202 Modified Open Concrete Bridge Rail w/ Metal Rail	54
405511-2	12/12/95	TTI	11	Van	Conventional	Vertical Concrete Bridge Railing	42

NA - Not available   TTI - Texas Transportation Institute

1 in. = 25.4 mm

Table 2. Summary of Test Information and Parameters for Selected Heavy, Tractor-Trailer Vehicle Crash Tests (Continued)

Test No.	Reference No.	Test Inertial Weight (lbs)	Individual Weights			Vehicle Dimensions			
			Tractor Front Axle (lbs)	Tractor Rear Tandem Axle (lbs)	Trailer Rear Tandem Axle (lbs)	Tractor Wheelbase (in.)	Trailer Wheelbase (in.)	Overall Tractor-Trailer Length (in.)	Trailer Length (in.)
7046-3	4	80,080	11,680	34,140	34,260	164.5	362.75	612.75	480
7046-4	4	79,900	11,840	33,570	34,490	236	350	665	439.5+
7046-9	4	50,000	8,540	19,790	21,670	169	430.5	703.5	538
7069-13	8-9	50,050	7,920	22,250	19,880	169	438	698	540
7069-10	8-9	50,000	9,400	21,760	18,840	182	434	710	538
4798-13	3	80,180	12,150	34,010	34,020	147.5	368.5	602.5	480
7162-1	2	80,000	11,580	34,350	34,070	171	429.6	688.8	536.4
1	5-6	80,120	12,070	34,050	34,000	201	346	650	439+
2416-1	7	80,080	12,020	34,170	33,890	199.5	377.75	685.25	480
6	10	79,770	11,490	33,760	34,520	162	351	647	480
405511-2	11	79,366	11,210	34,249	33,907	186	413	699	NA

NA - Not available
1 kg = 2.204623 lbs
1 in. = 25.4 mm

5

Table 3. Summary of Test Conditions and Results for Selected Heavy, Tractor-Trailer Vehicle Crash Tests

Test No.	Reference No.	Impact Speed (mph)	Impact Angle (degrees)	Impact Severity (kip-ft)		Peak 0.050-Sec Average Decelerations (G's)			
				Entire Truck	Tractor Rear Tandems	Lateral (Rear Tractor Tandem Axle)	Longitudinal (Rear Tractor Tandem Axle)	Lateral (Other Location)	Longitudinal (Other Location)
7046-3	4	55.0	15.3	563.9	240.4	9.7	-3.2	NA	NA
7046-4	4	54.8	16.0	609.4	256.0	12.3	2.1	NA	NA
7046-9	4	50.4	14.6	269.8	106.8	6.8 (Tractor C.G.)	-2.4 (Tractor C.G.)	NA	NA
7069-13	8-9	51.4	16.2	344.1	153.0	Est. 5.0	NA	3.7	-3.3
7069-10	8-9	52.2	14.0	266.6	116.0	Est. 7.5	NA	4.7	-2.2
4798-13	3	52.1	16.5	586.9	248.9	-9.3	-6.5	-9.3	-6.5
7162-1	2	49.6	15.1	446.5	191.7	-7.9	-1.2	-9.7	2
1	5-6	51.4	15	474.0	201.4	5.54	-1.77	6.92	NA
2416-1	7	48.4	14.5	393.1	167.8	5.5	-2.4	NA	NA
6	10	49.1	15	430.6	182.3	5.94	1.68	NA	NA
405511-2	11	49.8	14.5	412.5	178.0	Est. 8	NA	Est. 8	NA

NA - Not available
1 km/hr = 0.6213712 mph   1 Joule = 0.7375621 ft-lbs
1 lb = 0.2248089 N
1 in. = 25.4 mm

6

Table 4. Summary of Barrier Displacements and Barrier Capacities for Selected Heavy, Tractor-Trailer Vehicle Crash Tests.

Test No.	Reference No.	Barrier Displacement (in.)	Yield-Line Redirective Barrier Capacity, R_W (kips)	
			TTI	MwRSF
7046-3	4	NA	NA	NA
7046-4	4	NA	NA	NA
7046-9	4	NA	NA	NA
7069-13	8-9	NA	198	210
7069-10	8-9	NA	127	129
4798-13	3	NA	NA	Est. $\geq$ 793[1]
7162-1	2	NA	NA	Est. $\geq$ 158[2]
1	5-6	4.0 (Dynamic)	NA	NA
2416-1	7	10.8 (Dynamic)	NA	NA
6	10	12 (P.S.)	NA	NA
405511-2	11	NA	198	210

NA - Not available
P.S. - Permanent Set
[1] - Vertical steel reinforcement was not used to anchor the parapet to the foundation nor to provide the cantilevered moment capacity of the wall, M_C. An estimate for the torsional capacity of the reinforced wall provided a basis for M_C for use within the yield-line analysis procedure for concrete parapets. An estimate for the barrier's redirective capacity, R_W, is shown above.
[2] - Vertical steel reinforcement was not used to anchor the parapet to the foundation nor to provide the cantilevered moment capacity of the wall, M_C. An estimate for the torsional capacity of the un-reinforced wall provided a basis for M_C for use within the yield-line analysis procedure for concrete parapets. An estimate for the barrier's redirective capacity, R_W, is shown above.

1 lb = 0.2248089 N
1 in. = 25.4 mm

significantly influenced by the location of the impact region on the parapet. For example, an impact within an interior region of the parapet provides increased redirective capacity over that occurring near the end of or at an expansion joint within a similarly reinforced parapet. As shown in Table 4, R_W values for the F-shape and vertical concrete bridge railings have been determined by both TTI and MwRSF. For the F-shape bridge railing, TTI and MwRSF determined R_W to be 565 and 574 N (127 and 129 kips), respectively. For the vertical bridge railing, TTI and MwRSF determined R_W to be 881 and 934 N (198 and 210 kips), respectively. Therefore, it can be stated that the predicted barrier capacities correlated reasonably well when determined by independent research organizations.

In addition to these two single-faced parapets, two other concrete parapets were analyzed by MwRSF researchers - the un-reinforced and reinforced versions of the symmetric, New Jersey shape concrete median barrier. These two parapets were determined to be of special interest since they are included in AASHTO's *Roadside Design Guide* (14) and typically are used in median applications where protection for heavy trucks is desired. For both of these designs, no vertical steel reinforcement was utilized to anchor the barrier systems to their foundations. However, a 76-mm (3-in.) asphaltic concrete pad was placed near each barrier's base and on both sides in order to provide resistance to lateral movement.

During both crash tests, the full-size New Jersey barriers redirected the impacting tractor-trailer vehicles without significant consequence. For both configurations, the barriers appeared to have remained attached to the foundation surface without rotation upward nor backward. Since no physical attachment was provided between each barrier and its foundation, there must have been other mechanisms which contributed to the barrier's effective cantilevered moment capacity, and

8

ultimately to the barrier's overall redirective capacity. Other possible mechanisms for resisting barrier uplift and rotation may have included: (1) the barrier's torsional capacity; (2) the downward vehicular load applied to the barrier resulting from a trailer box leaning on the top of the parapet; (3) the barrier's dead weight based on an unknown effective length and limited by the barrier's bending capacity about the transverse barrier axis; (4) the translational and rotational inertial forces generated as a result of the significant barrier mass and resistance to movement; and (5) the frictional forces generated between the asphaltic concrete overlay and the toe of the concrete barrier's traffic-side face while based on some effective length.

Although several mechanisms may actually contribute to the cantilevered moment capacity, MwRSF researchers believed that the barrier's torsional capacity may have the largest influence on this M_C parameter out of the five items listed above. An attempt was then made to quantify the torsional capacities for both the un-reinforced and reinforced versions of the 1,067-mm (42-in.) high symmetric, New-Jersey shape concrete median barrier using the elementary procedures identified in reinforced concrete design texts published by Wang and Salmon (15) and MacGregor (16). For the un-reinforced Ontario tall wall, the minimum nominal torsional capacity was believed to be greater than or equal to 43.3 kN-m (489 kip-in). For the reinforced New Jersey parapet, the minimum nominal torsional capacity was believed to be greater than or equal to 163.3 kN-m (1,845 kip-in). Torsional capacities were then adjusted using a reduction factor of $\phi = 0.85$. Using the analytical procedures described above, the redirective capacities for the un-reinforced Ontario tall wall and reinforced New Jersey barrier were estimated to be greater than or equal to 703 N (158 kips) and 3,527 N (793 kips), respectively.

Based on these results, several conclusions can be made. First, the 1,067-mm (42-in.) tall,

reinforced New Jersey shape concrete median barrier provides significant reserve capacity above that needed to redirect TL-5 tractor-trailer vehicles. Therefore, it is believed that this barrier should be further optimized using a reduction of the longitudinal and vertical steel reinforcement.

Second, the redirective capacity of the non-reinforced Ontario tall wall was significantly lower than that provided by the other 1,067-mm (42-in.) tall concrete parapets evaluated according to the actual TL-5 impact conditions. Following a review of the test results, it should be noted that some of the vehicle ballast broke loose and fell out of the side of the trailer box during the impact event. It was also observed that the trailer's rear tandem axle assembly broke away from the trailer box prior to the impact between the barrier and the trailer's tandem axle. Therefore, the potential exists that the un-reinforced concrete median barrier may not have experienced the full impact load nor the double load pulse that would have been observed had the ballast remained in place and the rear tandem remained attached to the trailer. However, the non-reinforced Ontario tall wall was found to meet the heavy vehicle impact safety standards.

Although TL-5 heavy vehicle impacts into un-reinforced concrete median barriers may result in increased barrier damage, barrier performance is still judged acceptable when the vehicle is contained and redirected on the traffic-side face of the barrier system.

3 DESIGN IMPACT LOAD

3.1 Instrumented Wall Testing with Heavy Vehicles

In 1989, researchers at the TTI completed a study to determine the magnitude and duration of the dynamic lateral loads occurring when heavy vehicles impact rigid concrete barriers (4). In an effort to measure these loads, a 2,286-mm (90-in.) tall rigid concrete wall was constructed and instrumented with load cells. Methodologies were also presented for calculating the impact force from the onboard vehicle accelerometer data. For each test, a comparison was then made between the measured dynamic wall loads and that determined from the vehicle accelerometers. A total of ten full-scale vehicle crash tests were performed, consisting of a full-size sedan, pickup trucks, Chevrolet Suburbans, a single-unit truck, an inter-city bus, tractor van-trailers, and a tractor tank-trailer.

Three full-scale vehicle crash tests were performed with tractor-trailer vehicles ranging in weight from approximately 22,680 kg (50,000 lbs) to 36,287 kg (80,000 lbs), as summarized in Table 5. For the 36,287-kg (80,000-lb) vehicle tests, the peak impact forces were measured to be 979 N (220 kips) and 1,815 N (408 kips) for the van- and tanker-style trailers, respectively. During these same tests, the peak impact forces imparted to the wall by the tractor's rear tandem axles were found to be 783 N (176 kips) and 943 N (212 kips) for the van- and tanker-style trailers, respectively. For the 22,680-kg (50,000-lb) vehicle test, a peak impact force of 667 N (150 kips) was imparted to the wall, occurring as a result of the impact by the tractor's rear tandem axles.

Based on the 36,287-kg (80,000-lb) truck test results, a lateral impact force between 783 N (176 kips) and 943 N (212 kips) would seem appropriate for designing 1,067-mm (42-in.) high rigid parapets; since, the rail design would be governed by the load imparted by the tractor's rear tandem

Table 5. Tractor-Trailer Vehicle Crash Tests and Results for Instrumented Wall

| Test No. | Trailer Type | Vehicle Weight (lbs) | Impact Condition | | Impact Severity (kip-ft) | Maximum Impact Force[1] (kips) | Height of Maximum Resultant Force (in.) | Maximum Impact Force of Rear Tractor Tandem Axles[1] (kips) | Height of Resultant Force of Rear Tractor Tandem Axles (in.) |
			Speed (mph)	Angle (deg)					
7046-3	Van	80,080	55.0	15.3	563.9	220	70.0	176	44.0
7046-4	Tank	79,900	54.8	16.0	609.4	408	56.0	212	40.5
7046-9	Van	50,000	50.4	14.6	269.8	150	35.0	150	35.0

[1] - Maximum 0.050-sec average force as determined from the instrumented wall loads cells.
1 kg = 2.204623 lbs
1 in. = 25.4 mm
1 km/hr = 0.6213712 mph
1 lb = 0.2248089 N
1 Joule = 0.7375621 ft-lbs

12

axles versus the peak load measured higher up the instrumented "tall" wall. Additionally, if one considered the results from the 22,680-kg (50,000-lb) truck test, a higher lateral impact load may need to be considered than that discussed previously. In past research, it has been reported that the lateral impact force is approximately proportional to the impact severity for a given test. For convenience, the target impact severities for the 22,680-kg (50,000-lb) and 36,287-kg (80,000-lb) truck test conditions have been provided in Table 6. Therefore, if an adjustment were made to the lateral load based on an increase in impact severity for the TL-5 test condition, then the lateral impact force would be increased by nearly 63 percent or to a force level of 1,085 N (244 kips).

3.2 Load Estimation Using Linear Regression

Following a review of the instrumented wall results for both the 22,680-kg (50,000-lb) and 36,287-kg (80,000-lb) tractor-trailer crash tests, it was determined that a more rational method for estimating the design impact load was required. Therefore, MwRSF researchers performed a linear regression on the estimated lateral peak load versus impact severity for a selected number of tractor-trailer tests. This linear regression analysis was conducted for both the total impact severity of the tractor trailer as well as for the impact severity of the tractor's rear tandem axles. For this analysis, the lateral peak loads were calculated using the 50-msec average lateral accelerations multiplied by the corresponding weights (i.e., total vehicle weight or weight on tandems). The six tractor-trailer crash tests used for this investigation were TTI test nos. 7069-10, 4798-13, 7162-1, 2416-1, 6, and 405511-2, as shown in Tables 1 through 4.

For the linear regression analysis of the impact load and severity data, the general curve was determined to be of the general form:

$$y = m * x + b \tag{1}$$

13

Table 6. Target Impact Conditions for Tractor-Trailer Vehicle Tests According to NCHRP Report No. 350 and AASHTO

Test No.	Test Guidelines	Trailer Type	Test Designation	Vehicle Weight kg (lbs)	Impact Condition		Impact Severity kJ (kip-ft)	Suggested IS Tolerance kJ (kip-ft)
					Speed kph (mph)	Angle (deg)		
5-12	NCHRP (1)	Van	36000V	36,000 (79,366)	80.0 (49.71)	15.0	595.4 (439.2)	-72.3 to +76.9 (-53.3 to +56.7)
6-12	NCHRP (1)	Tank	36000T	36,000 (79,366)	80.0 (49.71)	15.0	595.4 (439.2)	-72.3 to +76.9 (-53.3 to +56.7)
PL-3	AASHTO (17)	Van	50 Kips	22,680 (50,000)	80.47 (50.0)	15.0	379.5 (279.9)	NA

1 kg = 2.204623 lbs
1 in. = 25.4 mm
1 km/hr = 0.6213712 mph
1 lb = 0.2248089 N
1 Joule = 0.7375621 ft-lbs

where y - barrier impact load, kips,
            x - calculated impact severity, kip-ft,
            m - slope of the line, and
            b - vertical ordinate for the line at x=0 and set equal to 0.

For this case, the slope coefficient, m, was determined using the following expression:

$$m = \sum x_i * y_i / \sum x_i^2 \tag{2}$$

where i = 1 to n (n = 6 for this analysis).

From the analysis based on using the total vehicle impact severity, the following linear relationship was determined:

$$Y = (0.5543) * X_{TV} \tag{3}$$

where Y - design impact load, kips, and
            X_{TV} - total vehicle impact severity, kip-ft.

This relationship is shown graphically in Figure 1.

From the analysis based on using the impact severity for the tractor's rear tandem axle, the following relationship was determined:

$$Y = (1.2988) * X_{RT} \tag{4}$$

where Y - design impact load, kips, and
            X_{RT} - impact severity for tractor's rear tandem axle, kip-ft.

This relationship is shown graphically in Figure 2.

Using Equation (3), the design impact load was estimated for two tractor-trailer vehicle test cases, as provided in Table 7a. For the TL-5 impact condition of NCHRP Report No. 350, a design impact load was calculated to be 1,081 N (243 kips). For the PL-3 impact condition found in AASHTO's *Guide Specifications for Bridge Railings* (17), a design impact load of 689 N (155 kips) was determined.

15
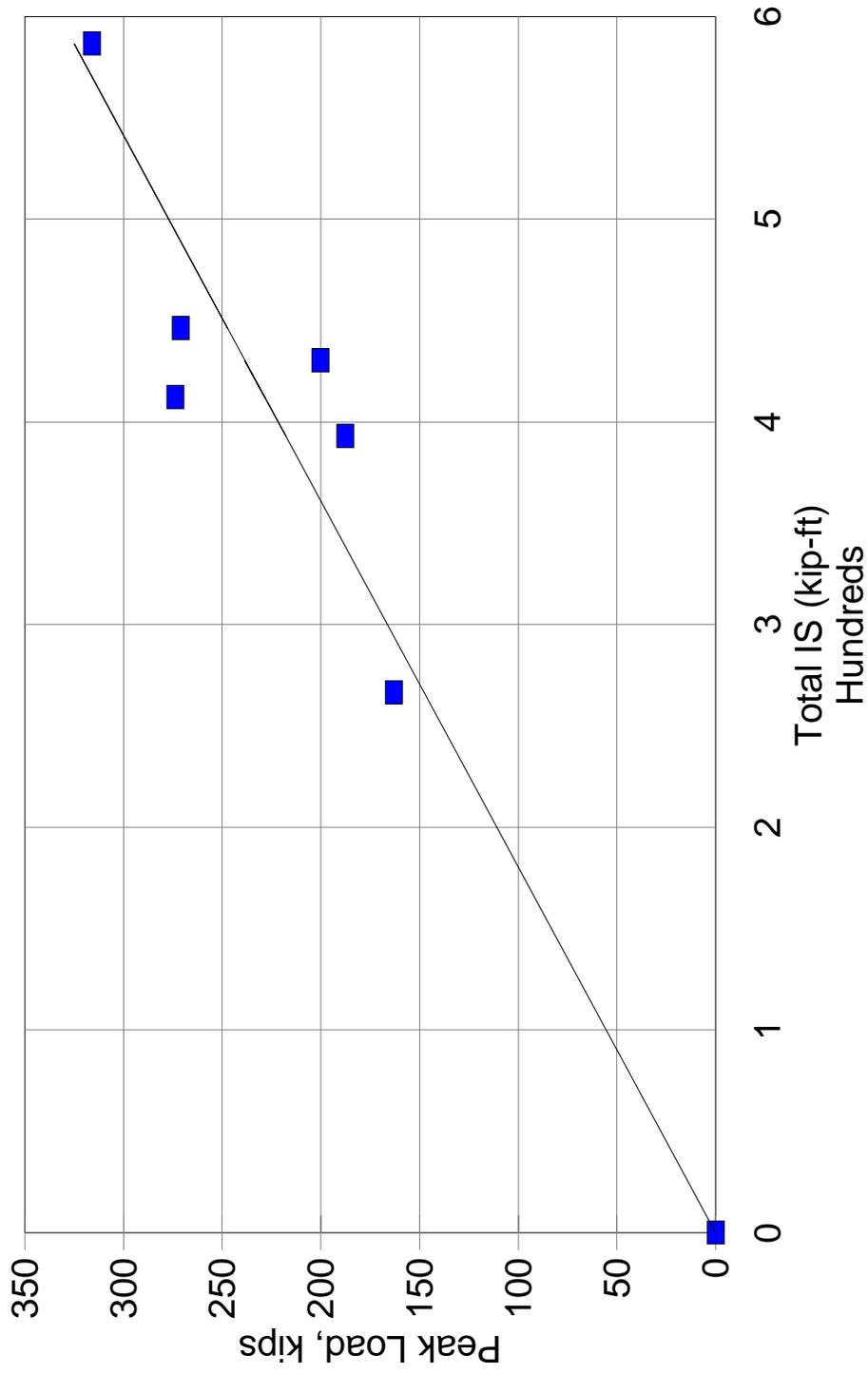
Figure 1. Peak Load and Total Impact Severity (Tractor-Trailer Impacts) [1lb=0.2248089 N and 1 Joule=0.7375621 ft-lbs]
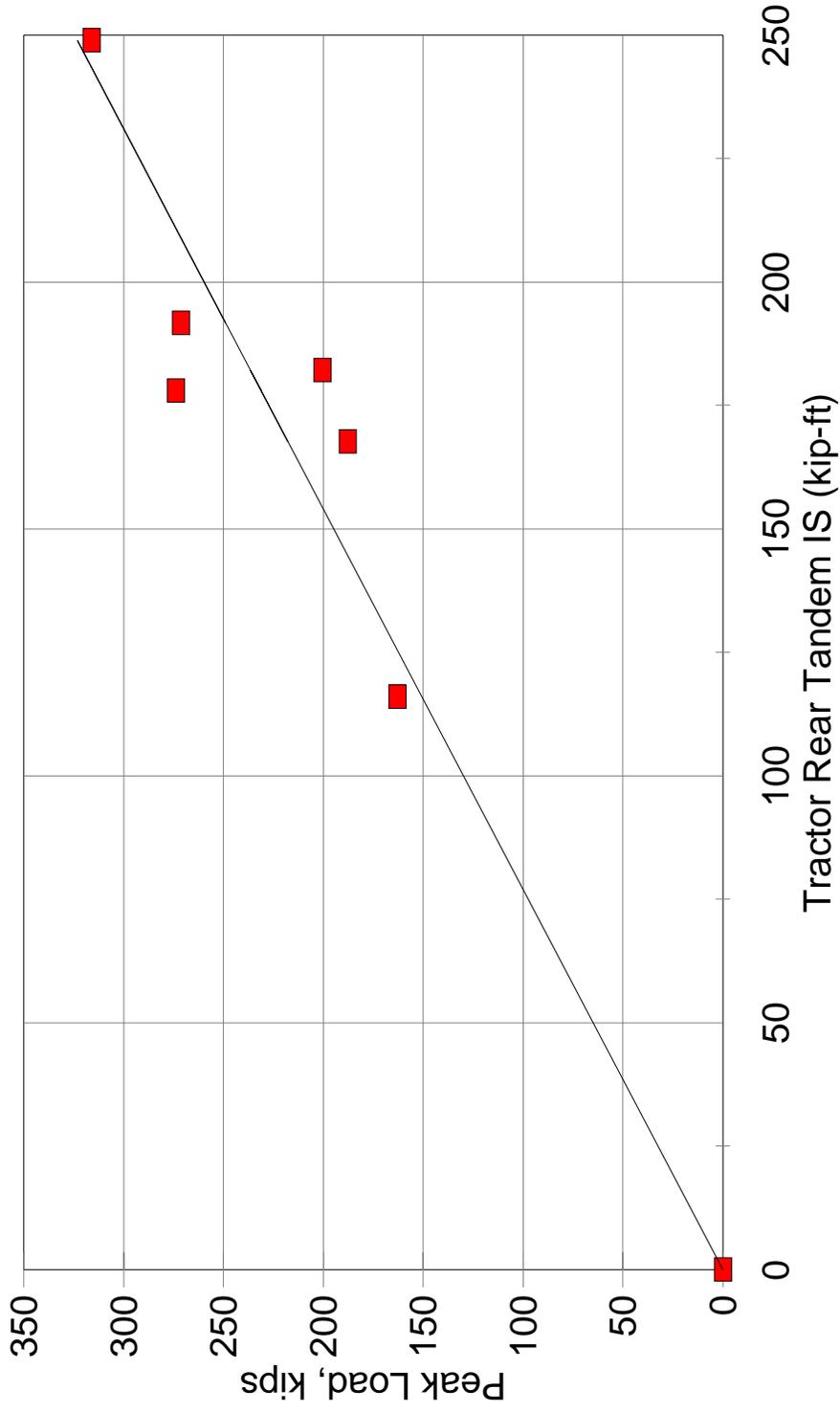
Figure 2. Peak Load and Impact Severity for Tractor's Rear Tandems [1lb=0.2248089 N and 1 Joule=0.7375621 ft-lbs]

In order to use Equation (4) to estimate the design impact load, it was first necessary to determine the weight carried by the tractor's rear tandem axles. For the eleven trucks identified in Tables 1 through 4, the average weight on the tractor's rear tandem axle for the 22,680-kg (50,000-lb) and 36,287-kg (80,000-lb) trucks were 9,640 kg (21,252 lbs) and 15,488 kg (34,145 lbs), respectively. Once the weights had been estimated, the corresponding impact severities were calculated using the appropriate impact speed and angle of the test conditions. As shown in Table 7b, the estimate for the design impact load was then determined using Equation (4) for the TL-5 and PL-3 tractor-trailer impact conditions. For the TL-5 impact condition of NCHRP Report No. 350, a design impact load was calculated to be 1,103 N (248 kips). For the PL-3 impact condition found in AASHTO's *Guide Specifications for Bridge Railings*, a design impact load of 681 N (153 kips) was determined.

3.3 Final Peak Design Load Range

In summary, the analytical investigation has resulted in a peak design load ranging between 681 to 689 N (153 to 155 kips) and 1,081 to 1,103 N (243 to 248 kips) for the AASHTO PL-3 and NCHRP 350 TL-5 impact conditions, respectively.

Table 7a. Design Impact Load Based on Total Vehicle Impact Severity (Target Impact Conditions)

Test No.	Test Guidelines	Test Designation	Vehicle Weight (lbs)	Total Vehicle Impact Severity (kip-ft)	Design Impact Load (kips)
5-12	NCHRP (1)	36000V	79,366	439.2	243
PL-3	AASHTO (17)	50 Kips	50,000	279.9	155

1 kg = 2.204623 lbs
1 in. = 25.4 mm
1 lb = 0.2248089 N
1 Joule = 0.7375621 ft-lbs

Table 7b. Design Impact Load Based on Impact Severity of Tractor's Rear Tandem Axle (Target Impact Conditions)

Test No.	Test Guidelines	Test Designation	Vehicle Weight (lbs)	Total Vehicle Impact Severity (kip-ft)	Tractor Rear Tandem Axle Weight[1] (lbs)	Tractor Rear Tandem Impact Severity (kip-ft)	Design Impact Load (kips)
5-12	NCHRP (1)	36000V	79,366	439.2	34,145	191.2	248
PL-3	AASHTO (17)	50 Kips	50,000	279.9	21,252	117.6	153

[1] - Average weight based on prior tractor-trailer truck tests conducted by TTI.

1 kg = 2.204623 lbs
1 in. = 25.4 mm
1 lb = 0.2248089 N
1 Joule = 0.7375621 ft-lbs

4 DESIGN METHODOLOGY

4.1 Barrier Capacity Considerations

Once peak lateral loads were determined, it was then necessary to compare that load to the predicted capacities of existing railing configurations. Four barrier systems were selected for further examination: (1) the 1,067-mm (42-in.) tall F-Shape, half-section bridge railing system [test no. 7069-10] (8-9), as shown in Figures 3 and 4; (2) the 1,067-mm (42-in.) tall, vertical concrete bridge railing system [test no. 405511-2] (11), as shown in Figures 5 and 6; (3) the 1,067-mm (42-in.) tall, non-reinforced New Jersey Shape concrete median barrier, or "Ontario tall wall," [test no. 7162-1] (2), as shown in Figure 7; and (4) the 1,067-mm (42-in.) tall, reinforced New Jersey shape concrete median barrier [test no. 4798-13] (3), as shown in Figure 8.

4.1.1 F-Shape, Half-Section Bridge Railing (PL-3 Impact Condition)

As shown in Table 4, the F-Shape, half-section bridge railing system was estimated to have a redirective barrier capacity, RW, ranging between 565 N (127 kips) and 574 N (129 kips) according to the yield-line analysis procedures provided in References (12) and (13). For test no. 7069-10, the actual impact severities for the entire vehicle and tractor's rear tandems were 361.5 kJ (266.6 kip-ft) and 157.3 kJ (116.0 kip-ft), respectively. These impact severities would have resulted in peak design loads, according to Equations 3 and 4, equal to 658 N (148 kips) and 672 N (151 kips), respectively.

During the crash test, the tractor-trailer vehicle was successfully redirected by the bridge railing system and without damage to the parapet. However, using the yield-line analysis procedure, greater damage to the barrier system would have been expected under this impact condition since the predicted peak load was approximately 17 percent greater than the rated redirective capacity.

This result may indicate that the yield-line analysis procedure underestimates the redirective barrier capacity of a solid, reinforced concrete parapet.
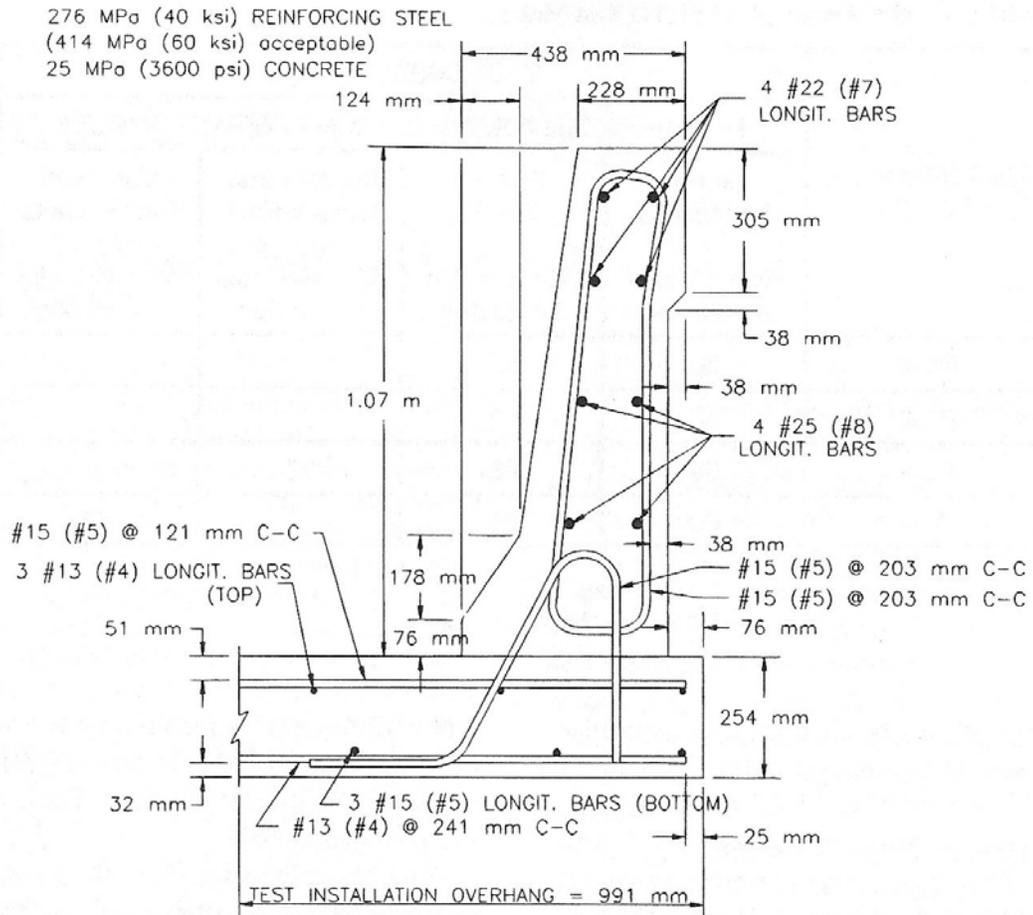
Figure 3. F-Shape, Half-Section Bridge Railing (PL-3 Impact Condition) [Reference No. 8]

22

GRADE 40 REINFORCING STEEL
3600 PSI CONCRETE

17¼"

4⅞" 9"

4 #7
LONGIT. BARS

12"

1½"

1½"

4 #8
LONGIT. BARS

42"

#5 @ 4¾" C–C

3 #4 LONGIT. BARS
(TOP)

7"

3"

1½"

#5 @ 8" C–C

#5 @ 8" C–C

3"

2"

10"

1¼"

3 #5 LONGIT. BARS (BOTTOM)

#4 @ 9½" C–C

1"

1 in = 25.4 mm
1 ft = 0.305 m

TEST INSTALLATION OVERHANG = 39"
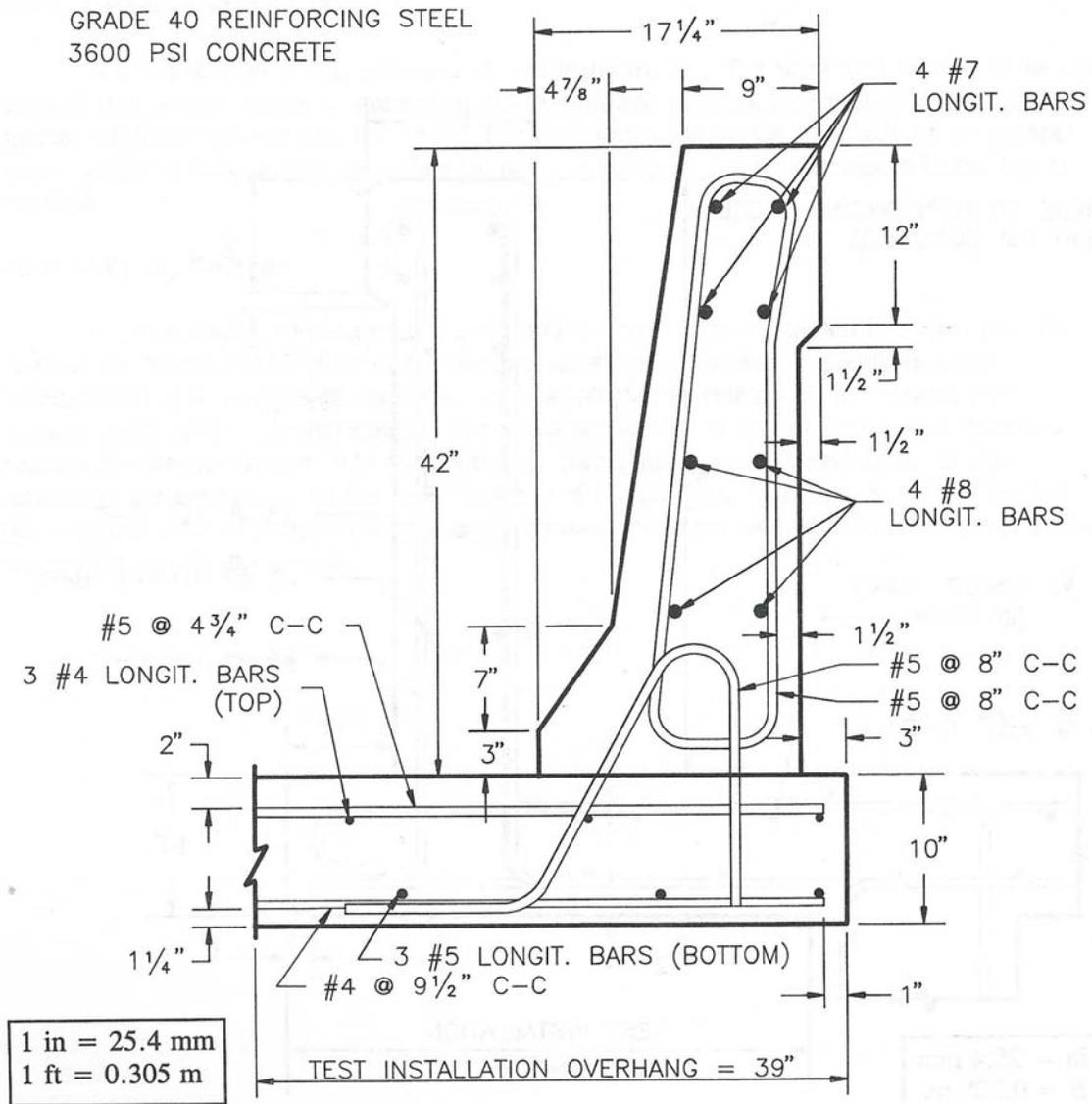
Figure 4. F-Shape, Half-Section Bridge Railing (PL-3 Impact Condition) [Reference No. 9]

23

414 MPa (40 ksi) REINFORCING STEEL
25 MPa (3600 psi) CONCRETE

305 mm

203 mm

25 mm

51 mm

38 mm

38 mm

1.07 m

#15 (#5) @ 305 mm C-C

10 #15 (#5) LONGIT. BARS
(IN SLAB)

10 #22 (#7) LONGIT. BARS

#15 (#5) @ 305 mm C-C

#15 (#5) @ 241 mm C-C

51 mm

191 mm

254 mm

51 mm

25 mm

TEST INSTALLATION
OVERHANG = 991 mm

1 mm = 0.039 in
1 m = 3.28 ft
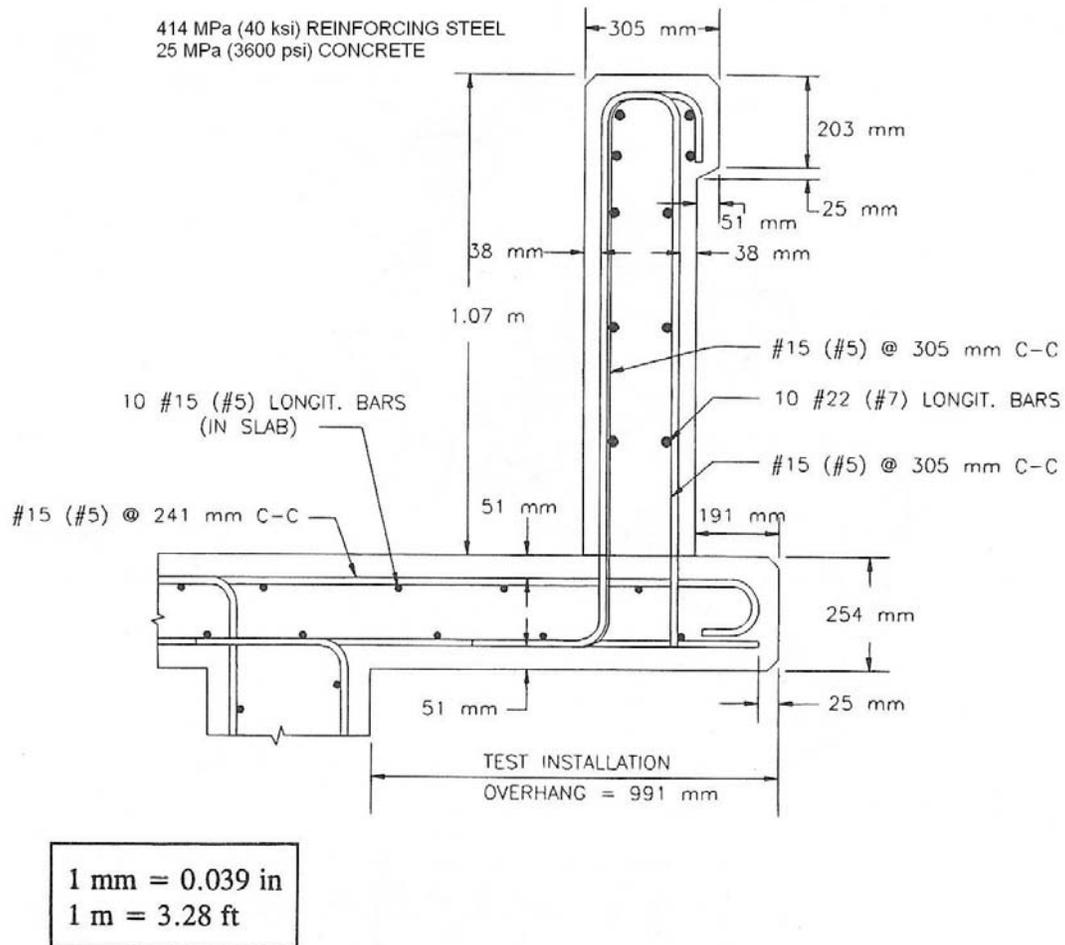
Figure 5. Vertical Bridge Railing (TL-5 Impact Condition) [Reference No. 8]

24

GRADE 60 REINFORCING STEEL
3600 PSI CONCRETE

12"

8"

2"

1"

1½"

1½"

42"

#5 @ 12" C-C

10 #5 LONGIT. BARS
(IN SLAB)

10 #7 LONGIT. BARS

#5 @ 12" C-C

#5 @ 9½" C-C

2"

7½"

10"

1"

2"

TEST INSTALLATION
OVERHANG = 39"

1 in = 25.4 mm
1 ft = 0.305 m
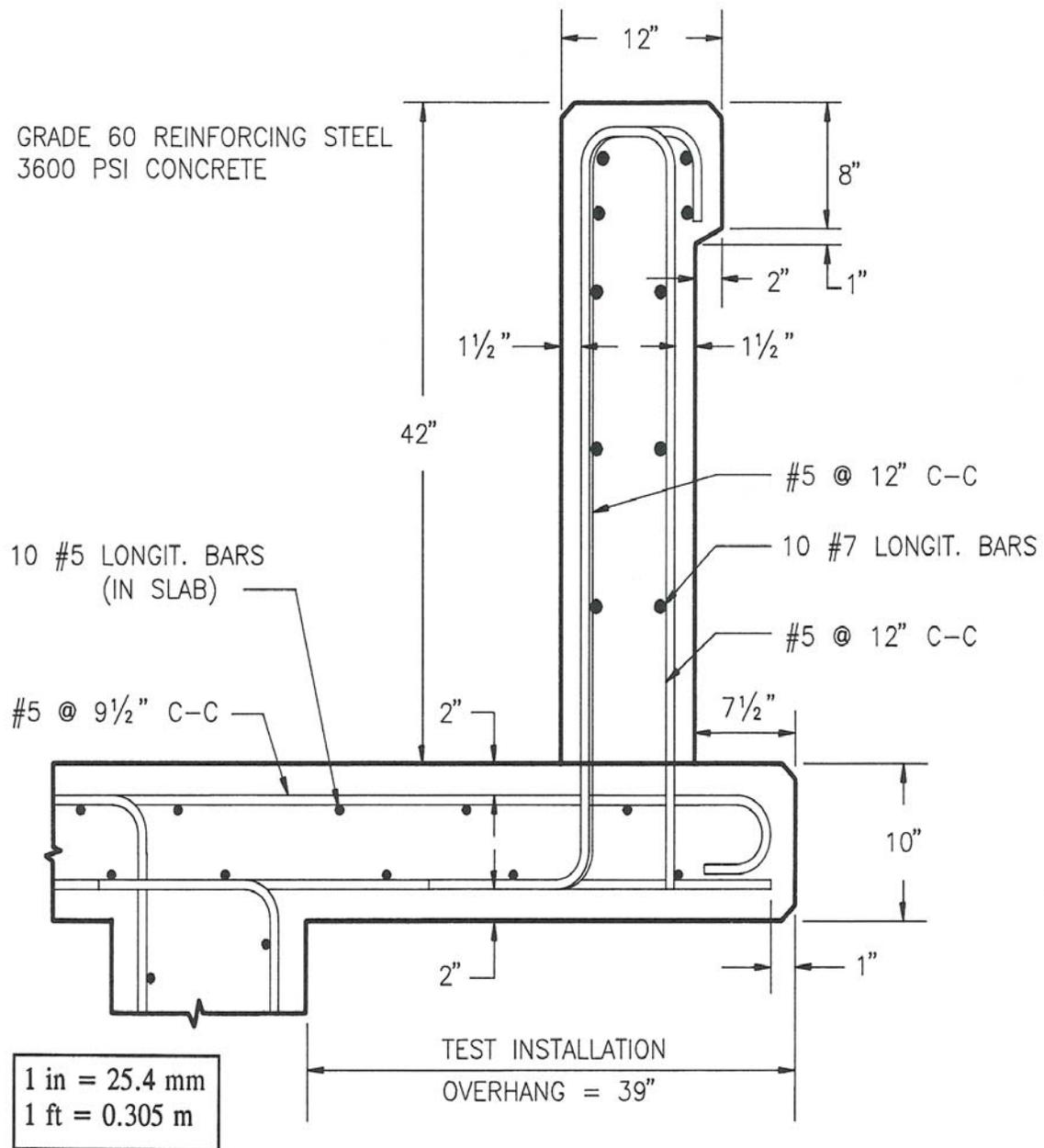
Figure 6. Vertical Bridge Railing (TL-5 Impact Condition) [Reference No. 9]
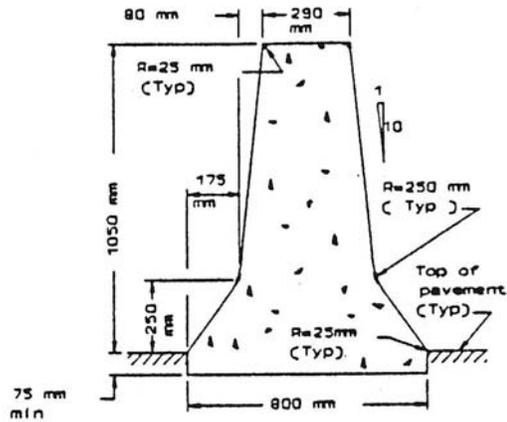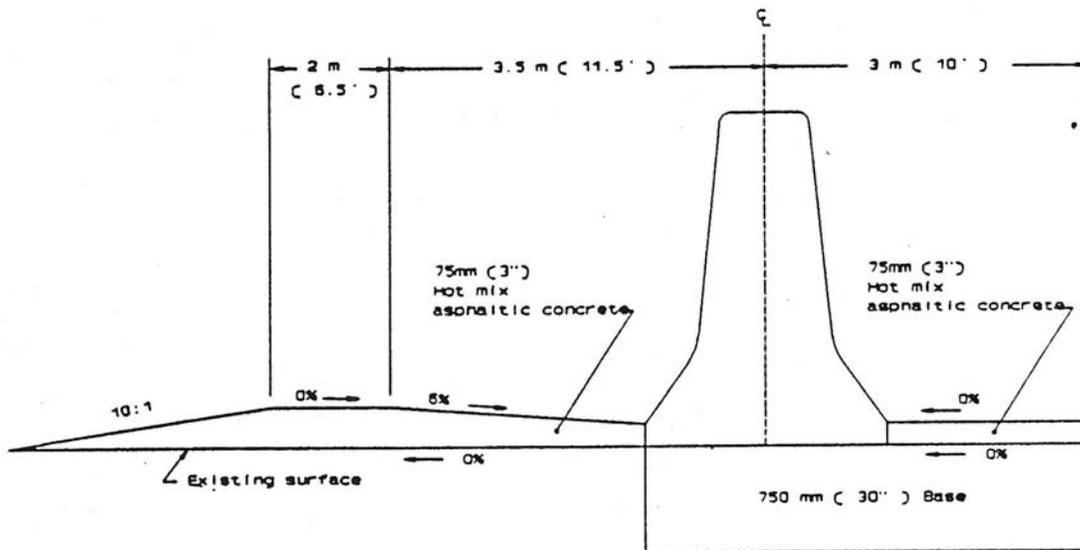
Figure 7. Ontario Tall Wall (TL-5 Impact Condition) [Reference No. 2]
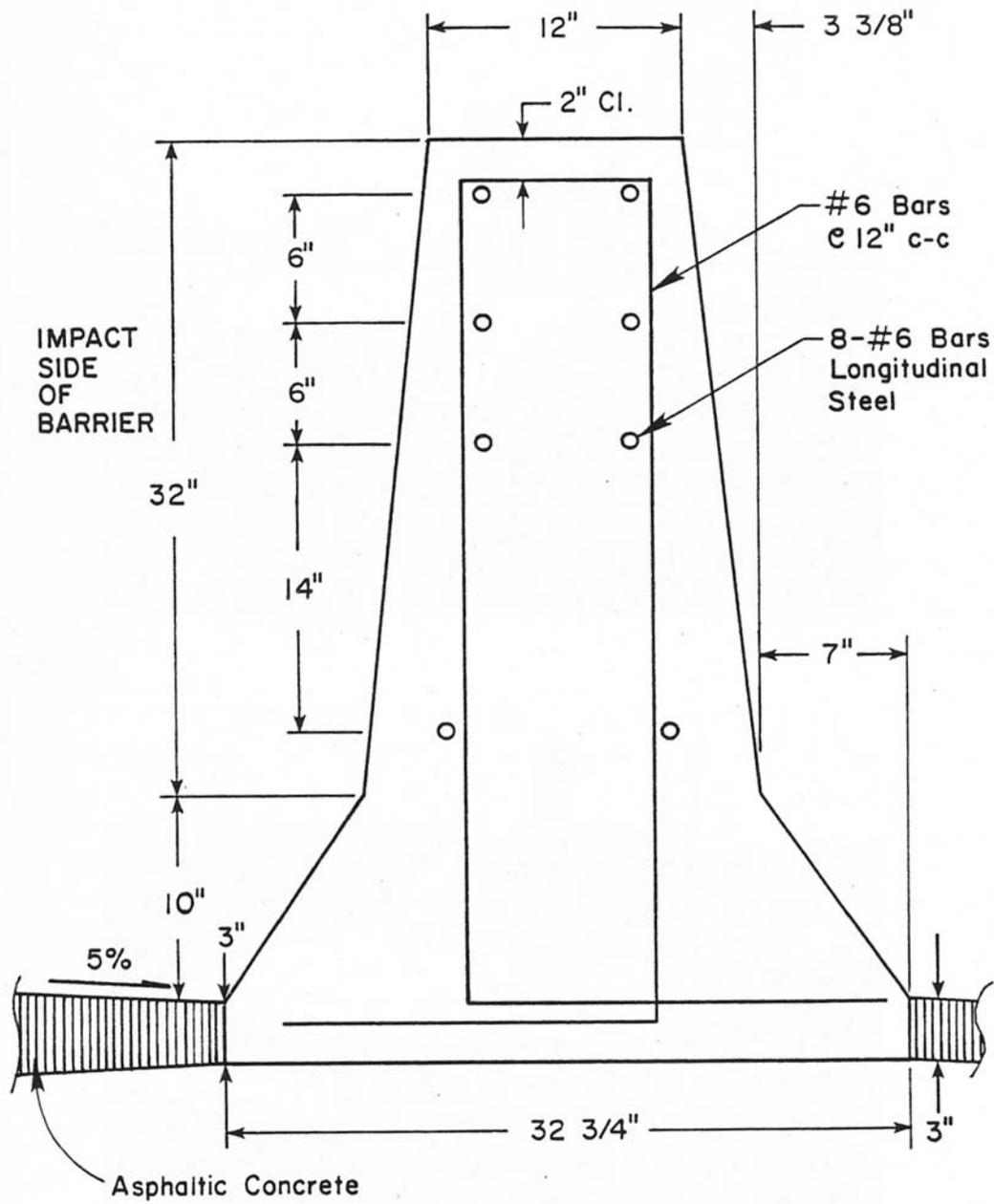
Figure 8. Reinforced, New Jersey Median Barrier (TL-5 Impact Condition) [Reference No. 3]

4.1.2 Vertical Bridge Railing (PL-5 Impact Condition)

As shown in Table 4, the vertical concrete bridge railing system was estimated to have a redirective barrier capacity, R_W, ranging between 881 N (198 kips) and 934 N (210 kips) according to the yield-line analysis procedures provided in References ([12]) and ([13]). For test no. 405511-2, the actual impact severities for the entire vehicle and tractor's rear tandems were 559.3 kJ (412.5 kip-ft) and 241.3 kJ (178.0 kip-ft), respectively. These impact severities would have resulted in peak design loads, according to Equations 3 and 4, equal to 1,019 N (229 kips) and 1,028 N (231 kips), respectively.

During the crash test, the tractor-trailer vehicle was successfully redirected by the bridge railing system, without damage to the parapet. From the yield-line analysis procedure, once again, greater damage to the barrier system would have been expected since the predicted peak load was approximately 13 percent greater than the rated redirective capacity. Again, this result may indicate that the yield-line analysis procedure underestimates the redirective barrier capacity of a solid, reinforced concrete parapet.

4.1.3 Non-Reinforced, New Jersey Shape Concrete Median Barrier (PL-5 Impact Condition)

As discussed in Chapter 2, the non-reinforced, New Jersey Shape concrete median barrier successfully redirected a heavy, tractor-trailer vehicle. During the impact event, however, some vehicle ballast became dislodged and fell outside of the trailer, and the trailer's rear tandem axle assembly broke away from the trailer. For test no. 7162-1, the actual impact severities for the entire vehicle and tractor's rear tandems were 605.4 kJ (446.5 kip-ft) and 259.9 kJ (191.7 kip-ft), respectively. These impact severities would have resulted in peak design loads, according to Equations 3 and 4, equal to 1,099 N (247 kips) and 1,108 N (249 kips), respectively. With the

shifting ballast and significant trailer damage, it is likely that these estimated peak loads would not likely have been imparted to the barrier system. However, a review of the peak 0.050-sec average lateral decelerations showed that a significant lateral load was likely imparted to the barrier by the tractor's rear tandems.

Before crash testing, five shrinkage cracks were noted in the barrier. During the test, the barrier appeared to have remained attached to the foundation without rotation upward nor backward. Following the test, one of the original five cracks increased in width from 4.8 mm (3/16 in.) to 6.35 mm (1/4 in.), and a new crack, measuring 1.6 mm (1/16 in.) wide, formed upstream of impact.

Due to the interest in this barrier, MwRSF researchers attempted to estimate the barrier's redirective capacity using estimates of strengths in lieu of the cantilevered moment capacity. Thus, as previously discussed in Chapter 2, researchers substituted the barrier's torsional capacity into the yield-line analysis expression in order to approximate a minimum redirective capacity. Using a conservative value for torsional strength, combined with a moment capacity of the wall set equal to zero, a conservative estimate for the barrier's redirective capacity was found to be at least 703 N (158 kips). It should be noted that this barrier capacity is much less than the 1,103-N (248-kip) estimated load imparted to this parapet. Therefore, it is believed that other factors may have contributed to the barrier's capacity. First, the torsional capacity may have been greater than the conservative value used in the analysis. Second, frictional forces generated between the asphalt overlay and the barrier's toe may have provided additional cantilevered capacity and resistance to overturning. Third, other factors identified in Chapter 2 may also have contributed to an increased barrier capacity. Finally, the translational and rotational inertial effects may have further aided in the vehicle's containment and redirection.

This analysis demonstrates that the yield-line analytical procedure underestimates a solid, concrete barrier's redirective capacity.

4.1.4 Reinforced, New Jersey Shape Concrete Median Barrier (PL-5 Impact Condition)

As discussed in Chapter 2, the reinforced, New Jersey Shape concrete median barrier successfully redirected a heavy, tractor-trailer vehicle. For test no. 4798-13, the actual impact severities for the entire vehicle and tractor's rear tandems were 795.7 kJ (586.9 kip-ft) and 337.5 kJ (248.9 kip-ft), respectively. These impact severities would have resulted in peak design loads, according to Equations 3 and 4, equal to 1,446 N (325 kips) and 1,437 N (323 kips), respectively. Using the peak 0.050-sec average lateral deceleration of 9.3 G's multiplied by the weight on the tractor's rear tandem axle of 15,427 kg (34,010 lbs), a peak lateral load imparted to the reinforced barrier was approximated to be 1,406 N (316 kips). This result correlates very well with the results obtained from Equations 3 and 4.

During the test, the barrier appeared to have remained attached to the foundation without rotation upward or backward. Due to the interest in this barrier, MwRSF researchers attempted to estimate the barrier's redirective capacity using alternative strengths in lieu of the cantilevered moment capacity. Researchers substituted the barrier's torsional capacity into the yield-line analysis expression in order to approximate a minimum redirective capacity. Using a conservative value for torsional strength, combined with a calculated moment capacity of the wall, a conservative estimate for the barrier's redirective capacity was found to be at least 3,527 N (793 kips). This barrier capacity is much greater than the peak design load ranging between 1,081 N (243 kips) and 1,103 N (248 kips) for the TL-5 impact conditions. It should be noted that this estimated barrier capacity would not be possible without the consideration of the torsional strength of the reinforced concrete

parapet in the yield-line analytical procedure.

Once again, this analysis demonstrated that the yield-line analytical procedure underestimates a solid, concrete barrier's redirective capacity.

4.2 Two Design Philosophies

Based on the impact load investigation and the evaluation of existing barrier configurations previously presented, MwRSF researchers evaluated the two basic philosophies for designing the 813-mm (42-in.) and 1,295-mm (51-in.) tall, F-shape, half-section concrete barriers to meet the TL-5 safety performance criteria. The first design philosophy consisted of using the new TL-5 design impact load, which ranged between 1,081 N (243 kips) and 1,103 N (248 kips), in combination with a "modified" yield-line analysis procedure. The "modified" yield-line analysis procedure incorporates the torsional capacity of the solid, concrete parapet. Since limited analysis has been conducted in order to investigate this hypothesis, it does not seem appropriate to employ this "modified" analytical procedure at this time.

The second design philosophy utilized the existing yield-line analytical procedure in combination with a scaled-down design impact load. This scaled-down design impact load considered two major factors: (1) the redirective capacity of the successfully crash tested vertical wall, as determined by both TTI and MwRSF, and (2) the difference between the actual impact severity of test no. 405511-2 and the target impact severity for the TL-5 impact condition. As shown in Table 4, the redirective barrier capacity for the vertical wall was determined to be 881 N (198 kips) and 934 N (210 kips), as determined by TTI and MwRSF, respectively, thus resulting in an average capacity of 907 N (204 kips). The target impact severity for the TL-5 impact condition was 595.5 kJ (439.2 kip-ft) or approximately 6.5 percent greater than the impact severity for the actual

31

crash test. Therefore, it was deemed appropriate to increase the required barrier capacity by 6.5

percent to the design impact load ranging between 939 N (211 kips) and 996 N (224 kips) or to an

average design impact load value of approximately 965 N (217 kips).

5 CONCEPTUAL DEVELOPMENT OF A NEW BRIDGE RAILING

5.1 Structural and Geometric Considerations

As previously noted, the objective of this research project was to develop an aesthetic, open concrete bridge railing to meet the TL-5 safety performance criteria. For this effort and as discussed in Chapter 4, a design impact load value of approximately 965 N (217 kips) was utilized to size bridge railing system, more specifically, the reinforced concrete post and rail members as well as the connection between the posts and the bridge deck. For the design, several configurations were analyzed in order to obtain a reasonable bridge railing system that met the design impact load. As such, redirective barrier capacities were obtained using the yield-line analytical procedures previously outlined for open concrete railings (12-13) and using a 2.44-m (8-ft) distributed length for the applied load. A total of 513 design combinations were analyzed using clear gap openings ranging between 0.91 to 2.44 m (3 to 8 ft) and variations in steel reinforcement and post and rail geometries.

For the final open concrete rail design, a redirective capacity of approximately 925 N (208 kips) was calculated using a height of 813 mm (32 in.) for the main longitudinal structural member's top front corner. This analysis utilized a minimum 28-day concrete compressive strength of 34 MPa (5,000 psi) and Grade 60 steel reinforcement. An upper cap railing, measuring 10-in. tall, was placed on top of the main longitudinal structural member in order to bring the total barrier height to 1,067 mm (42 in.). The upper cap railing was deemed necessary for reducing the roll motion of the trailer box over the top of the railing by providing vertical support for the lower edge of the impact side of the trailer. It is noted that the redirective capacity of the cap rail was not incorporated into the barrier's overall capacity for two reasons. First, it was not believed to significantly add to the

33

barrier's overall lateral resistance. Second, during the vehicle to barrier contact, it was believed that the cap rail may encounter moderate damage and/or fracture such that its lateral flexural resistance would be negated even though its compressive strength would remain adequate to resist truck roll and lean onto its upper surface.

The upper cap rail was also setback (distance) from the front face of the main longitudinal structural member, starting at a height of 870 mm (34.25 in.) and continuing to the 1,067-mm (42-in.) top height. This upper rail setback distance was incorporated in order to reduce the potential for the occupant's head to extend out of the side windows during oblique small car impacts and contact the barrier face. MwRSF researchers believed that the incorporation of an upper rail setback, varying between 114 to 140 mm (4½ and 5½-in.), would significantly reduce the serious risk to the occupants during head-slap against the upper face of tall, rigid parapets.

Below the rail and at the post locations, the front face of the posts were setback approximately 51mm (2 in.) from front face of the lower rail and approximately 89 mm (3½ in.) away from the front face of two protruding longitudinal asperities. In addition, the leading edge of the post on both the upstream and downstream sides was setback an additional 76 mm (3 in.), thus bringing the total setback away from the front face of the lower rail to 127 mm (5 in.). MwRSF researchers determined that the propensity for small car and pickup truck wheel snag against the posts would be virtually eliminated by this setback.

The final open concrete bridge railing was configured with an 1,829-mm (6-ft 0-in.) long clear gap opening between the outer ends of the 762-mm (30-in.) long by 267-mm (10½-in.) wide by 305-mm (12-in.) tall posts. The concrete posts were spaced on 2,591-mm (8-ft 6-in.) centers. This configuration provided a sufficient gap opening width under the rail for water runoff and was

believed to provide a more open and aesthetic appearance for the motoring public. As previously mentioned, two protruding longitudinal asperities were placed along the rail's front face for both aesthetic and performance reasons. With regard to performance, MwRSF researchers believed that the asperities would provide increased vehicle to barrier interlock, thereby reducing the propensity for small cars and light trucks to climb and/or vault the barrier system as well as decrease vehicle instabilities during redirection.

Final and complete design details for the TL-5 open concrete bridge railing system are provided in Chapter 7 of this report.

6 TEST REQUIREMENTS AND EVALUATION CRITERIA

6.1 Test Requirements

Longitudinal barriers, such as aesthetic open concrete bridge rails, must satisfy the requirements provided in NCHRP Report No. 350 to be accepted for use on National Highway System (NHS) construction projects or as a replacement for existing systems not meeting current safety standards. According to TL-5 criteria found in NCHRP Report No. 350, the bridge railing system must be subjected to three full-scale vehicle crash tests. The three crash tests are as follows:

1. Test Designation 5-10: An 820-kg (1,808-lb) small car impacting the bridge railing system at a nominal speed and angle of 100.0 km/h (62.1 mph) and 20 degrees, respectively.

2. Test Designation 5-11: A 2,000-kg (4,409-lb) pickup truck impacting the bridge railing system at a nominal speed and angle of 100.0 km/h (62.1 mph) and 25 degrees, respectively.

3. Test Designation 5-12: A 36,000-kg (79,366-lb) tractor-trailer unit impacting the bridge railing system at a nominal speed and angle of 80.0 km/h (49.7 mph) and 15 degrees, respectively.

Although the small car and pickup truck tests are used to evaluate the overall performance of the length-of-need section and occupant risk problems arising from the snagging or overturning of the vehicle, both tests were deemed unnecessary based on previous testing of open concrete bridge railing systems. Performed by ENSCO, Inc. (18), an open concrete bridge railing system, with a clear opening height of 330 mm (13 in.) and a post setback distance of 51 mm (2 in.), had been successfully tested and evaluated in accordance with the performance criteria of NCHRP Report No. 230, *Recommended Procedures for the Safety Performance Evaluation of Highway Appurtenances* (19). Therefore, on the basis of the previous small car test results, an 820-kg (1,808-lb) small car crash test was considered unnecessary for this project. In addition, MwRSF researchers

have conducted several studies involving the analysis, design, testing, and evaluation of open concrete bridge railing systems (20-23). For these research efforts, two different safety performance criteria were utilized - the Performance Level 1 and 2 criteria provided in American Association of State Highway and Transportation Officials (AASHTO's) *Guide Specifications for Bridge Rails* (17) and the Test Level 3 criteria in NCHRP Report No. 350 (1). Once again, the crash test results have demonstrated that the use of a 330-mm (13-in.) clear opening height and a 51-mm (2-in.) post setback distance were adequate for preventing excessive pickup truck wheel for oblique impacts with ¾-ton pickup trucks. Therefore, a 2,000-kg (4,409-lb) pickup truck crash test was also considered unnecessary for this project. The test conditions for TL-5 longitudinal barriers are summarized in Table 8.

6.2 Evaluation Criteria

Evaluation criteria for full-scale vehicle crash testing are based on three appraisal areas: (1) structural adequacy; (2) occupant risk; and (3) vehicle trajectory after collision. Criteria for structural adequacy are intended to evaluate the ability of the bridge railing to contain, redirect, or allow controlled vehicle penetration in a predictable manner. Occupant risk evaluates the degree of hazard to occupants in the impacting vehicle. Vehicle trajectory after collision is a measure of the potential for the post-impact trajectory of the vehicle to cause subsequent multi-vehicle accidents. This criterion also indicates the potential safety hazard for the occupants of other vehicles or the occupants of the impacting vehicle when subjected to secondary collisions with other fixed objects. These three evaluation criteria are defined in Table 9. The full-scale vehicle crash test was conducted and reported in accordance with the procedures provided in NCHRP Report No. 350.

Table 8. NCHRP Report No. 350 Test Level 5 Crash Test Conditions

Test Article	Test Designation	Test Vehicle	Impact Conditions			Evaluation Criteria [1]
			Speed		Angle (degrees)	
			(km/h)	(mph)		
Longitudinal Barrier	5-10	820C	100	62.1	20	A,D,F,H,I,K,M
	5-11	2000P	100	62.1	25	A,D,F,K,L,M
	5-12	36000V	80	49.7	15	A,D,G,K,M

[1] Evaluation criteria explained in Table 9.

Table 9. NCHRP Report No. 350 Evaluation Criteria for Crash Tests (1)

Structural Adequacy	A.	Test article should contain and redirect the vehicle; the vehicle should not penetrate, underride, or override the installation although controlled lateral deflection of the test article is acceptable.
Occupant Risk	D.	Detached elements, fragments or other debris from the test article should not penetrate or show potential for penetrating the occupant compartment, or present an undue hazard to other traffic, pedestrians, or personnel in a work zone. Deformations of, or intrusions into, the occupant compartment that could cause serious injuries should not be permitted.
	F.	The vehicle should remain upright during and after collision although moderate roll, pitching, and yawing are acceptable.
	G.	It is preferable, although not essential, that the vehicle remain upright during and after collision.
	H.	Longitudinal and lateral occupant impact velocities should fall below the preferred value of 9 m/s (29.53 ft/s), or at least below the maximum allowable value of 12 m/s (39.37 ft/s).
	I.	Longitudinal and lateral occupant ridedown accelerations should fall below the preferred value of 15 g's, or at least below the maximum allowable value of 20 g's.
Vehicle Trajectory	K.	After collision it is preferable that the vehicle's trajectory not intrude into adjacent traffic lanes.
	L.	The occupant impact velocity in the longitudinal direction should not exceed 12 m/sec (39.37 ft/sec), and the occupant ridedown acceleration in the longitudinal direction should not exceed 20 G's.
	M.	The exit angle from the test article preferably should be less than 60 percent of test impact angle measured at time of vehicle loss of contact with test device.

7 DESIGN DETAILS

The test installation consisted of a reinforced, open concrete bridge rail attached to a reinforced bridge deck system, as shown in Figures 9 through 13. The corresponding English-unit drawings are shown in Appendix A. Photographs of the test installation are shown in Figures 14 through 19.

7.1 Bridge Substructure

One grade beam was constructed adjacent to the existing concrete slab. This grade beam measured 457-mm (18-in.) wide by 318-mm (12.5-in.) high to the bottom of the bridge deck and spanned the entire 37.03 m (121 ft - 6 in.) of bridge deck length. Steel reinforcement for this grade beam consisted of No. 6 vertical bars spaced 305 mm (12 in.) on center which were tied to the corresponding transverse deck bars. All steel reinforcement in the concrete grade beams was Grade 60 epoxy-coated rebar.

Another grade beam was constructed 1,626 mm (64 in.) away from the existing concrete slab. This grade beam measured 457-mm (18-in.) wide by 457-mm (18-in.) high and spanned the entire 37.03 m (121 ft - 6 in.) of bridge deck length. The steel reinforcement for the grade beam utilized No. 3 and 4 longitudinal bars and No. 6 vertical bars. Each of the four runs of No. 3 and six runs of No. 4 longitudinal rebar was 36.93-m (121-ft 2-in.) long. The spacing of the longitudinal bars are shown in Figures 9 through 11, 14, and 15. The length of the longitudinal bar can be varied as long as the minimum lap length of 610 mm (24 in.) is maintained. The vertical bars in the grade beam were 838-mm (33-in.) long and spaced 305 mm (12 in.) on center, as shown in Figures 9 through 11, 14, and 15.

The bridge deck measured 3,404-mm (134-in.) wide by 203-mm (8-in.) thick by 37.03-m

(121-ft 6-in.) long. The concrete used for the concrete grade beams and the concrete deck consisted of a Nebraska 47-BD Mix, with a minimum compressive strength of 34.47 MPa (5,000 psi). The actual concrete compressive strength for the bridge deck on test day, as determined from concrete cylinder testing, was found to be approximately 41.25 MPa (5,983 psi). A minimum concrete cover of 51 mm (2 in.) was used for all the rebar placed within the bridge deck, except for the bottom of the bridge deck between the grade beam and existing concrete slab.

The steel reinforcement for the bridge deck utilized No. 4 and 5 longitudinal bars and No. 4, 5, and 6 transverse bars. Each of the eleven runs of No. 4 and twelve runs of No. 5 longitudinal rebar was 36.93-m (121-ft 2-in.) long and spaced 305 mm (12 in.) on center. The length of the longitudinal bar can be varied as long as the minimum lap length of 610 mm (24 in.) is maintained. The transverse bars in the bridge deck were 3.05-m (10-ft) long. The No. 4 and 6 transverse bars in the top layer were alternated and spaced 152 mm (6 in.) on center. The No. 5 transverse bars in the bottom layer were spaced 305 mm (12 in.) on center. The No. 6 bent bars in the bridge deck were positioned near the existing concrete slab and spaced 305 mm (12 in.) on center. These bent bars were lapped with and tied to the corresponding transverse deck bars. In addition, 1,067-mm (42-in.) long No. 8 transverse bars were embedded 305 mm (12 in.) into the existing apron and spaced 305 mm (12 in.) and 610 mm (24 in.) on center in the impact and non-impact region, respectively. These bars were lapped with and tied to the longitudinal deck bars. Bridge deck reinforcement details are shown in Figures 9 through 15 and Appendix A.

7.2 Bridge Rail

The 37.03-m (121-ft 6-in.) long, aesthetic open concrete bridge rail consisted of a reinforced concrete parapet, as shown in Figures 9, 11, 18, and 19 . The entire system was 356-mm (14-in.)

41

wide by 762-mm (30-in.) deep with a 1,067-mm (42-in.) top mounting height, as measured from the top of the concrete bridge deck to the top of the rail. The bridge rail was cast in place on top of the concrete bridge posts with a 51-mm (2-in.) overhang on the front face of the posts and flush with the back side of the posts. Fifteen bridge posts, measuring 267-mm (10.5-in.) wide by 762-mm (30-in.) long by 305-mm (12-in.) high, were used to support the bridge rail. Bridge posts were spaced 2,591 mm (8 ft - 6 in.) on centers along the length of the bridge railing, as shown in Figures 9 through 11, 18, and 19.

The concrete used for the bridge rail and posts consisted of Nebraska 47-BD Mix, with a minimum compressive strength of 34.47 MPa (5,000 psi).The bridge rail and posts were cast in place in two separate pours, half of the bridge rail and posts cast during each pour. The actual concrete compressive strength for the first-half and second-half of the bridge rail and posts on test day, as determined from concrete cylinder testing, were found to be approximately 37.46 MPa (5,434 psi) and 39.43 MPa (5,720 psi), respectively. A minimum concrete cover of 51 mm (2 in.) was used for all the rebar placed within the bridge rail and posts. All steel reinforcement in the bridge rail and posts was Grade 60 epoxy-coated rebar. The bridge rail and post reinforcement details are shown in Figures 9 through 17.

The steel reinforcement for the bridge rail utilized No. 6 longitudinal bars and No. 4 vertical loop and U-shaped bars. Each of the ten longitudinal rebar was 36.93-m (121-ft 2-in.) long. The length of the longitudinal bar can be varied as long as the minimum lap length of 610 mm (24 in.) is maintained. The transverse and vertical spacings of the longitudinal bars varied, as shown in Figures 10 through 12. The vertical loop bars were 1,276-mm (50.25-in.) long and were bent into a rectangular shape. The longitudinal spacings of the vertical loop bars were 152 mm (6 in.) on

42

center. The vertical U-shaped bars were 1,143-mm (45-in.) long and were bent into a "U" shape. The longitudinal spacings of the vertical U-shaped bars were 305 mm (12 in.) on center.

The steel reinforcement for the bridge posts consisted of No. 4 bars for the horizontal loop bars and No. 6 bars for the vertical L-shaped bars, as shown in Figures 10 through 13. The horizontal loop bars were 1,441-mm (56.75-in.) long and were bent into a rectangular shape. The vertical spacings of the post loop bars were 95 mm (3.75 in.) on center. The post-to-deck attachment utilized thirteen vertical, L-shaped bars in each post, as shown in Figures 10 through 13. The No. 6 bars were 2,007-mm (79-in.) long. The longitudinal and transverse spacings of the vertical, L-shaped bars were approximately 102 mm (4 in.) on center.

NOTES:
(1) No. 8 BARS @ 610mm CENTERS FOR 0 to 3.81 m AND 13.26 m to 36.42 m FROM THE RIGHT
(2) No. 8 BARS @ 305mm CENTERS FOR 3.81 m to 13.26 m, 36.42 m to 137.03 m, AND BARS LONGITUDINAL TO BRIDGE DECK ON SOUTH END

NDOR's TL-5 Aesthetic Open Concrete Bridge Rail

Plan View

Midwest Roadside Safety Facility

Drawing Name:	Scale:
NDOR TL-5 R4.dwg	None

Sheet:	1 of 5
Date:	4/13/2004
By:	JL/GEP
Dwg:	RKF/KAP

Figure 9. Layout for NDOR's TL-5 Aesthetic Open Concrete Bridge Rail

44

Figure 10. NDOR's TL-5 Aesthetic Open Concrete Bridge Rail Design Details
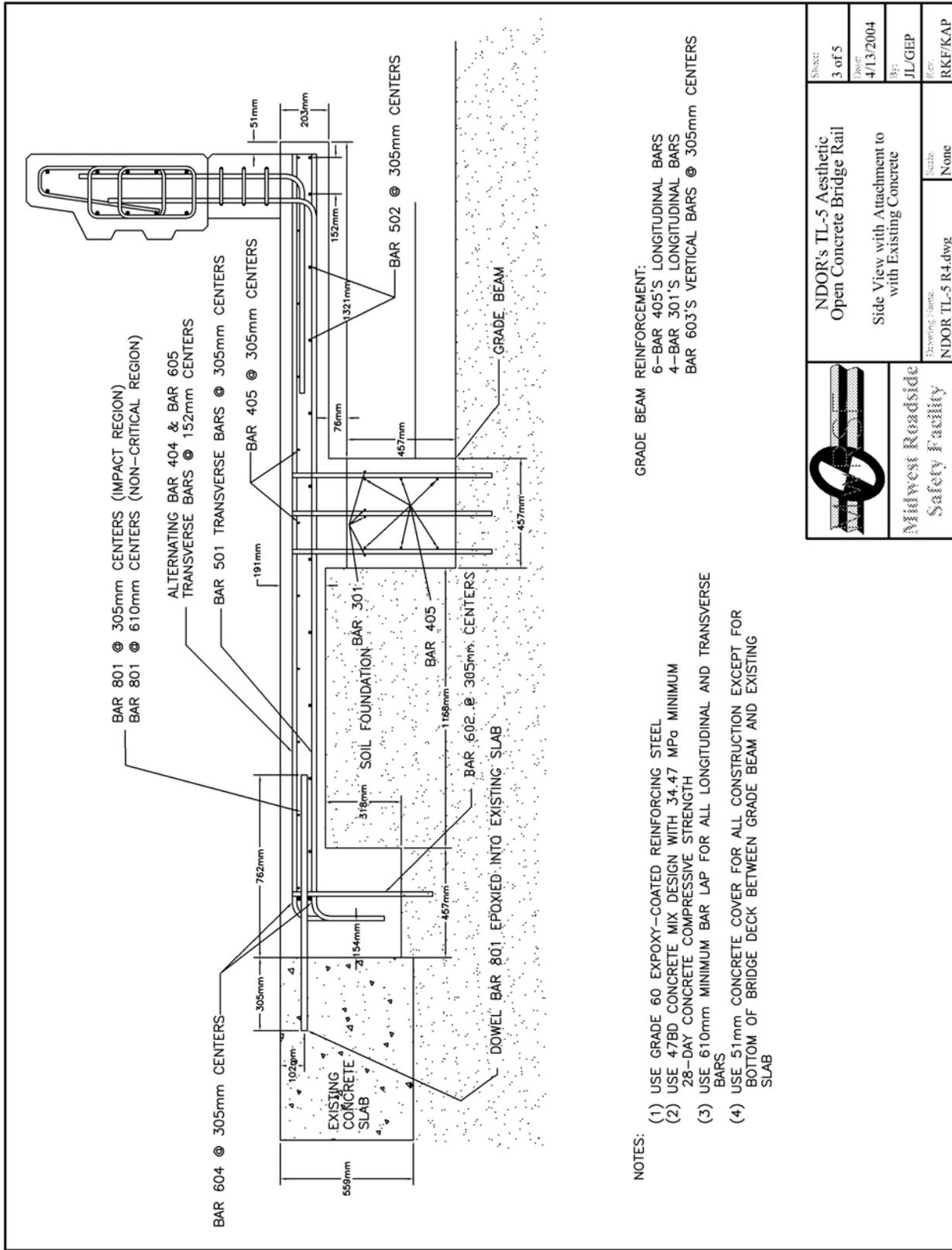
Figure 11. NDOR's TL-5 Aesthetic Open Concrete Bridge Rail Attachment to Existing Concrete Design Details
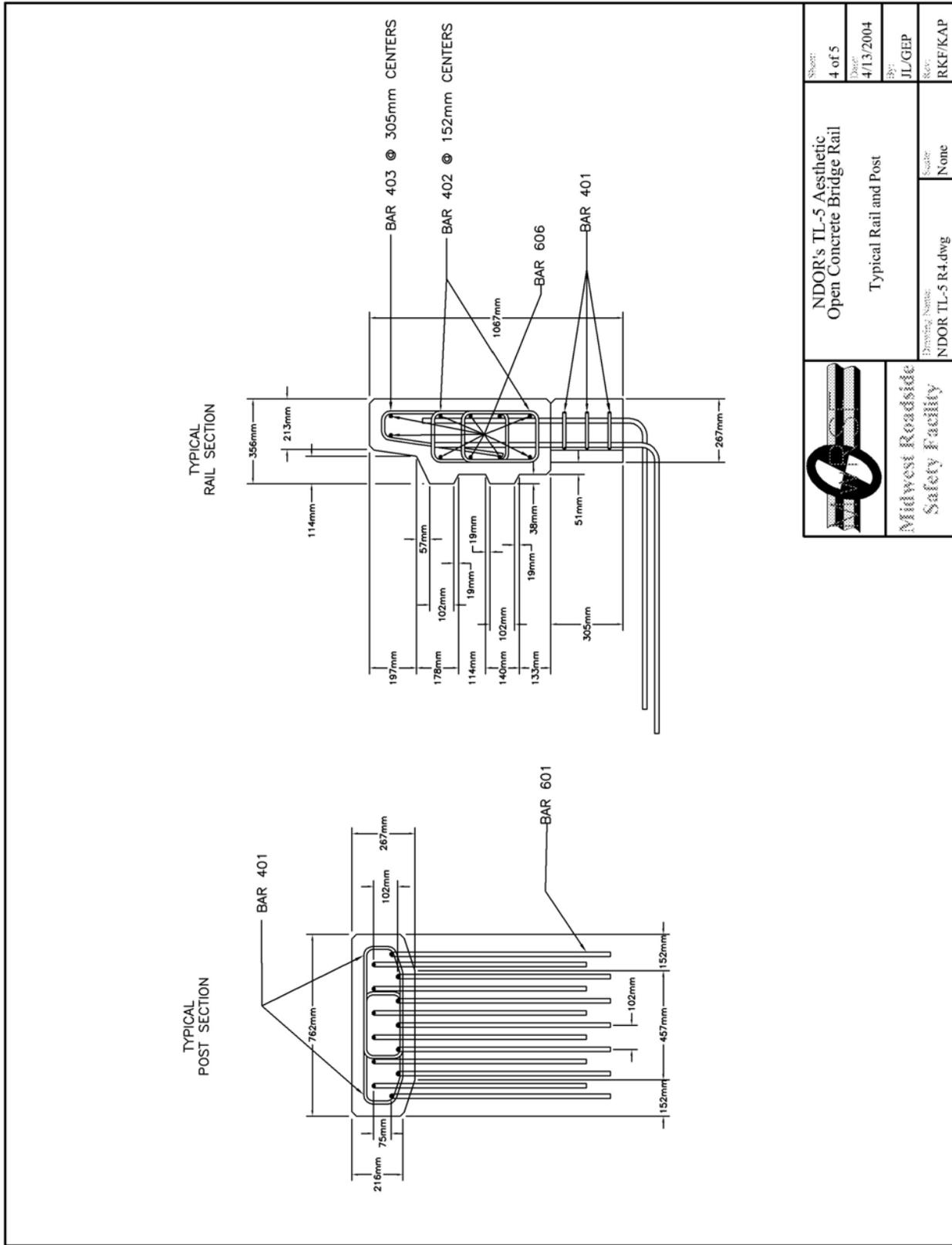
Figure 12. NDOR's TL-5 Aesthetic Open Concrete Bridge Rail Design Typical Rail and Post Details

Shape	Bar No.	Quantity	Length
301	3	27	6096mm
401	4	90	1441mm
402	4	486	1276mm
403	4	122	1143mm
404	4	122	3048mm
405	4	113	6096mm
501	5	122	3048mm
502	5	79	6096mm
601	6	195	2007mm
602	6	122	591mm
603	6	366	838mm
604	6	244	1016mm
605	6	122	3048mm
606	6	33	12192mm
801	8	85	1067mm

NOTES:
(1) ALL No. 4 BARS BENT WITH 51mm I.D.
(2) ALL No. 6 BARS BENT WITH 114mm I.D.
(3) ALL BARS GRADE 60 EPOXY COATED STEEL

Midwest Roadside Safety Facility

NDOR's TL-5 Aesthetic Open Concrete Bridge Rail

Bill of Bars

Drawing Name:	Scale:
NDOR TL-5 R4.dwg	None

| Sheet: 5 of 5 |
| Date: 4/13/2004 |
| By: JL/GEP |
| Rev: RKF/KAP |

801 — 1067mm

601 — 991mm, 991mm, 90°

603 — 838mm

602 — 591mm

604 — 686mm, 305mm

401 — 137mm, 82mm, 470mm, 108°, 76mm, 354mm, 165mm

402 — 74mm, 216mm, 324mm

403 — 123mm, 508mm, 82, 191mm, 480mm

Figure 13. NDOR's TL-5 Aesthetic Open Concrete Bridge Rail Design Reinforcement Details

Figure 14. Bridge Deck Rebar Reinforcement

Figure 15. Bridge Deck Construction

Figure 16. NDOR's TL-5 Aesthetic Open Concrete Bridge Rail Rebar Reinforcement
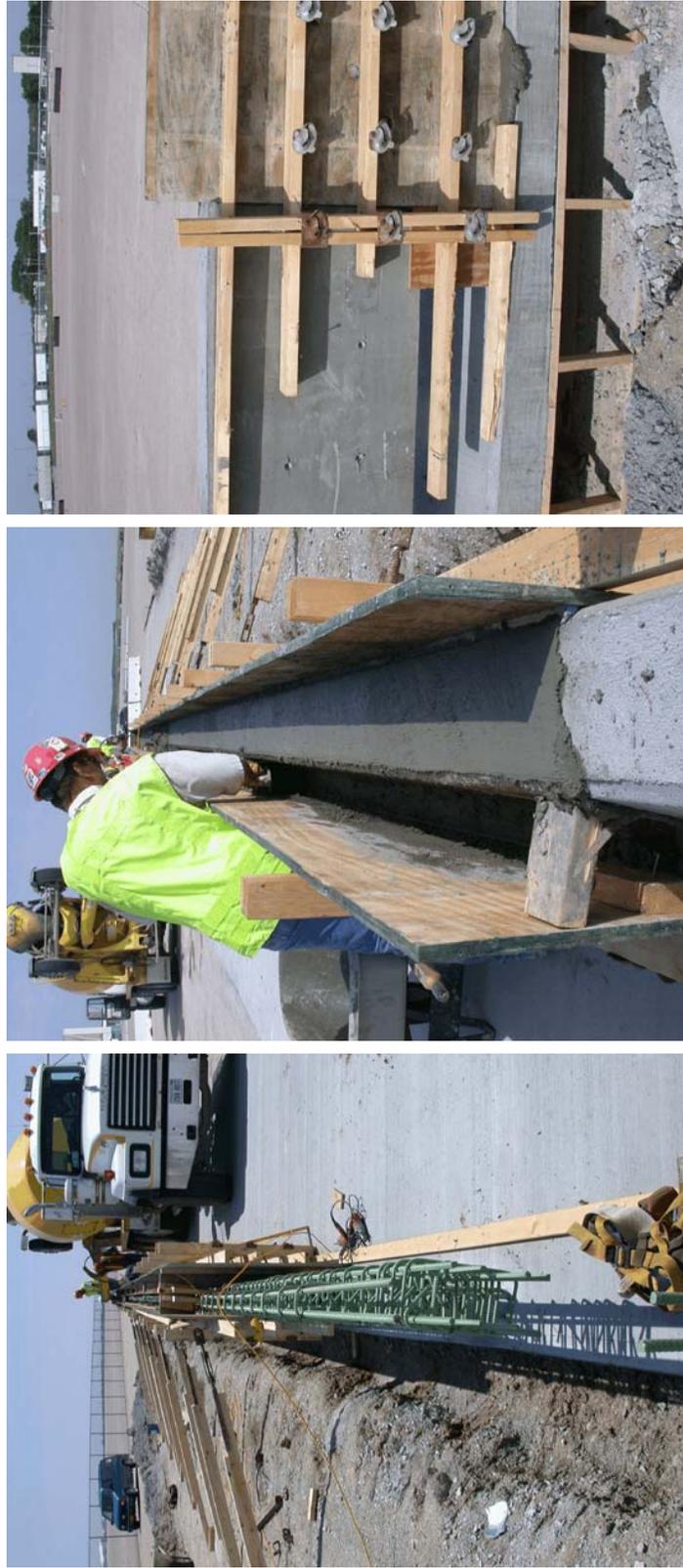
Figure 17. NDOR's TL-5 Aesthetic Open Concrete Bridge Rail Construction

Figure 18. NDOR's TL-5 Aesthetic Open Concrete Bridge Rail

Figure 19. NDOR's TL-5 Aesthetic Open Concrete Bridge Rail

8 TEST CONDITIONS

8.1 Test Facility

The testing facility is located at the Lincoln Air-Park on the northwest (NW) side of the Lincoln Municipal Airport and is approximately 8.0 km (5 mi.) NW of the University of Nebraska-Lincoln.

8.2 Vehicle Tow and Guidance System

A reverse cable tow system with a 1:2 mechanical advantage was used to propel the test vehicle. The distance traveled and the speed of the tow vehicle were one-half that of the test vehicle. The test vehicle was released from the tow cable before impact with the bridge rail system. A digital speedometer was located on the tow vehicle to increase the accuracy of the test vehicle impact speed.

A vehicle guidance system developed by Hinch (24) was used to steer the test vehicle. A guide-flag, attached to the front-right wheel and the guide cable, was sheared off before impact with the bridge rail system. The 9.5-mm (0.375-in.) diameter guide cable was tensioned to approximately 15.6 kN (3,500 lbf), and supported laterally and vertically every 30.48 m (100 ft) by hinged stanchions. The hinged stanchions stood upright while holding up the guide cable, but as the vehicle was towed down the line, the guide-flag struck and knocked each stanchion to the ground. For test ACBR-1, the vehicle guidance system was 929.6-m (3,050-ft) long.

8.3 Test Vehicles

For test ACBR-1, a 1989 GMC Brigadier T/S Tractor with a 1989 Great Dane Trailer was used as the test vehicle. The test inertial and gross static weights were 35,822 kg (78,975 lbs). The test vehicle is shown in Figure 20, and vehicle dimensions are shown in Figure 21.

Figure 20. Test Vehicle, Test ACBR-1

Date: 8/21/03   Test Number: ACBR-1

Tractor:
VIN No.: 4GTT9C4C3KV800398   Make: General Motors   Model: Brigadier
Year: 1989   Odometer: 754,596

Trailer:
VIN No.: 1GAA9623LB056236   Make: Great Dane   Model: Brigadier
Year: 1989
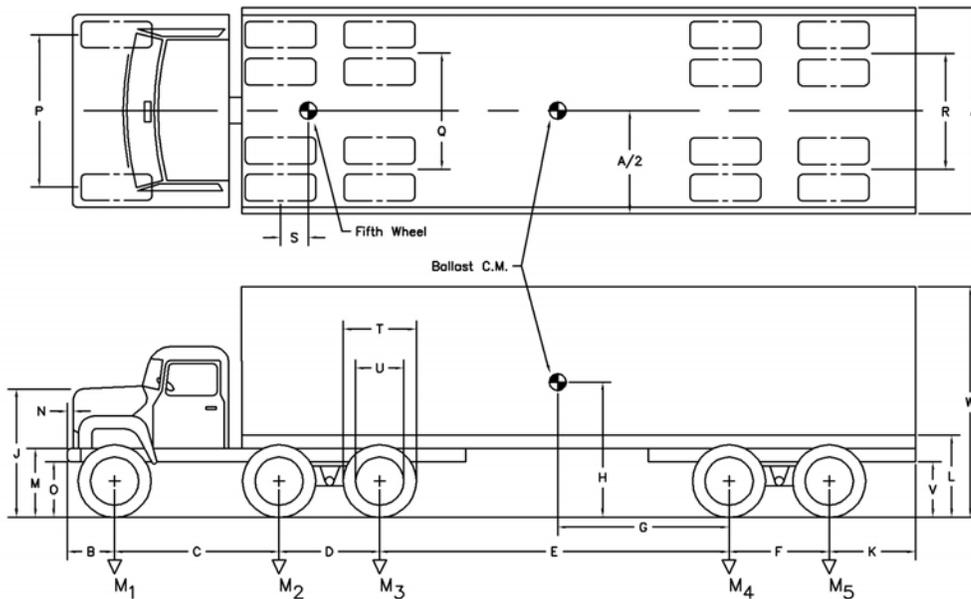
Vehicle Geometry — mm (in.)

A	2600 (102.375)	G	5525 (217.5)	N	83 (3.25)	T	1080 (42.5)
B	711 (28)	H	1854 (73)	O	556 (21.875)	U	648 (25.5)
C	3683 (145)	J	1797 (70.75)	P	2019 (79.5)	V	940 (37)
D	1302 (51.25)	K	927 (36.5)	Q	1822 (71.75)	W	4007 (157.75)
E	8331 (328)	L	1232 (48.5)	R	1965 (77.375)		
F	1245 (49)	M	984 (38.75)	S	610 (24)		

Mass — kg (lb.)	Curb	Test Inertial	Gross Static
M_1	3651 (8050)	3844 (8475)	3844 (8475)
M_2	3368 (7425)	8596 (18950)	8596 (18950)
M_3	2495 (5500)	8063 (17775)	8063 (17775)
M_4	2234 (4925)	7269 (16025)	7269 (16025)
M_5	2098 (4625)	8051 (17750)	8051 (17750)
M_T	13846 (30525)	35822 (78975)	35822 (78975)

Note any damage prior to test: Minor cosmetic, rusty tractor cab

Figure 21. Vehicle Dimensions, Test ACBR-1

57

The longitudinal component of the center of gravity was determined using the measured axle weights. The location of the final centers of gravity are shown in Figures 20 and 21. Vehicle ballast, consisting of steel panels, concrete barriers, and foam blocks, was used to obtain the desired test weight.

Square black and white-checkered targets were placed on the vehicle to aid in the analysis of the high-speed film and E/cam and Photron video, as shown in Figure 22. Checkered targets were placed on the center of gravity, on the driver's side door, on the passenger's side door, and on the roof of the vehicle. The remaining targets were located for reference so that they could be viewed from the high-speed cameras for film analysis.

The front wheels of the test vehicle were aligned for camber, caster, and toe-in values of zero so that the vehicle would track properly along the guide cable. Two 5B flash bulbs were mounted on both the hood and roof of the vehicle to pinpoint the time of impact with the bridge rail on the high-speed film, E/cam video, and Photron video. The flash bulbs were fired by a pressure tape switch mounted on the front face of the bumper. A remote-controlled brake system was installed in the test vehicle so the vehicle could be brought safely to a stop after the test.

8.4 Data Acquisition Systems

8.4.1 Accelerometers

One triaxial piezoresistive accelerometer system with a range of ±200 G's was used to measure the acceleration in the longitudinal, lateral, and vertical directions at a sample rate of 10,000 Hz. The environmental shock and vibration sensor/recorder system, Model EDR-4M6, was developed by Instrumented Sensor Technology (IST) of Okemos, Michigan and includes three differential channels as well as three single-ended channels. The EDR-4 was configured with 6 Mb

Figure 22. Vehicle Target Locations, Test ACBR-1

59

of RAM memory and a 1,500 Hz lowpass filter. Computer software, "DynaMax 1 (DM-1)" and "DADiSP", was used to analyze and plot the accelerometer data.

Another triaxial piezoresistive accelerometer system with a range of ±200 G's was also used to measure the acceleration in the longitudinal, lateral, and vertical directions at a sample rate of 3,200 Hz. The environmental shock and vibration sensor/recorder system, Model EDR-3, was developed by Instrumental Sensor Technology (IST) of Okemos, Michigan. The EDR-3 was configured with 256 Kb of RAM memory and a 1,120 Hz lowpass filter. Computer software, "DynaMax 1 (DM-1)" and "DADiSP", was used to analyze and plot the accelerometer data.

It should be noted that the EDR-4 unit was located just beneath the tractor's frame at the centerline of the rear tandems. In addition, the EDR-3 unit was located at the longitudinal center of gravity of the ballast on the trailer but below the trailer floor.

8.4.2 Rate Transducers

A Humphrey 3-axis rate transducer with a range of 360 degrees/sec in each of the three directions (pitch, roll, and yaw) was used to measure the rates of motion of the test vehicle. The rate transducer was rigidly attached to the vehicle near the center of gravity of the test vehicle. Rate transducer signals, excited by a 28-volt DC power source, were received through the three single-ended channels located externally on the EDR-4M6 and stored in the internal memory. The raw data measurements were then downloaded for analysis and plotted. Computer software, "DynaMax 1 (DM-1)" and "DADiSP", was used to analyze and plot the rate transducer data.

8.4.3 High-Speed Photography

For test ACBR-1, three high-speed 16-mm Red Lake Locam cameras, with operating speeds of approximately 500 frames/sec, were used to film the crash test. One Photron high-speed video

camera and five high-speed Red Lake E/cam video cameras, all with operating speeds of 500 frames/sec, were also used to film the crash test. Six Canon digital video cameras, with a standard operating speed of 29.97 frames/sec, were also used to film the crash test. A Locam (with a wide-angle 12.5-mm lens), a high-speed Photron video camera (with a 12.5-mm lens), and three Canon digital video camera were placed above the test installation to provide a field of view perpendicular to the ground. A Locam, a Canon digital video camera, and a Nikon F5 35-mm camera were placed downstream from the impact point and had a field of view parallel to the barrier. A high-speed E/cam video camera was placed downstream from the impact point and behind the barrier. A Locam, a high-speed E/cam video camera, and a Canon digital video camera were placed upstream from the impact point and had a field of view parallel to the barrier. A high-speed E/cam video camera was placed upstream from the point of impact and behind the barrier and focused on post no. 3 of the system. Another high-speed E/cam video camera was placed downstream from the point of impact and behind the barrier and focused on post no. 4 of the system. Another high-speed E/cam video camera was placed downstream from the point of impact and behind the barrier and focused on post no. 5 of the system. A Canon digital video camera was placed on the traffic side of the barrier and had a field of view perpendicular to the barrier. A schematic of all sixteen camera locations for test ACBR-1 is shown in Figure 23. The Locam films, Photron video, and E/cam videos were analyzed using the Vanguard Motion Analyzer, ImageExpress MotionPlus software, and Redlake Motion Scope software, respectively. Actual camera speed and camera divergence factors were considered in the analysis of the high-speed film.

8.4.4 Pressure Tape Switches

For test ACBR-1, five pressure-activated tape switches, spaced at 2-m (6.56-ft) intervals,

were used to determine the speed of the vehicle before impact. Each tape switch fired a strobe light which sent an electronic timing signal to the data acquisition system as the right-front tire of the test vehicle passed over it. Test vehicle speed was determined from electronic timing mark data recorded using the "Test Point" software. Strobe lights and high-speed film analysis are used only as a backup in the event that vehicle speed cannot be determined from the electronic data.
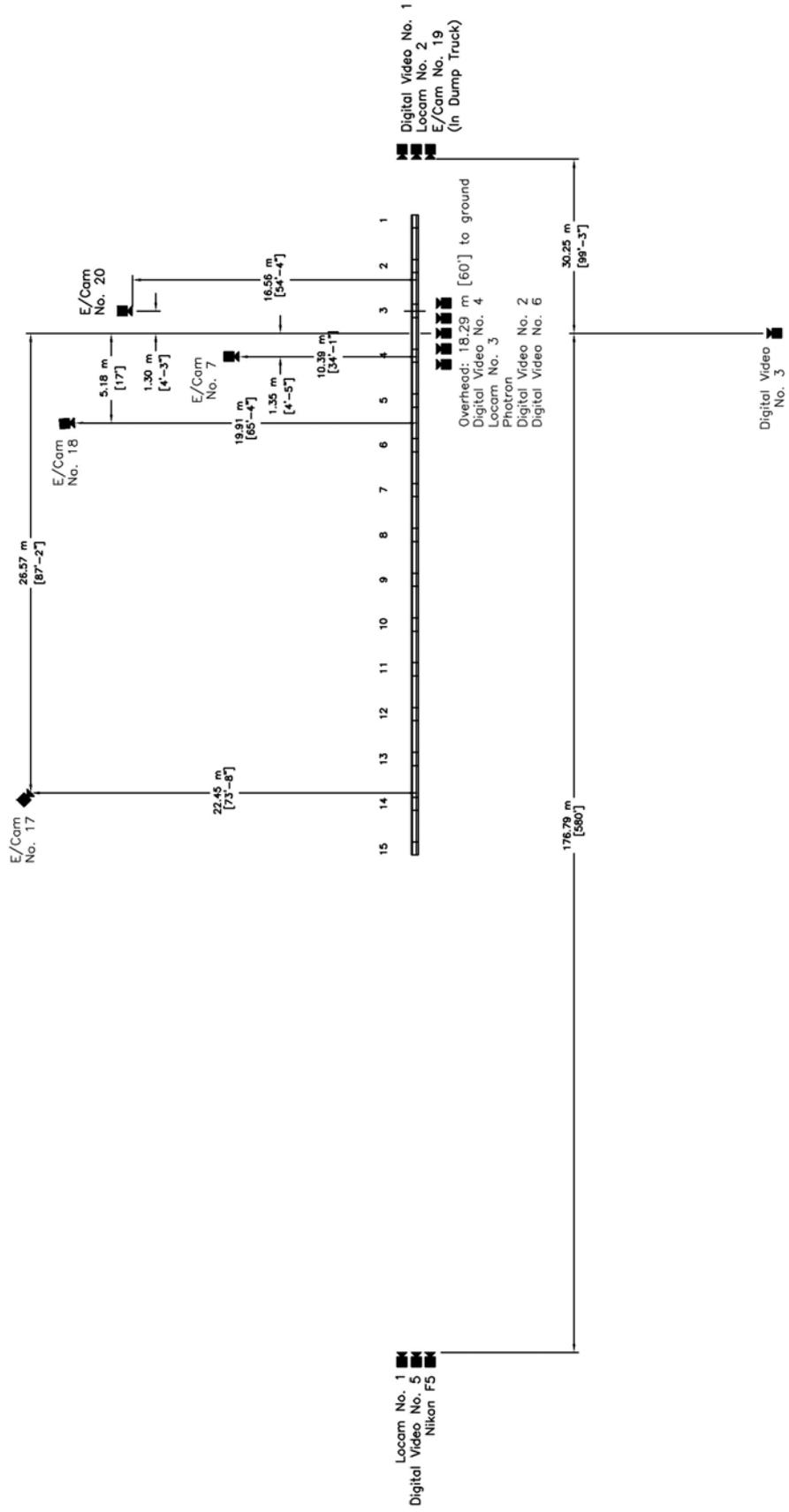
Figure 23. Location of High-Speed Cameras, Test ACBR-1

9 CRASH TEST NO. 1

9.1 Test ACBR-1

The 35,822-kg (78,975-lb) tractor-trailer unit impacted the open concrete bridge rail at a speed of 79.6 km/h (49.4 mph) and at an angle of 16.3 degrees. A summary of the test results and sequential photographs are shown in Figure 24. The summary of the test results and sequential photographs in English units are shown in Appendix B. Additional sequential photographs are shown in Figures 25 through 29. Documentary photographs of the crash test are shown in Figures 30 and 31.

9.2 Test Description

Initial vehicle impact occurred at the midspan between post nos. 3 and 4, as shown in Figure 32. Shortly after impact, the right-front corner of the right-front fender impacted the bridge rail slightly downstream of the midspan between post nos. 3 and 4. At 0.018 sec after impact the tractor's right-front fender crushed inward and upward and mounted the top of the barrier. At 0.056 sec, the tractor's left-front wheel rotated inward toward the engine as the tractor rolled clockwise (CW). At 0.070 sec, the right-front fender mounted the bridge rail completely as the right-front corner of the hood impacted the bridge rail and damaged the concrete. At this same time, the tractor began to redirect, and the trailer continued along the line of impact. At 0.090 sec, the tractor rolled counter-clockwise (CCW) toward the bridge rail. At this same time, the right-front corner of the fender intruded over the back edge of the bridge rail, and the concrete sustained extensive damage. At 0.138 sec, the right-front corner of the hood intruded over the back edge of the bridge rail and damage to the top of the concrete bridge rail continued. At this same time, the left edge of the hood near the windshield began to tear. At 0.160 sec, the tractor continued to roll CCW toward the rail

64

with the right-side exhaust pipe in contact with the bridge rail. At 0.172 sec, the right-front corner of the trailer impacted the bridge rail near the original impact point and caused more extensive concrete damage. At this same time, the tractor yawed CW, and the roof hatch jarred open. At 0.206 sec, the tractor continued to yaw CW and the trailer, which remained in contact with the bridge rail, rolled slightly CW toward the barrier. At this same time, the center of the hood was positioned near the front edge of the bridge rail, the back portion of the hood continued to fracture near the windshield, and the gap between the left-side door and left-front fender increased. At 0.238 sec, the crack in the hood propagated toward the right side as the tractor continued to roll CW toward the bridge rail. At this same time, the deformed left-front tire assembly was airborne. At 0.260 sec, the right-front corner of the trailer intruded over the back-side edge of the bridge rail. At this same time, the CW roll of the tractor increased. At 0.290 sec, the tractor appeared to be redirecting. At 0.356 sec, the right-rear corner of the tractor contacted the bridge rail. At this same time, the extent of intrusion of the trailer's right-front corner increased. At 0.387 sec, the trailer pitched slightly toward the right-front corner. At 0.455 sec, the back edge of the tractor's hood pitched forward. At 0.483 sec, concrete damage increased due to trailer contact. At 0.495 sec, the front of the tractor pitched downward as the right-front fender disengaged from the tractor. At 0.519 sec, the right edge of the front grill disengaged. At 0.545 sec, the trailer exhibited significant CW roll toward the bridge rail with the left-rear tandems off the ground. At 0.627 sec, the trailer continued to roll CW toward the bridge rail, and the right-rear corner of the trailer began to intruded over the bridge rail. At 0.679 sec, the trailer's right-rear corner intruded over the back side of the bridge rail as the trailer experienced extensive CW roll. At 0.767 sec, a large area of concrete, slightly upstream of impact, began to crack as the trailer tire contacted that area. At 0.809 sec, this same large area of concrete

crumbled and disengaged from the rest of the bridge rail system. At 0.919 sec, the trailer experienced increased CW roll and the bridge rail experienced increased concrete damage as the trailer traveled along the system. At about 2 sec after impact, the vehicle lost all contact with the bridge rail and exited the system at an angle of approximately 5 degrees. The vehicle came to rest 125.25 m (410 ft - 11 in.) downstream from impact and 52.82 m (173 ft - 3 in.) laterally behind a line projected parallel to the traffic-side face of the open concrete bridge rail. The trajectory and final position of the tractor-trailer unit are shown in Figures 24 and 33.

9.3 Barrier Damage

Damage to the open concrete bridge rail was moderate, as shown in Figures 34 through 52. Barrier damage consisted of contact and gouge marks, concrete deck, post, and rail cracking, and spalling of the concrete. The length of vehicle contact along the concrete bridge rail was approximately 19 m (63 ft), which spanned from the upstream edge of post no. 3 through 305 mm (12 in.) downstream from the downstream edge of post no. 10.

Black contact marks were found on the bottom groove of the rail starting at 584 mm (23 in.) upstream from the upstream edge of post no. 4 through the upstream edge of post no. 5. Minor black marks were also found on the bottom edge of the rail's bottom groove between post nos. 5 and 6. Black contact marks were also found on the lower asperity of the rail beginning 381 mm (15 in.) downstream from the downstream edge of post no. 3 and continuing for 610 mm (24 in.) downstream. Black contact marks were also found on the lower asperity from the downstream edge of post no. 5 through 457 mm (18 in.) upstream from the upstream edge of post no. 8. Additional black contact marks were found on the lower asperity 940 mm (37 in.) downstream from the upstream edge of post no. 9 through 1,041 mm (41 in.) upstream from the upstream edge of post no. 11. Black contact marks were found on the middle groove from the center of post no. 4 through

66

midpoint between post nos. 5 and 6. From 203 mm (8 in.) downstream from the upstream edge of post no. 3 through post no. 8, black contact marks were found on the upper asperity. A 2,718-mm (107-in.) long black mark was also found on the upper asperity beginning 178 mm (7 in.) downstream from the downstream edge of post no. 9. A 610-mm (24-in.) long black mark was found on the top portion of the rail at the downstream edge of post no. 3. A 38-mm (1.5-in.) wide black mark was found on the center of the rail's top portion between post nos. 3 and 6. Rusty-yellow colored markings were found on the top of the rail from post no. 4 to post no. 6.

Damage to the rail also consisted of major cracking. One 1.6-mm (0.0625-in.) wide crack originated at the bottom edge of the bottom groove at 813 mm (32 in.) upstream of the upstream edge of post no. 3 and continued to the top edge of the top of the rail at the downstream edge of post no. 3. Another 1.6-mm (0.0625-in.) wide crack originated on the bottom edge of the bottom groove at 864 mm (34 in.) upstream of the upstream edge of post no. 6 and continued up to the top edge of the top of the rail near the upstream edge of post no. 6. A third 1.6-mm (0.0625-in.) wide crack originated at the bottom edge of the bottom groove at 406 mm (16 in.) downstream of the upstream edge of post no. 6 and propagated to the top edge of the rail's top portion near the upstream edge of post no. 7. A fourth 1.6-mm (0.0625-in.) wide crack originated at the bottom edge of the bottom groove at 457 mm (18 in.) upstream of the upstream edge of post no. 7 and continued to the top edge of the top of the rail at the downstream edge of post no. 7. A fifth 1.6-mm (0.0625-in.) wide crack originated at the bottom edge of the bottom groove at 610 mm (24 in.) downstream from the downstream edge of post no. 7 and propagated to the damage at the top edge of the rail at post no. 8. A final 1.6-mm (0.0625-in.) wide crack originated at the bottom edge of the bottom groove at 508 mm (20 in.) upstream of the upstream edge of post no. 8 and continued to the top edge of the top of

the rail at the center of post no. 8. Minor cracks were also found in the rail between post nos. 1 and 10.

A 76-mm by 76-mm (3-in. by 3-in.) piece of concrete was removed from the rail's bottom groove at 432-mm (17-in.) upstream from the upstream edge of post no. 7. Another piece of concrete, measuring 76 mm by 102 mm (3 in. by 4 in.), was removed from the rail's bottom groove at 1,168-mm (46-in.) upstream from the upstream edge of post no. 8. Concrete surface damage was found on the lower asperity between post nos. 3 and 6 and post nos. 9 and 11. The rail's lower asperity was completely removed between 381 mm (15 in.) and 610 mm (24 in.) upstream of the upstream edge of post no. 4 and also from 686 (27 in.) upstream from the upstream edge of post no. 5 through the center of post no. 5. Concrete surface damage, approximately 178-mm (7-in.) long, was found on the upper asperity beginning at the upstream edge of post no. 3. Concrete surface damage was found on the top edge of the upper asperity from post no. 7 to post no. 8. Concrete surface damage, 965-mm (38-in.) long, was found on the upper asperity beginning 762 mm (30 in.) upstream of the upstream edge of post no. 9. A major piece of concrete was removed from the top portion of the rail at post no. 3, as shown in Figures 34 and 36 through 42. The top portion of the rail encountered minor concrete surface damage from post no. 3 through the midspan between post nos. 7 and 8. The top portion of the rail also encountered major concrete damage at the midspan between post nos. 7 and 8, as shown in Figures 34, 37, 39, 41, and 43. Minor concrete damage was found on the rail's top portion from post no. 8 to post no. 9.

Damage to the deck consisted of cracking and concrete spalling at the posts, as shown in Figures 46 through 52. At post no. 1, a 406-mm (16-in.) long crack originated at the backside of the deck and propagated toward the center of the deck. At post no. 2, a 660-mm (26-in.) long crack originated at the back side of the deck and propagated toward the center of the deck. At both post

68

nos. 3 and 7, a 559-mm (22-in.) long crack originated at the backside of the deck and propagated toward the center of the deck. At post no. 4, a 635-mm (25-in.) long crack originated at the back side of the deck and propagated toward the center of the deck. At both post nos. 5 and 6, a 483-mm (19-in.) long crack originated at the back side of the deck and propagated toward the center of the deck. At post no. 8, a 305-mm (12-in.) long crack originated at the back side of the deck and propagated toward the center of the deck. Concrete spalling of the concrete bridge deck was found at post nos. 1 through 6, as shown in Figure 46 through 52. Detailed sketches of the concrete failure and cracking at post nos. 1 through 8 are shown in Appendix C.

The bridge rail encountered minor permanent set deflections, and minor dynamic deflections were also observed. The maximum dynamic lateral deflection, as determined from high-speed film analysis, was 285 mm (11.22 in.). The working width of the system was found to be 1,916 mm (75.43 in.).

9.4 Vehicle Damage

Exterior vehicle damage was moderate, as shown in Figures 53 through 57. Occupant compartment deformations were negligible, as shown in Figure 58. The left side of the floorboard opened up and the frame channel section was protruding into the occupant compartment, as shown in Figure 58. The hood was fractured and disengaged from the rest of the tractor. The front bumper disengaged from the lower-left connection on the long frame horn but remained attached at the upper-left connection. The front bumper also buckled around the right-side frame horn and at the left-side end. The left-side fiberglass fuel tank cover was creased and also fractured at its midpoint. The outer and front faces of the right-side fuel tank encountered heavy contact marks, the front face was also crushed inward approximately 305 mm (12 in.), and the inner-lower corner was torn open. The left-side fender disengaged at the lower-front connection and the fiberglass was fractured. The

69

right-side fender and lower fiberglass piece also disengaged. The right-side steel frame encountered major deformations at the front, especially near the bumper attachment, and the long steel frame member remained undamaged on the left-side. The lower-left side shock attachment and two of the three left-side leaf springs disengaged; however, the right-rear suspension, springs, and right side of the drive shaft remained undamaged. The bottom shock mount and the right-side axle disengaged. The inner left-side tie rod connection fractured at the ball joint. The side wall of the outer-left rear tandem tire encountered a 610-mm (24-in.) long slice, and the rim encountered a 406-mm (16-in.) long bend. The left-front tire only encountered scuff marks on the tire wall. Both right-rear tandem tires encountered heavy scuff marks on their sidewalls and major rim damage around their entire perimeters. The right-side front wheel assembly was deformed upward and backward into the engine compartment. The right-front wheel lug nuts were ground down and had concrete embedded in them. The right-front wheel's steel rim encountered a 203-mm (8-in.) long dent, and minor scuff marks were found on the tire's sidewall. All components above the bottom of the left- and right-side doors, above the front axle and frame, and under the hood along with the left-side fuel tank and battery box, as well as all window glass remained undamaged.

Scrape marks were found along the entire lower portion of the trailer's right side due to contact with the concrete bridge rail. The support frame was also deformed along the right side. The trailer's right-rear tandem wheels encountered significant steel rim damage and scuff marks on the tire's outer sidewalls. The trailer's left-rear tandem wheels remained undamaged.

9.5 Occupant Risk Values

Although not required and assuming the accelerometer recorder readings could privide some measure of occupant risk, the tractor's longitudinal and lateral occupant impact velocities were determined to be 0.91 m/sec (2.99 ft/sec) and 5.50 m/sec (18.05 ft/sec), respectively, at the locations

70

of the EDR-4 and EDR-3 boxes. Likewise, the trailer's longitudinal and lateral occupant impact velocities were determined to be 1.08 m/sec (3.55 ft/sec) and 2.32 m/sec (7.60 ft/sec), respectively. Similarly, the tractor's maximum 0.010-sec average occupant ridedown decelerations in the longitudinal and lateral directions were 8.05 g's/-6.98 g's and 6.06 g's/-7.91 g's, respectively. The trailer's maximum 0.010-sec average occupant ridedown decelerations in the longitudinal and lateral directions were 3.52 g's/-2.17 g's and 11.74 g's/-7.88 g's, respectively. Once again and although ot required, it is noted that the occupant impact velocities (OIV's) and occupant ridedown decelerations (ORD's) were within the suggested limits provided in NCHRP Report No. 350. The results of the occupant risk, determined from the accelerometer data, are summarized in Figure 24. Results are shown graphically in Appendix D.

9.6 Discussion

The analysis of the test results for test ACBR-1 showed that the aesthetic open concrete bridge rail adequately contained and redirected the vehicle with controlled lateral displacements of the bridge rail. There were no detached elements nor fragments which showed potential for penetrating the occupant compartment nor presented undue hazard to other traffic. Deformations of, or intrusion into, the occupant compartment that could have caused serious injury did not occur. The test vehicle did not penetrate nor ride over the bridge rail and remained upright during and after the collision. Vehicle roll, pitch, and yaw angular displacements were noted, but they were deemed acceptable because they did not adversely influence occupant risk safety criteria nor cause rollover. After collision, the vehicle's trajectory did not intrude into adjacent traffic lanes. In addition, the vehicle's exit angle was less than 60 percent of the impact angle. Therefore, test ACBR-1 conducted on the open concrete bridge rail was determined to be acceptable according to the TL-5 safety performance criteria found in NCHRP Report No. 350.
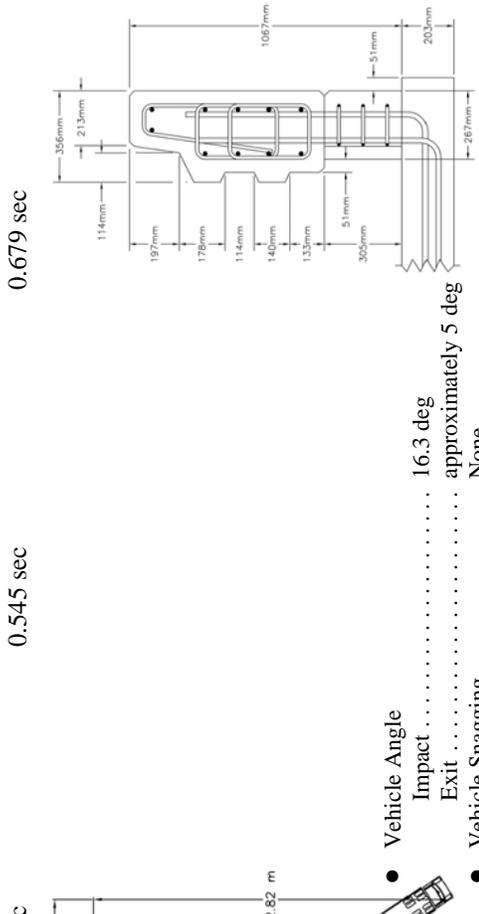
| 0.000 sec | 0.138 sec | 0.238 sec | 0.545 sec | 0.679 sec |

- Test Number ACBR-1
- Date 8/28/03
- Appurtenance . . . . Nebraska Aesthetic Open
  Concrete Bridge Rail
- Total Length . . . . 37.03 m
- Concrete Material . . . . Nebraska 47-BD Mix
- Reinforcing Steel Material . . . . Grade 60 Rebar - Epoxy Coated
- Concrete Bridge Rail
    Length . . . . 37.03 m
    Width . . . . 356 mm
    Depth . . . . 762 mm
    Top Mounting Height . . . . 1,067 mm
- Concrete Bridge Posts
    Length . . . . 762 mm
    Width . . . . 267 mm
    Height . . . . 305 mm
    Spacing . . . . 2,591 mm
    Offset from Back Edge of Deck . . . . . 51 mm
- Concrete Bridge Deck
    Length . . . . 37.03 m
    Width . . . . 3,403 mm
    Thickness . . . . 203 mm
- Vehicle Model . . . . 1989 General Motors Brigadier Tractor
  1989 Great Dane Brigadier Trailer
    Curb . . . . 13,846 kg
    Test Inertial . . . . 35,822 kg
    Gross Static . . . . 35,822 kg
- Vehicle Speed
    Impact . . . . 79.6 km/h
    Exit . . . . NA

- Vehicle Angle
    Impact . . . . 16.3 deg
    Exit . . . . approximately 5 deg
- Vehicle Snagging . . . . None
- Vehicle Pocketing . . . . None
- Vehicle Stability . . . . Satisfactory
- Occupant Ridedown Deceleration (10 msec avg.) – Tractor
    Longitudinal (not required) . . . 8.05/-6.98 g's < 20 g's
    Lateral (not required) . . . . 6.06/-7.91 g's
- Occupant Impact Velocity – Tractor
    Longitudinal (not required) . . . 0.91 m/s < 12 m/s
    Lateral (not required) . . . . 5.50 m/s
- Occupant Ridedown Deceleration (10 msec avg.) – Trailer
    Longitudinal (not required) . . . 3.52/-2.17 g's < 20 g's
    Lateral (not required) . . . . 11.74/-7.88 g's
- Occupant Impact Velocity – Trailer
    Longitudinal (not required) . . . 1.08 m/s < 12 m/s
    Lateral (not required) . . . . 2.32 m/s
- Vehicle Damage . . . . Moderate
    TAD[25] . . . . 1-RFQ-3 and 1-RD-3
    SAE[26] . . . . 1-FREN3 and 1-RDES2
- Vehicle Stopping Distance . . . . 125.25 m downstream
  52.82 m laterally behind
- Barrier Damage . . . . Moderate
- Maximum Rail Deflections
    Permanent Set . . . . NA
    Dynamic . . . . 285 mm
- Working Width . . . . 1,916 mm

Figure 24. Summary of Test Results and Sequential Photographs, Test ACBR-1

0.000 sec

0.311 sec

0.050 sec

0.373 sec

0.110 sec

0.475 sec

0.207 sec

0.539 sec

Figure 25. Additional Sequential Photographs, Test ACBR-1

0.000 sec	0.288 sec
0.050 sec	0.355 sec
0.076 sec	0.435 sec
0.146 sec	0.775 sec
0.198 sec	0.877 sec

Figure 26. Additional Sequential Photographs, Test ACBR-1

0.000 sec

0.000 sec

0.082 sec

0.133 sec

0.124 sec

0.300 sec

0.160 sec
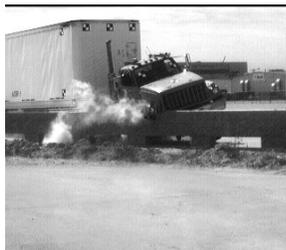
0.467 sec

0.186 sec

0.534 sec

Figure 27. Additional Sequential Photographs, Test ACBR-1

75

0.000 sec

0.133 sec

0.234 sec

0.334 sec

0.434 sec
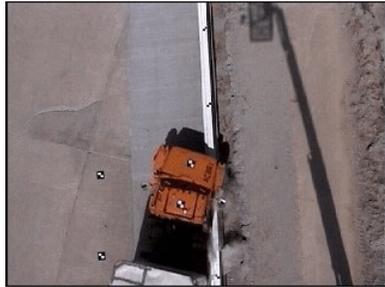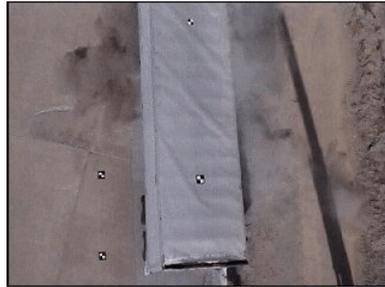
0.868 sec

1.001 sec

1.235 sec

Figure 28. Additional Sequential Photographs, Test ACBR-1

0.000 sec

1.001 sec

0.234 sec

1.401 sec

0.367 sec

1.768 sec

0.534 sec

2.169 sec

0.801 sec

Figure 29. Additional Sequential Photographs, Test ACBR-1

Figure 30. Documentary Photographs, Test ACBR-1

Figure 31. Documentary Photographs, Test ACBR-1
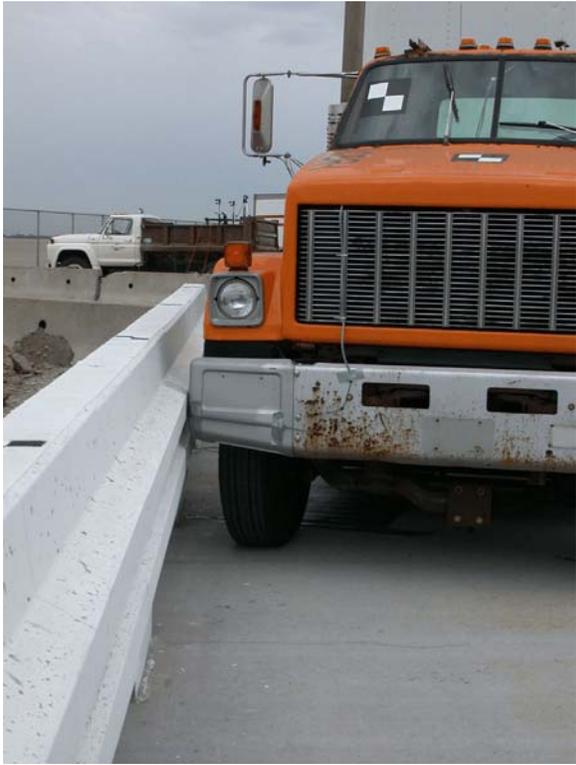
Figure 32. Impact Location, Test ACBR-1

Figure 33. Vehicle Final Position and Trajectory Marks, Test ACBR-1

Figure 34. Bridge Rail Damage, Test ACBR-1

Figure 35. Bridge Rail Damage, Test ACBR-1

Figure 36. Bridge Rail Damage, Test ACBR-1

Figure 37. Bridge Rail Damage, Test ACBR-1

Figure 38. Traffic-Side Bridge Rail Damage at Spans Between Post Nos. 1 through 5, Test ACBR-1

Figure 39. Traffic-Side Bridge Rail Damage at Spans Between Post Nos. 5 through 8, Test ACBR-1

Figure 40. Back-Side Bridge Rail Damage at Spans Between Post Nos. 1 through 5, Test ACBR-1

Figure 41. Back-Side Bridge Rail Damage at Spans Between Post Nos. 5 through 8, Test ACBR-1

89

Figure 42. Traffic-Side Bridge Rail Damage at Post Nos. 1 through 4, Test ACBR-1

Figure 43. Traffic-Side Bridge Rail Damage at Post Nos. 5 through 8, Test ACBR-1

Figure 44. Traffic-Side Bridge Rail Damage at Post Nos. 9 through 12, Test ACBR-1

Figure 45. Traffic-Side Bridge Rail Damage at Post Nos. 13 through 15, Test ACBR-1

Figure 46. Back-Side Bridge Rail and Deck Damage at Post Nos. 1 through 3, Test ACBR-1

Figure 47. Back-Side Bridge Rail and Deck Damage at Post Nos. 4 through 6, Test ACBR-1

Figure 48. Back-Side Bridge Rail and Deck Damage at Post Nos. 7 through 9, Test ACBR-1

Figure 49. Bridge Post Nos. 1 and 2 Damage, Test ACBR-1

Figure 50. Bridge Post Nos. 3 and 4 Damage, Test ACBR-1

Figure 51. Bridge Post Nos. 5 and 6 Damage, Test ACBR-1

Figure 52. Bridge Post No. 7 Damage, Test ACBR-1

Figure 53. Vehicle Damage, Test ACBR-1
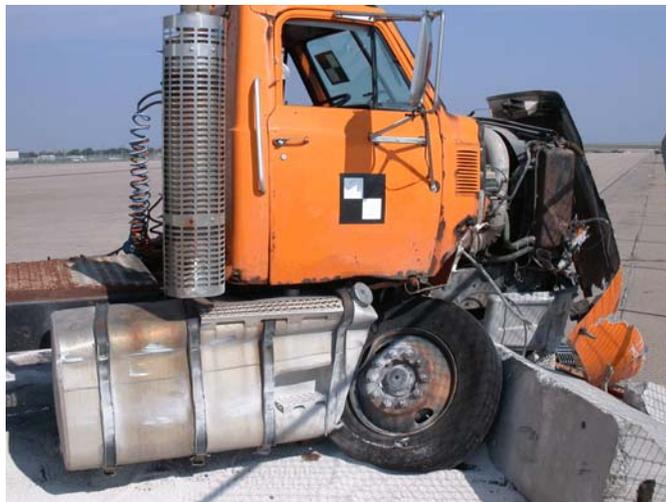
Figure 54. Vehicle Damage, Test ACBR-1

Figure 55. Vehicle Damage, Test ACBR-1

Figure 56. Vehicle Damage, Test ACBR-1
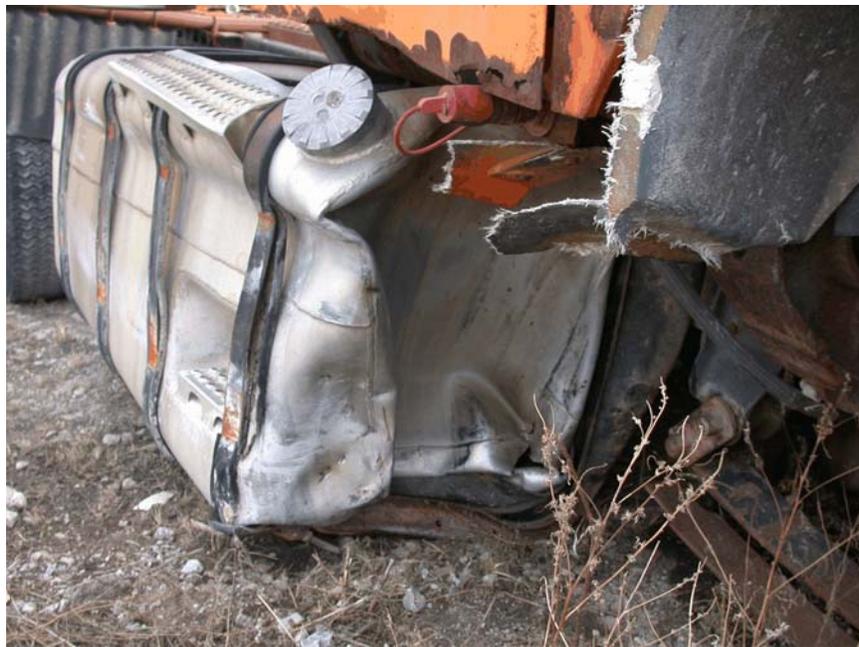
Figure 57. Vehicle Damage, Test ACBR-1

Figure 58. Occupant Compartment Damage, Test ACBR-1

10 SUMMARY AND CONCLUSIONS

An aesthetic, open concrete bridge rail was developed, constructed, and full-scale vehicle crash tested. One full-scale vehicle crash test, using a tractor-trailer vehicle, was performed on the bridge railing system and was determined to be acceptable according to the TL-5 safety performance criteria presented in NCHRP Report No. 350. The bridge railing safely redirected the tractor-trailer vehicle with moderate barrier deflections. A summary of the safety performance evaluation is provided in Table 3.

Table 10. Summary of Safety Performance Evaluation Results

Evaluation Factors	Evaluation Criteria		Test ACBR-1
Occupant Risk	A.	Test article should contain and redirect the vehicle; the vehicle should not penetrate, underride, or override the installation although controlled lateral deflections of the test article is acceptable.	S
	D.	Detached elements, fragments or other debris from the test article should not penetrate or show potential for penetrating the occupant compartment, or present an undue hazard to other traffic, pedestrians, or personnel in a work zone. Deformations of, or intrusions into, the occupant compartment that could cause serious injuries should not be permitted.	S
	G.	It is preferable, although not essential, that the vehicle remain upright during and after collision.	S
Vehicle Trajectory	K.	After collision it is preferable that the vehicle's trajectory not intrude into adjacent traffic lanes.	S
	M.	The exit angle from the test article preferably should be less than 60 percent of test impact angle measured at time of vehicle loss of contact with test device.	S

S - Satisfactory
M - Marginal
U - Unsatisfactory
NA - Not Available

11 RECOMMENDATIONS

An open concrete bridge rail, as described in this report, was developed and successfully crash tested according to the TL-5 criteria found in NCHRP Report No. 350. The results of this test indicate that this design is a suitable design for use on Federal-aid highways. However, any design modifications made to the bridge railing system can only be verified through the use of full-scale crash testing.

12 REFERENCES

1. Ross, H.E., Sicking, D.L., Zimmer, R.A., and Michie, J.D., *Recommended Procedures for the Safety Performance Evaluation of Highway Features*, National Cooperative Research Program (NCHRP) Report No. 350, Transportation Research Board, Washington, D.C., 1993.

2. Mak, K.K., and Campise, W.L., *Test and Evaluation of Ontario "Tall Wall" Barrier with an 80,000-Pound Tractor-Trailer*, Project No. RF 71620, Performed for the Ontario Ministry of Transportation, Performed by Texas Transportation Institute, Texas A&M Research Foundation, College Station, Texas, September 1990, [Test no. 7162-1].

3. Campise, W.L., and Buth, C.E., *Performance Limits of Longitudinal Barrier Systems - Volume III - Appendix B - Details of Full-Scale Crash Tests on Longitudinal Barriers*, Final Report, Performed for the Office of Research, Federal Highway Administration, Performed by the Texas Transportation Institute, Texas A&M University System, College Station, Texas, May 1985, [Test no. 4798-13].

4. Beason, W.L., Hirsch, T.J., and Campise, W.L., *Measurement of Heavy Vehicle Impact Forces and Inertia Properties*, Report No. FHWA-RD-89-120, Performed for the Office of Safety and Traffic Operations R&D, Federal Highway Administration, Performed by the Texas Transportation Institute, Texas A&M University, College Station, Texas, May 1989, [Test nos. 7046-3, 7046-4, and 7046-9].

5. Hirsch, T.J., and Fairbanks, W.L., *Bridge Rail to Contain and Redirect 80,000-lb Tank Trucks*, Transportation Research Record No. 1024, Transportation Research Board, National Research Council, Washington, D.C., 1985, [Test no. 1].

6. Hirsch, T.J., and Fairbanks, W.L., *Bridge Rail to Restrain and Redirect 80,000 LB Tank Trucks*, Report No. FHWA/TX-84/911-1F, Performed for the Texas State Department of Highways and Public Transportation, Performed by the Texas Transportation Institute, Texas A&M University System, College Station, Texas, January 1984, [Test no. 1].

7. Hirsch, T.J., Fairbanks, W.L., and Buth, C.E., *Concrete Safety Shape with Metal Rail on Top to Redirect 80,000-lb Trucks*, Transportation Research Record No. 1065, Transportation Research Board, National Research Council, Washington, D.C., 1986, [Test no. 2416-1].

8. Menges, W.L., Buth, C.E., Bullard, D.L., Jr., and McDevitt, C.F., *Performance Level 3 Bridge Railings*, Transportation Research Record No. 1500, Transportation Research Board, National Research Council, Washington, D.C., July 1995, [Test nos. 7069-13 and 7069-10].

9. Buth, C.E., Hirsch, T.J., and Menges, W.L., *Testing of New Bridge Rail and Transition Designs - Volume I: Technical Report*, Report No. FHWA-RD-93-058, Performed for the Office of Safety and Traffic Operations R&D, Federal Highway Administration, Performed

by the Texas Transportation Institute, Texas A&M University System, College Station, Texas, June 1997, [Test nos. 7069-13 and 7069-10].

10. Hirsch, T.J., and Arnold, A., *Bridge Rail to Restrain and Redirect 80,000-lb Trucks*, Transportation Research Record No. 942, Transportation Research Board, National Research Council, Washington, D.C., 1983, [Test no. 6].

11. Alberson, D.C., Zimmer, R.A., and Menges, W.L., *NCHRP Report 350 Compliance Test 5-12 of the 1.07-m Vertical Wall Bridge Railing*, Report No. FHWA-RD-96-199, Performed for the Office of Safety and Traffic Operations R&D, Federal Highway Administration, Performed by the Texas Transportation Institute, Texas A&M University System, College Station, Texas, January 1997, [Test nos. 405511-2].

12. Hirsch, T.J., *Analytical Evaluation of Texas Bridge Rails to Contain Buses and Trucks*, Report No. FHWA TX 78-230-2, Performed for the Texas State Department of Highways and Public Transportation, Performed by Texas Transportation Institute, Texas A&M University, College Station, Texas, August 1978.

13. *AASHTO LRFD Bridge Design Specifications - U.S. Units - 2003 Interim Revisions*, American Association of State Highway and Transportation Officials (AASHTO), Washington, D.C., April 2003.

14. *Roadside Design Guide*, 2002 Edition, American Association of State Highway and Transportation Officials (AASHTO), Washington, D.C., 2002.

15. Wang, C.K., and Salmon, C.G., *Reinforced Concrete Design*, Fourth Edition, Harper & Row, Publishers, New York, 1985.

16. MacGregor, J.G., *Reinforced Concrete Mechanics and Design*, Third Edition, Prentice Hall, Publishers, New Jersey, 1997.

17. *Guide Specifications for Bridge Railings*, American Association of State Highway and Transportation Officials (AASHTO), Washington, D.C., 1989.

18. Stout, D. and Hinch, J., *Test and Evaluation of Traffic Barriers: Final Report - Technical*, Report No. FHWA-RD-89-119, Submitted to the Office of Safety and Traffic Operations R & D, Federal Highway Administration, Performed by ENSCO, Inc., Springfield, VA, April 1989.

19. Michie, J.D., *Recommended Procedures for the Safety Performance Evaluation of Highway Appurtenances*, National Cooperative Highway Research Program (NCHRP) Report No. 230, Transportation Research Board, Washington, D.C., March 1981.

20. Holloway, J.C., Faller, R.K., Wolford, D.F., Dye, D.L., and Sicking, D.L., *Performance Level 2 Tests on a 29-in. Open Concrete Bridge Rail*, Final Report to the Midwest States' Regional Pooled Fund Program, Transportation Research Report No. TRP-03-51-95, Project No. SPR-03(017)-Fiscal Year 1994, Midwest Roadside Safety Facility, University of Nebraska-Lincoln, Lincoln, NE, June 1996.

21. Holloway, J.C., Sicking, D.L., and Faller, R.K., *A Reduced Height Performance Level 2 Bridge Rail*, Transportation Research Record No. 1528, Transportation Research Board, National Research Council, Washington, D.C., 1996.

22. Faller, R.K., Holloway, J.C., Pfiefer, B.G., and Rosson, B.T., *Performance Level 1 Tests on the Nebraska Open Concrete Bridge Rail*, Final Report to the Nebraska Department of Roads, Transportation Research Report No. TRP-03-28-91, Midwest Roadside Safety Facility, University of Nebraska-Lincoln, Lincoln, NE, February 1992.

23. Polivka, K.A., Faller, R.K., Rohde, J.R., Reid, J.D., Sicking, D.L., and Holloway, J.C., *Safety Performance Evaluation of the Nebraska Open Concrete Bridge Rail on an Inverted Tee Bridge Deck*, Final Report to the Nebraska Department of Roads, Transportation Research Report No. TRP-03-133-04, Midwest Roadside Safety Facility, University of Nebraska-Lincoln, January 21, 2004.

24. Hinch, J., Yang, T.L., and Owings, R., *Guidance Systems for Vehicle Testing*, ENSCO, Inc., Springfield, VA, 1986.

25. *Vehicle Damage Scale for Traffic Investigators*, Second Edition, Technical Bulletin No. 1, Traffic Accident Data (TAD) Project, National Safety Council, Chicago, Illinois, 1971.

26. *Collision Deformation Classification - Recommended Practice J224 March 1980*, Handbook Volume 4, Society of Automotive Engineers (SAE), Warrendale, Pennsylvania, 1985.

13 APPENDICES

APPENDIX A

English-Unit System Drawings

Figure A-1. Layout for NDOR's TL-5 Aesthetic Open Concrete Bridge Rail (English)

Figure A-2. NDOR's TL-5 Aesthetic Open Concrete Bridge Rail Design Details (English)

Figure A-3. NDOR's TL-5 Aesthetic Open Concrete Bridge Rail Attachment to Existing Concrete Design Details (English)

Figure A-4. NDOR's TL-5 Aesthetic Open Concrete Bridge Rail Design Typical Rail and Post Details (English)

Figure A-5. NDOR's TL-5 Aesthetic Open Concrete Bridge Rail Design Reinforcement Details (English)

NOTES:
(1) No. 8 BARS @ 24" CENTERS FOR 0 to 12'-6" AND 43'-6" to 119'-6" FROM THE RIGHT
(2) No. 8 BARS @ 12" CENTERS FOR 12'-6" to 43'-6", 119'-6" to 121'-6", AND BARS LONGITUDINAL TO BRIDGE DECK ON SOUTH END

1	2	3	4	5	6	7	8	9	10	11	12	13	14	15

SPAN C_L (IMPACT LOCATION)

8'-6" (Typical)

121'-6"

Midwest Roadside Safety Facility

NDOR's TL-5 Aesthetic Open Concrete Bridge Rail

Plan View

Drawing Name: NDOR TL-5 R4.dwg	Scale: None
Sheet:	1 of 5
Date:	4/13/2004
By:	JL/GEP
Dwg:	RKF/KAP

Figure A-1. Layout for NDOR's TL-5 Aesthetic Open Concrete Bridge Rail (English)

115

Figure A-2. NDOR's TL-5 Aesthetic Open Concrete Bridge Rail Design Details (English)

Figure A-3. NDOR's TL-5 Aesthetic Open Concrete Bridge Rail Attachment to Existing Concrete Design Details (English)

BAR 604 @ 12" CENTERS

BAR 801 @ 12" CENTERS (IMPACT REGION)
BAR 801 @ 24" CENTERS (NON-CRITICAL REGION)

ALTERNATING BAR 404 & BAR 605
TRANSVERSE BARS @ 6" CENTERS

BAR 501 TRANSVERSE BARS @ 12" CENTERS

BAR 405 @ 12" CENTERS

BAR 502 @ 12" CENTERS

GRADE BEAM

DOWEL BAR 801 EPOXIED INTO EXISTING SLAB

BAR 602 @ 12" CENTERS

BAR 405

SOIL FOUNDATION BAR 301

EXISTING CONCRETE SLAB

GRADE BEAM REINFORCEMENT:
6—BAR 405'S LONGITUDINAL BARS
4—BAR 301'S LONGITUDINAL BARS
BAR 603'S VERTICAL BARS @ 12" CENTERS

NOTES:
(1) USE GRADE 60 EXPOXY—COATED REINFORCING STEEL
(2) USE 47BD CONCRETE MIX DESIGN WITH 5,000 PSI MINIMUM 28—DAY CONCRETE COMPRESSIVE STRENGTH
(3) USE 24" MINIMUM BAR LAP FOR ALL LONGITUDINAL AND TRANSVERSE BARS
(4) USE 2" CONCRETE COVER FOR ALL CONSTRUCTION EXCEPT FOR BOTTOM OF BRIDGE DECK BETWEEN GRADE BEAM AND EXISTING SLAB

Midwest Roadside Safety Facility

NDOR's TL-5 Aesthetic Open Concrete Bridge Rail

Side View with Attachment to with Existing Concrete

Sheet:	3 of 5
Date:	4/13/2004
By:	JL/GEP
Rev:	RKF/KAP

Drawing Name: NDOR TL-5 R4.dwg
Scale: None

Figure A-4. NDOR's TL-5 Aesthetic Open Concrete Bridge Rail Design Typical Rail and Post Details (English)

Shape	Bar No.	Quantity	Length
301	3	27	20'
401	4	90	56¾"
402	4	486	50¼"
403	4	122	45"
404	4	122	10'
405	4	113	20'
501	5	122	10'
502	5	79	20'
601	6	195	79"
602	6	122	23¼"
603	6	366	33"
604	6	244	40"
605	6	122	10'
606	6	33	40'
801	8	85	42"

NOTES:
(1) ALL No. 4 BARS BENT WITH 2" I.D.
(2) ALL No. 6 BARS BENT WITH 4½" I.D.
(3) ALL BARS GRADE 60 EPOXY COATED STEEL

801 — 42"

601 — 39", 39", 90°
603 — 33"
602 — 23¼"
604 — 27", 12"

401 — 5⅝", 3¼", 18½", 3", 13⁵⁄₁₆", 106°, 6½"
402 — 8¼", 12¼", 3"
403 — 20", 7⅞", 8²⁄", 18⅞", 4⅞"

Millwest Roadside Safety Facility

NDOR's TL-5 Aesthetic Open Concrete Bridge Rail

Bill of Bars

Drawing Name: NDOR TL-5 R4.dwg
Scale: None

Sheet: 5 of 5
Date: 4/13/2004
By: JL/GEP
Rev: RKF/KAP

Figure A-5. NDOR's TL-5 Aesthetic Open Concrete Bridge Rail Design Reinforcement Details (English)

119

APPENDIX B

Test Summary Sheet in English Units, Test ACBR-1

Figure B-1. Summary of Test Results and Sequential Photographs (English), Test ACBR-1
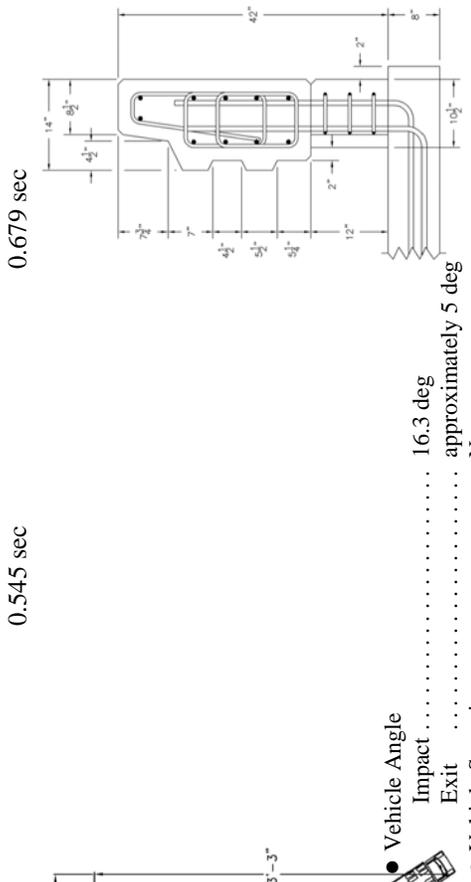
0.000 sec   0.138 sec   0.238 sec   0.545 sec   0.679 sec

- Test Number ACBR-1
- Date 8/28/03
- Appurtenance .... Nebraska Aesthetic Open
  Concrete Bridge Rail
- Total Length .... 121 ft-6 in.
- Concrete Material .... Nebraska 47-BD Mix
- Reinforcing Steel Material .... Grade 60 Rebar - Epoxy Coated
- Concrete Bridge Rail
  - Length .... 121 ft-6 in.
  - Width .... 14 in.
  - Depth .... 30 in.
  - Top Mounting Height .... 42 in.
- Concrete Bridge Posts
  - Length .... 30 in.
  - Width .... 10.5 in.
  - Height .... 12 in.
  - Spacing .... 8 ft-6 in.
  - Offset from Back Edge of Deck ...... 2 in.
- Concrete Bridge Deck
  - Length .... 121 ft-6 in.
  - Width .... 134 in.
  - Thickness .... 8 in.
- Vehicle Model .... 1989 General Motors Brigadier Tractor
  1989 Great Dane Brigadier Trailer
  - Curb .... 30,525 lbs
  - Test Inertial .... 78,975 lbs
  - Gross Static .... 78,975 lbs
- Vehicle Speed
  - Impact .... 49.4 mph
  - Exit .... NA
- Vehicle Angle
  - Impact .... 16.3 deg
  - Exit .... approximately 5 deg
- Vehicle Snagging .... None
- Vehicle Pocketing .... None
- Vehicle Stability .... Satisfactory
- Occupant Ridedown Deceleration (10 msec avg.) – Tractor
  - Longitudinal (not required) .... 8.05/-6.98 g's < 20 g's
  - Lateral (not required) .... 6.06/-7.91 g's
- Occupant Impact Velocity – Tractor
  - Longitudinal (not required) .... 2.99 ft/s < 39.37 ft/s
  - Lateral (not required) .... 18.05 ft/s
- Occupant Ridedown Deceleration (10 msec avg.) – Trailer
  - Longitudinal (not required) .... 3.52/-2.17 g's < 20 g's
  - Lateral (not required) .... 11.74/-7.88 g's
- Occupant Impact Velocity – Trailer
  - Longitudinal (not required) .... 3.55 ft/s < 39.37 ft/s
  - Lateral (not required) .... 7.60 ft/s
- Vehicle Damage .... Moderate
  - TAD[25] .... 1-RFQ-3 and 1-RD-3
  - SAE[26] .... 1-FREN3 and 1-RDES2
- Vehicle Stopping Distance .... 410 ft-11 in. downstream
  173 ft-3 in. laterally behind
- Barrier Damage .... Moderate
- Maximum Rail Deflections
  - Permanent Set .... NA
  - Dynamic .... 11.2 in
  - Working Width .... 75.4 in.

Figure B-1. Summary of Test Results and Sequential Photographs (English), Test ACBR-1

121

APPENDIX C

Concrete Damage Sketches, Test ACBR-1

Figure C-1. Concrete Damage – Back-side of Rail at Post No. 1, Test ACBR-1
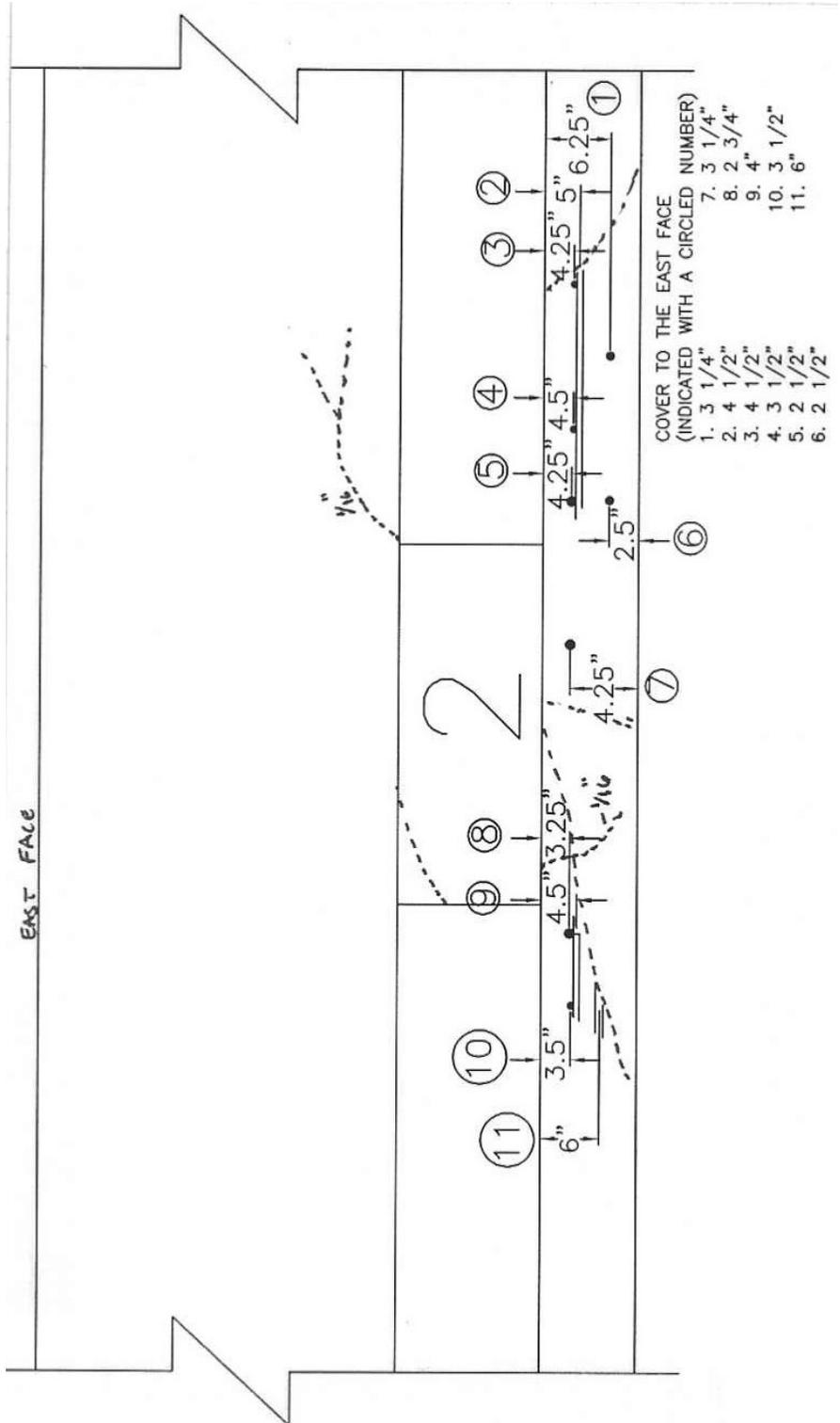
Figure C-2. Concrete Damage – Back-side of Rail at Post No. 2, Test ACBR-1

124
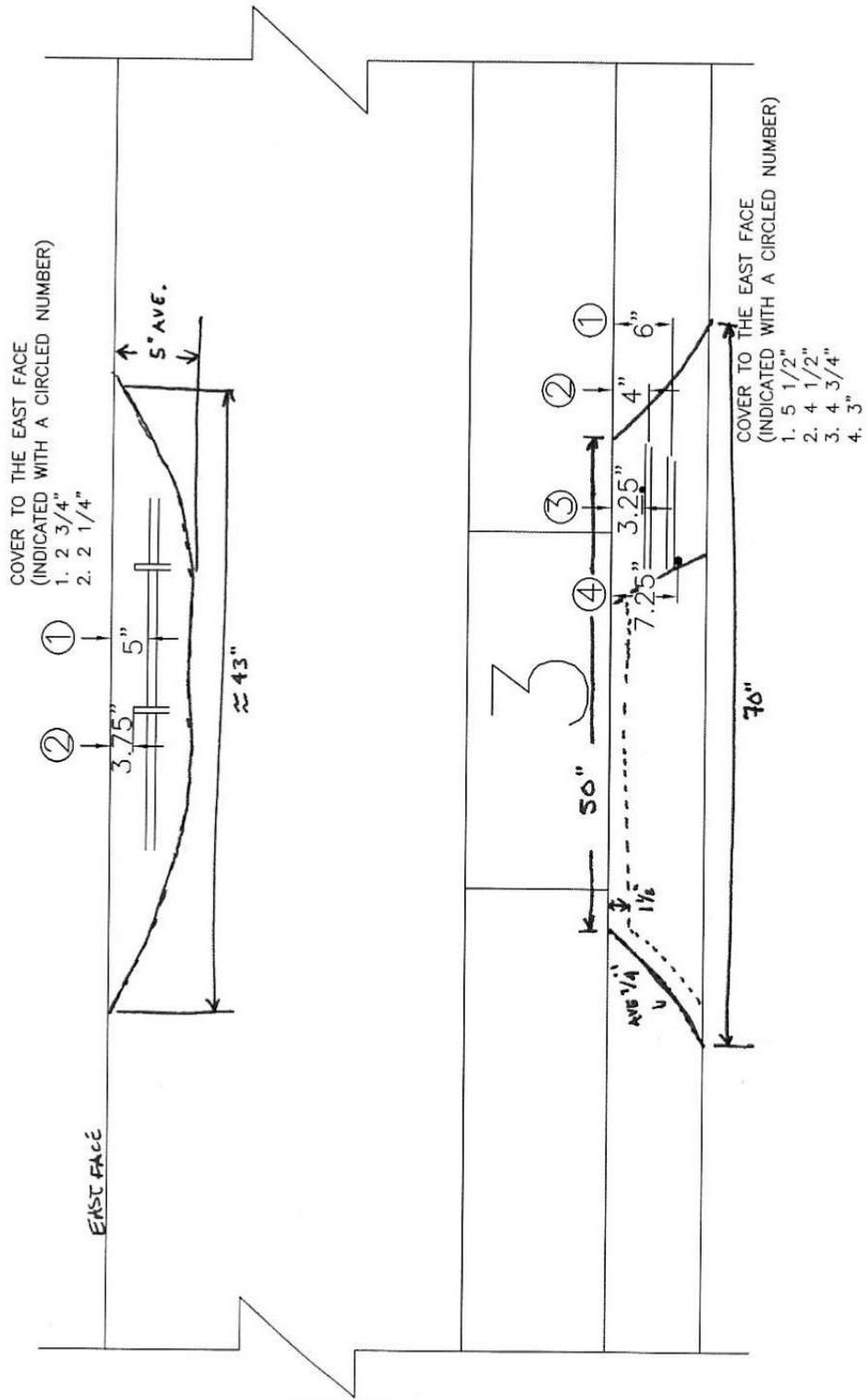
Figure C-3. Concrete Damage – Back-side of Rail at Post No. 3, Test ACBR-1
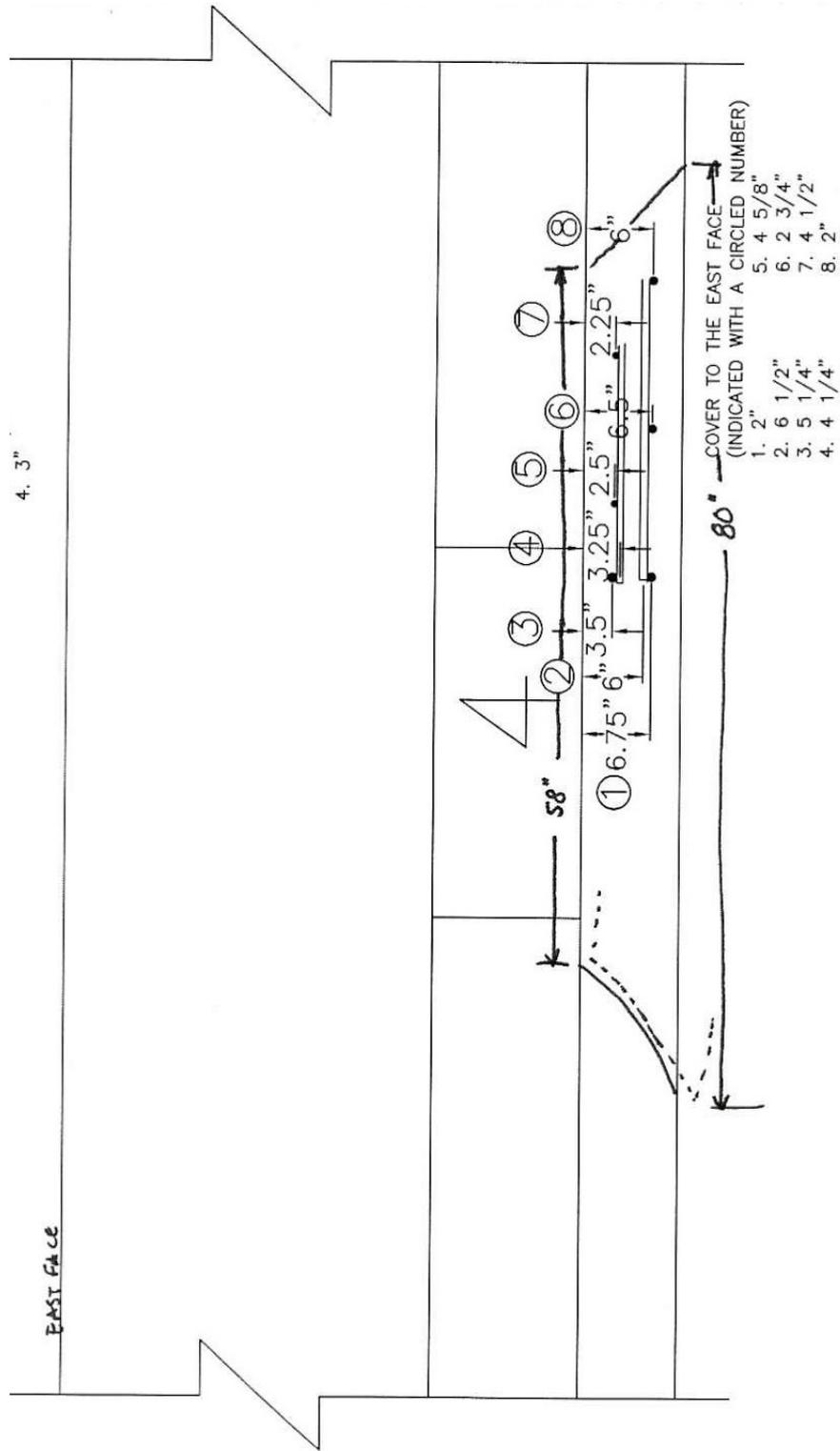
Figure C-4. Concrete Damage – Back-side of Rail at Post No. 4, Test ACBR-1

COVER TO THE EAST FACE
(INDICATED WITH A CIRCLED NUMBER)
1. 4"   7. 4 1/4"
2. 3"   8. 4"
3. 4 1/4"   9. 2 3/8"
4. 4 1/2"   10. 5 1/2"
5. 3"   11. 4 1/2"
6. 4 1/4"   12. 5"
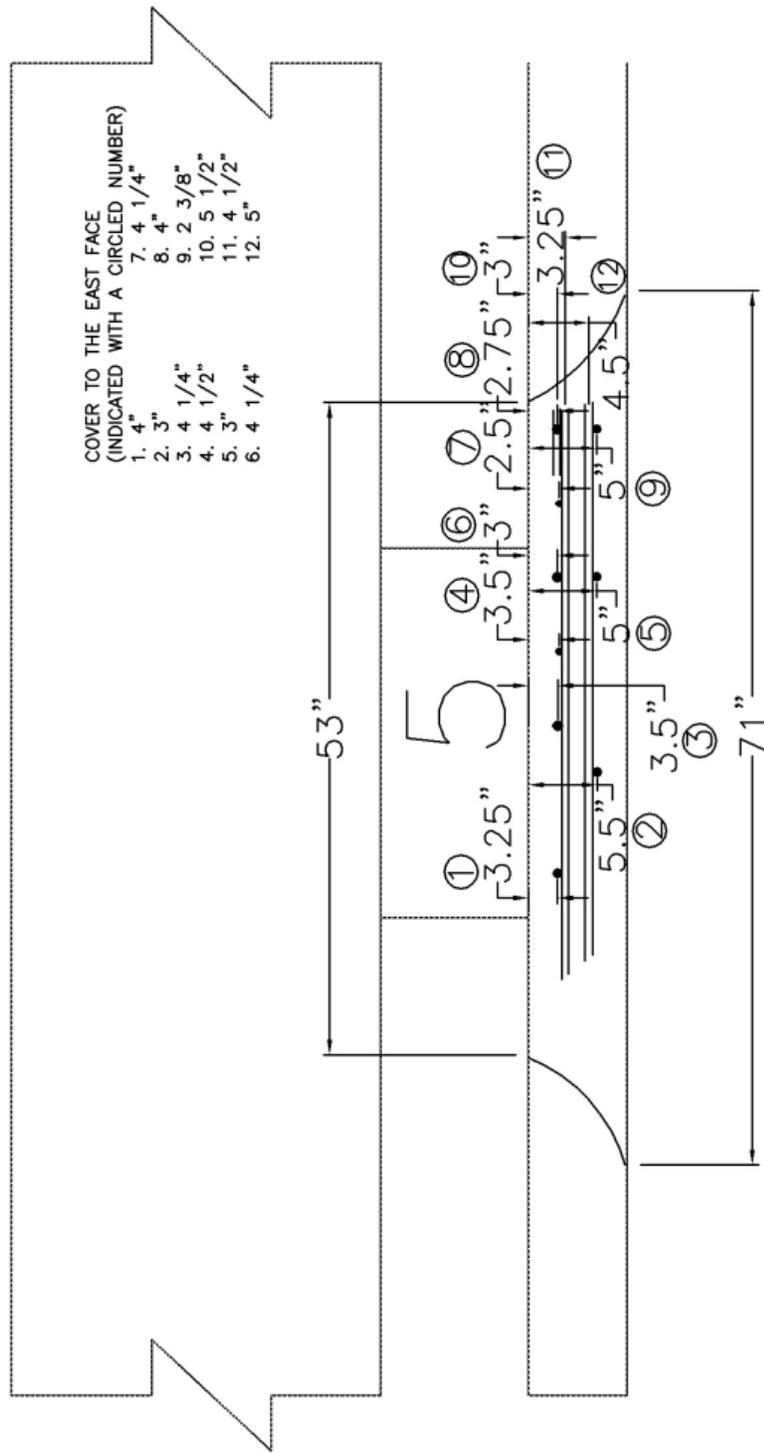
Figure C-5. Concrete Damage – Back-side of Rail at Post No. 5, Test ACBR-1

COVER TO THE EAST FACE
(INDICATED WITH A CIRCLED NUMBER)
1. 2 3/4"   7. 3 1/2"
2. 5 3/4"   8. 3 1/2"
3. 4 1/2"   9. 3 1/2"
4. 3"   10. 3 1/2"
5. 4 1/2"   11. 3 1/2"
6. 4 3/4"   12. 4 3/4"
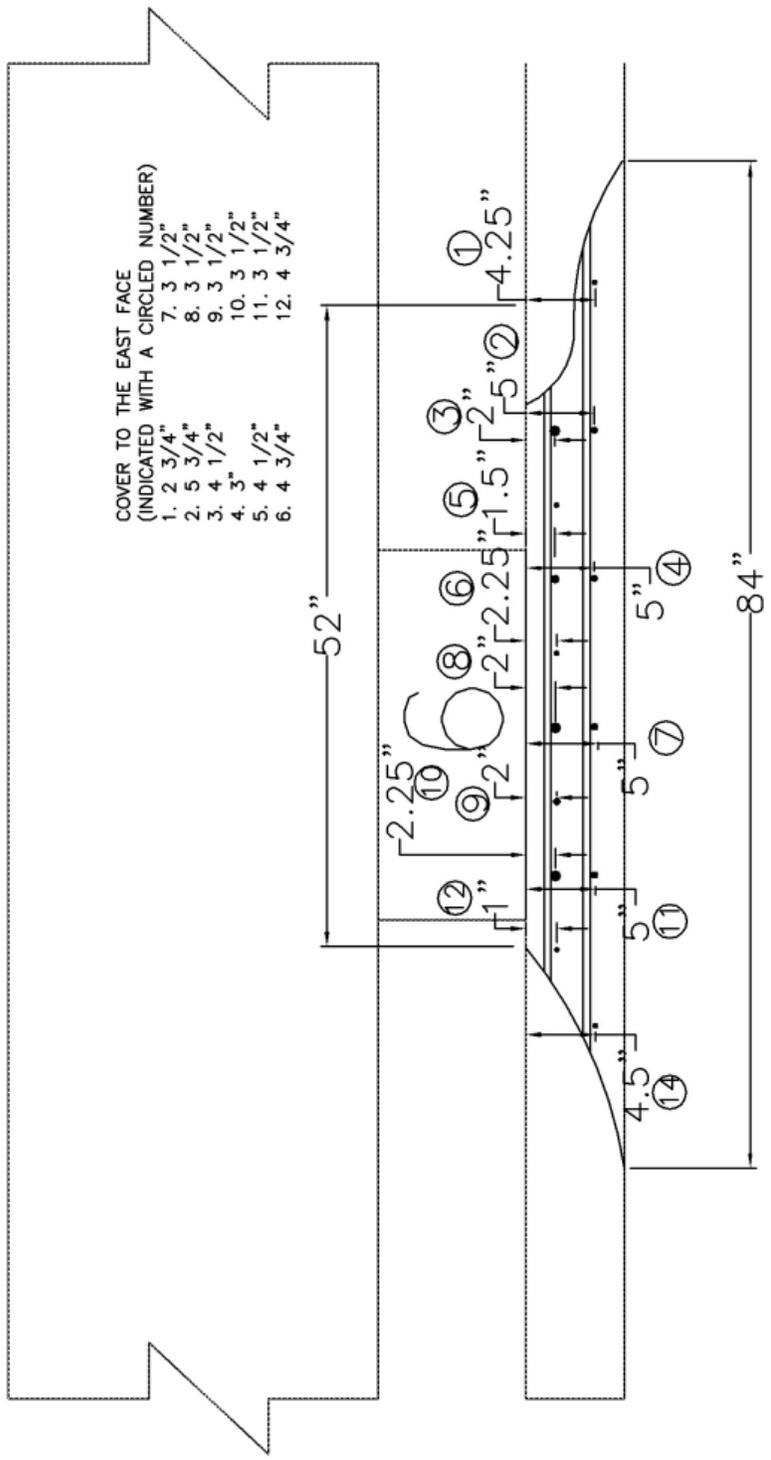
Figure C-6. Concrete Damage – Back-side of Rail at Post No. 6, Test ACBR-1

Figure C-7. Concrete Damage – Back-side of Rail at Post No. 7, Test ACBR-1

EAST FACE

COVER TO THE EAST FACE
(INDICATED WITH A CIRCLED NUMBER)
1. 2 1/4"

51"

5"

1/8"

3/16"

1/8"

55"

83"
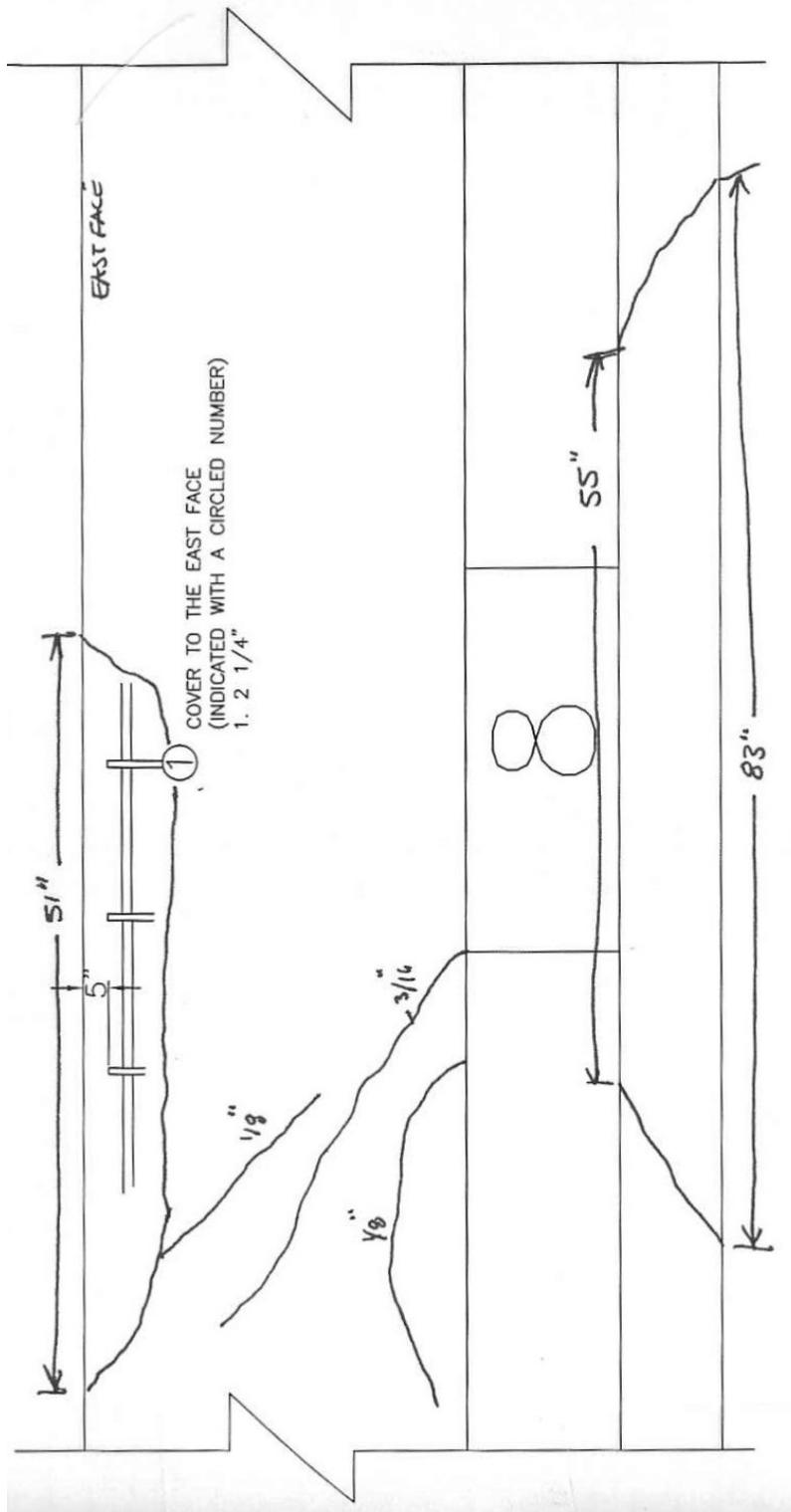
Figure C-8. Concrete Damage – Back-side of Rail at Post No. 8, Test ACBR-1

APPENDIX D

Accelerometer and Rate Transducer Data Analysis, Test ACBR-1

Figure D-1. Graph of 10-ms Average Longitudinal Deceleration (CFC 180 Filtered) of the Tractor, Test ACBR-1

133

Figure D-2. Graph of Longitudinal Occupant Impact Velocity (CFC 180 Filtered) of the Tractor, Test ACBR-1

Figure D-3. Graph of Longitudinal Occupant Displacement (CFC 180 Filtered) of the Tractor, Test ACBR-1

135
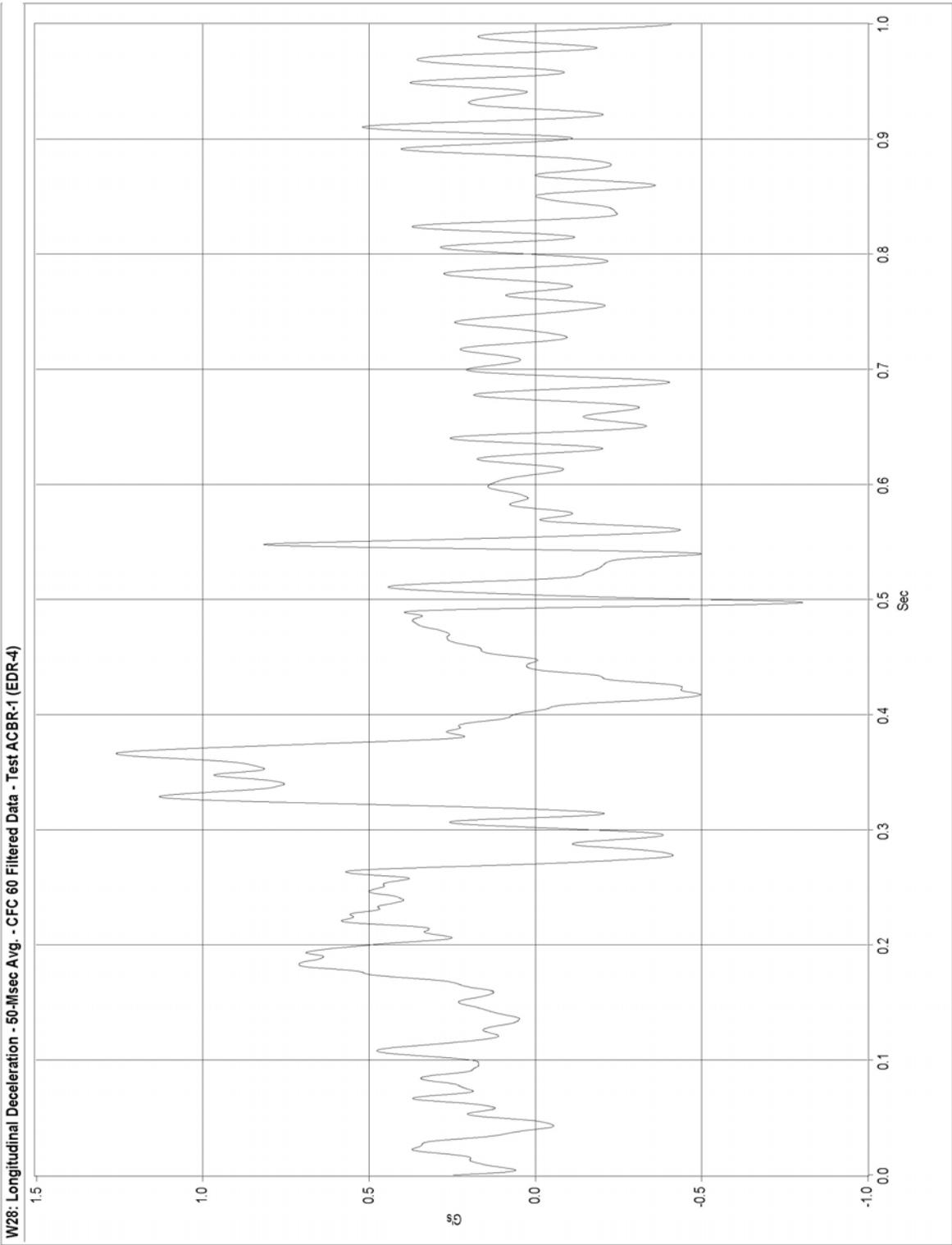
Figure D-4. Graph of 50-ms Average Longitudinal Deceleration (CFC 60 Filtered) of the Tractor, Test ACBR-1
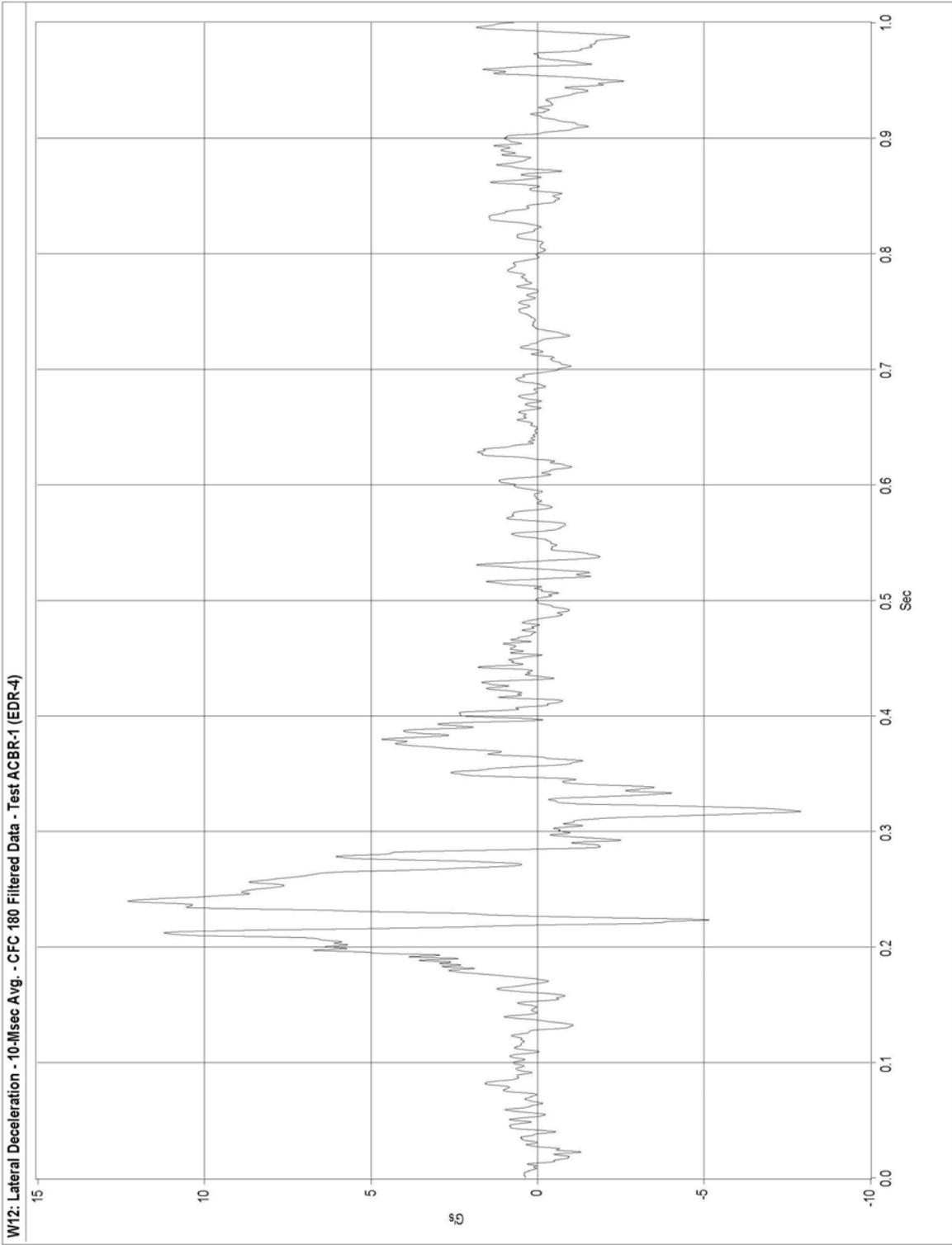
Figure D-5. Graph of 10-ms Average Lateral Deceleration (CFC 180 Filtered) of the Tractor, Test ACBR-1

137
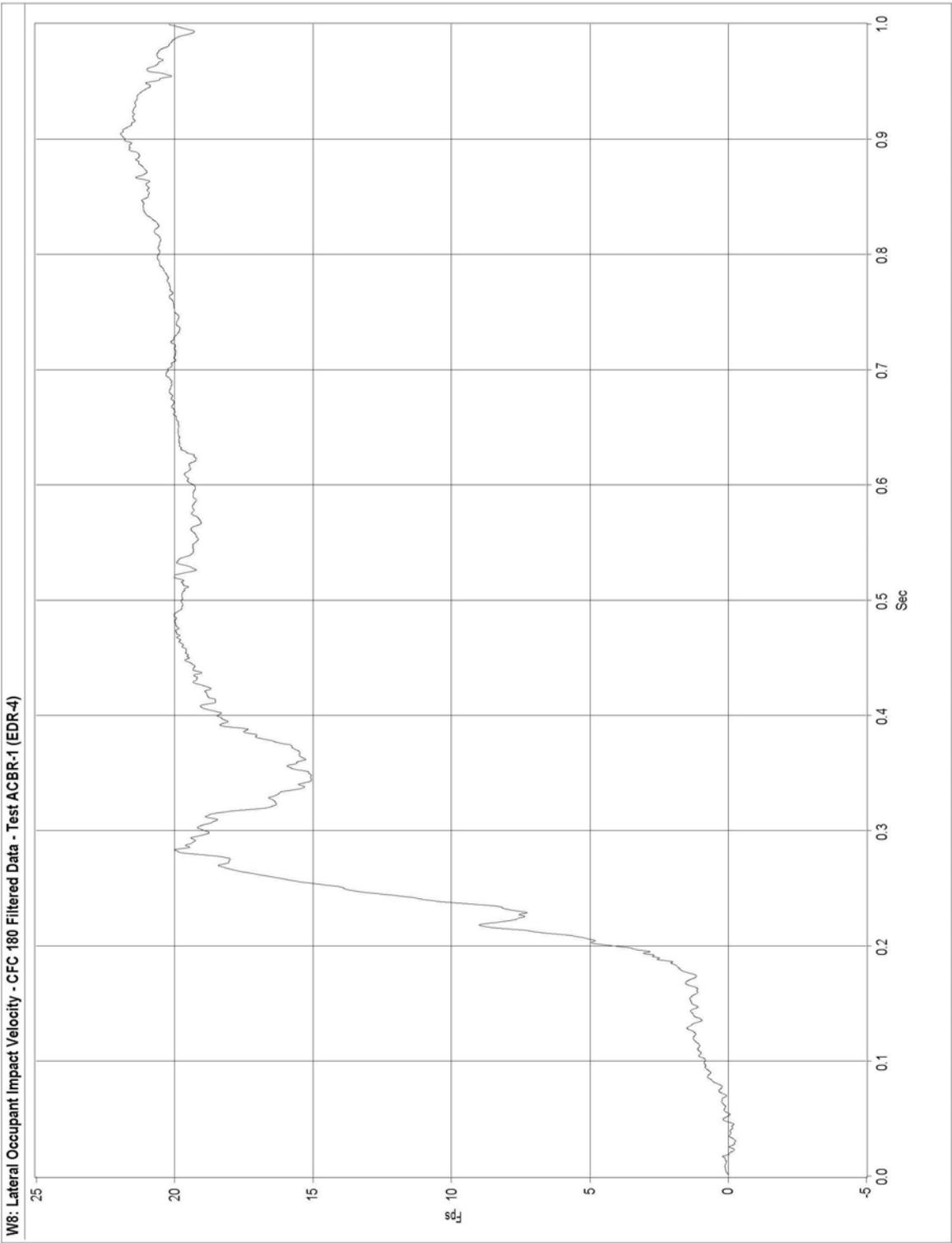
Figure D-6. Graph of Lateral Occupant Impact Velocity (CFC 180 Filtered) of the Tractor, Test ACBR-1
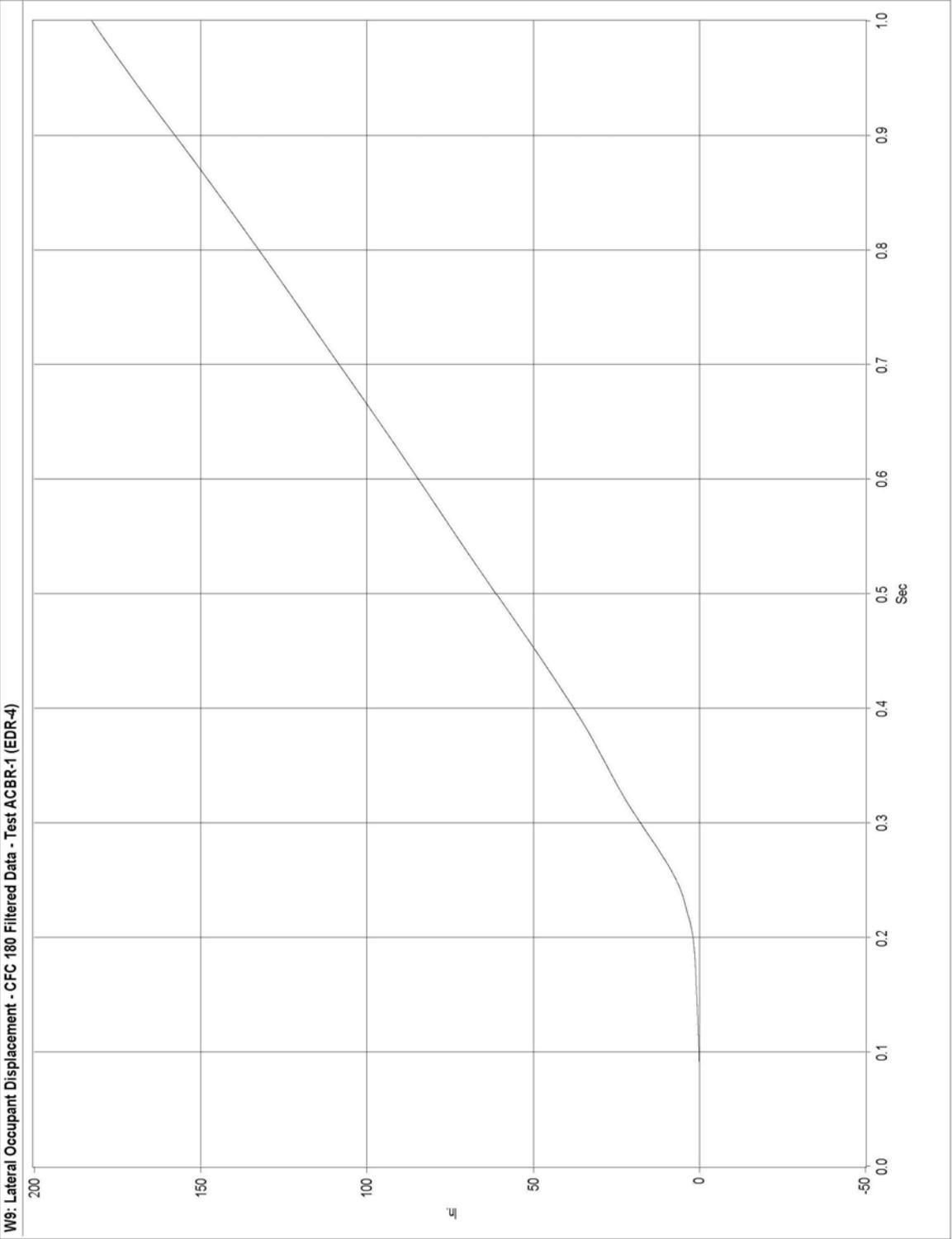
Figure D-7. Graph of Lateral Occupant Displacement (CFC 180 Filtered) of the Tractor, Test ACBR-1
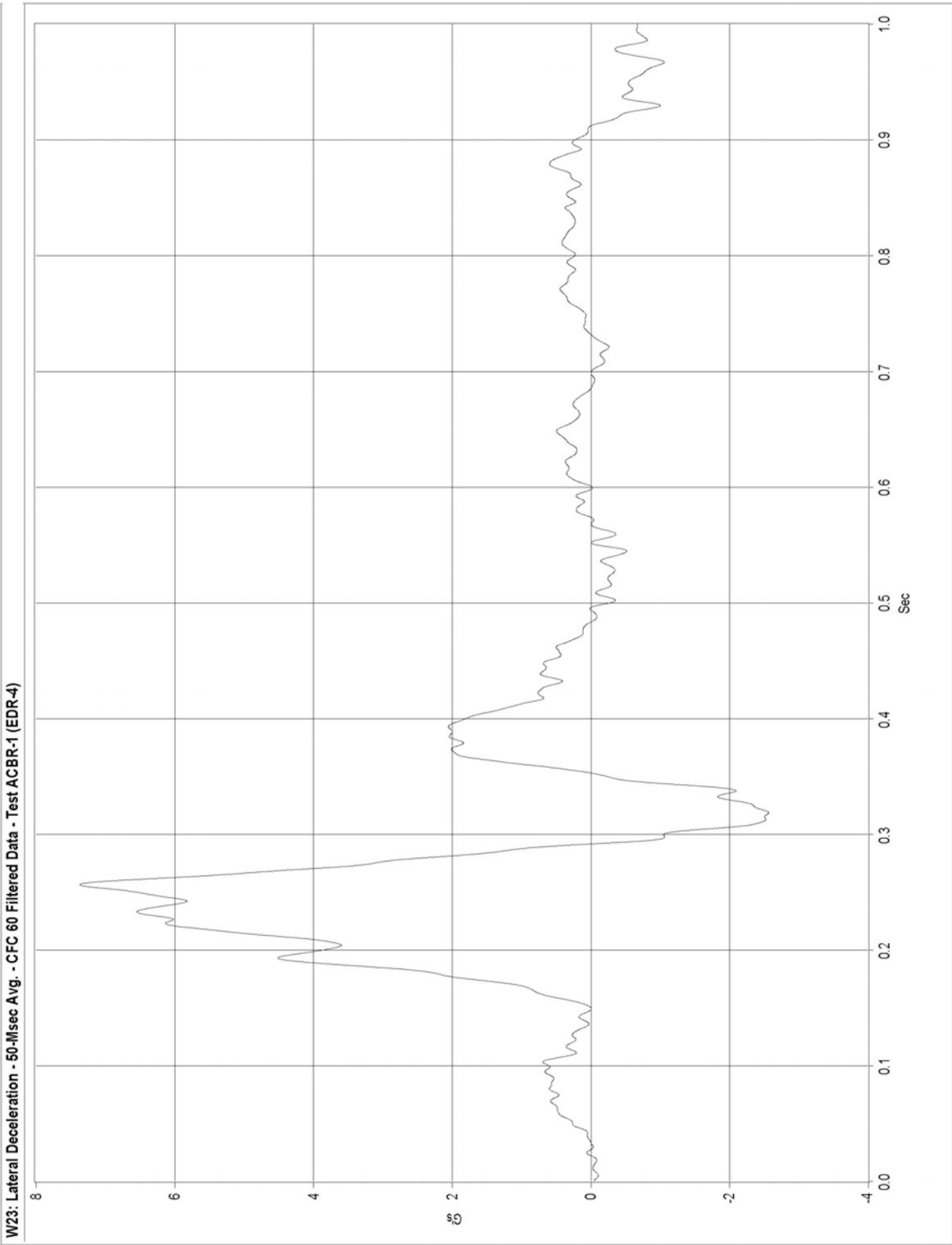
Figure D-8. Graph of 50-ms Average Lateral Deceleration (CFC 60 Filtered) of the Tractor, Test ACBR-1

Figure D-9. Comparison Graph of Vehicle Accelerations (CFC 60 Filtered) of the Tractor, Test ACBR-1

Figure D-10. Comparison Graph of 50-ms Average Vehicle Accelerations (CFC 60 Filtered) of the Tractor, Test ACBR-1

Figure D-11. Comparison Graph of Vehicle Velocity Change (CFC 180 Filtered) of the Tractor, Test ACBR-1
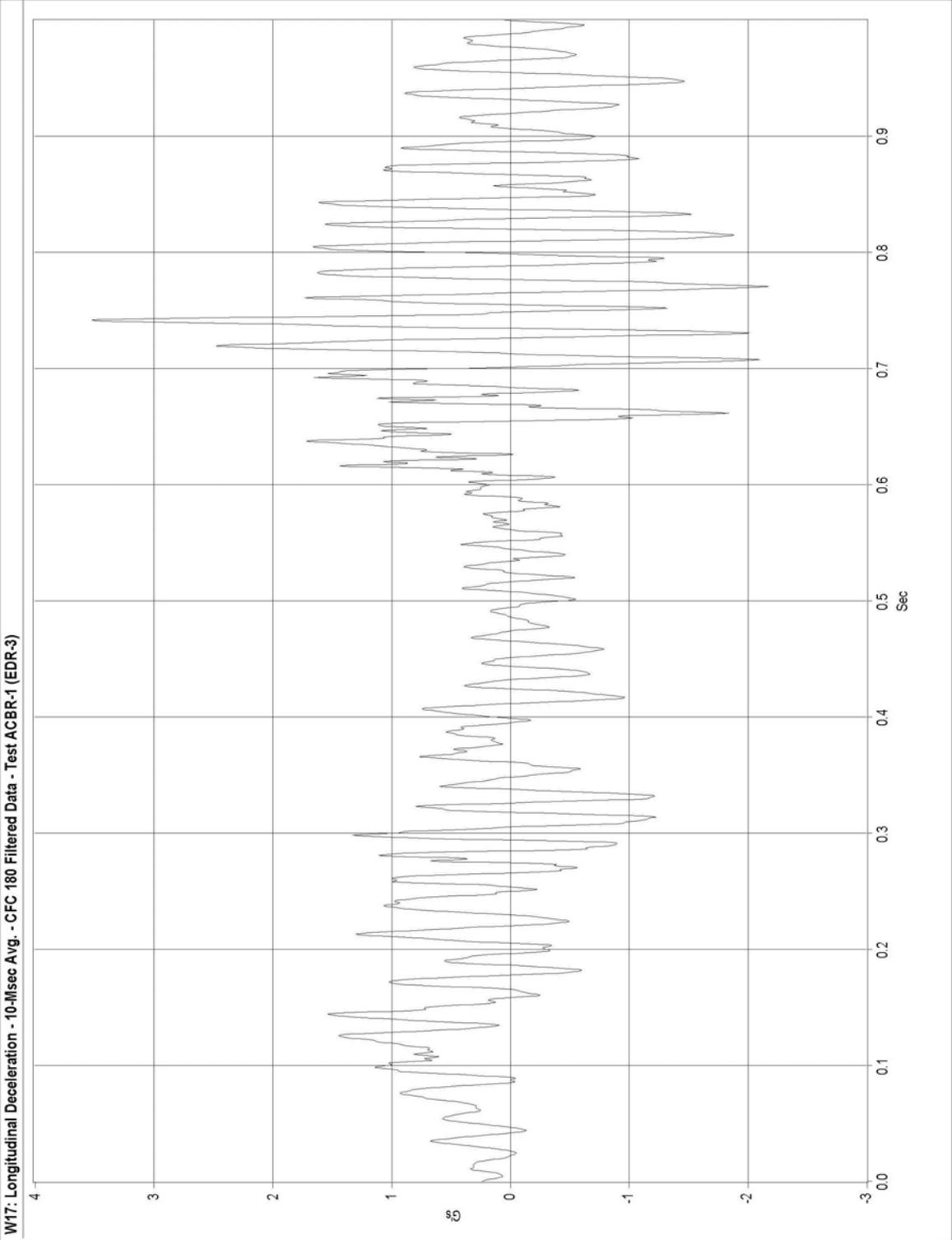
Figure D-12. Graph of 10-ms Average Longitudinal Deceleration (CFC 180 Filtered) of the Trailer, Test ACBR-1

144
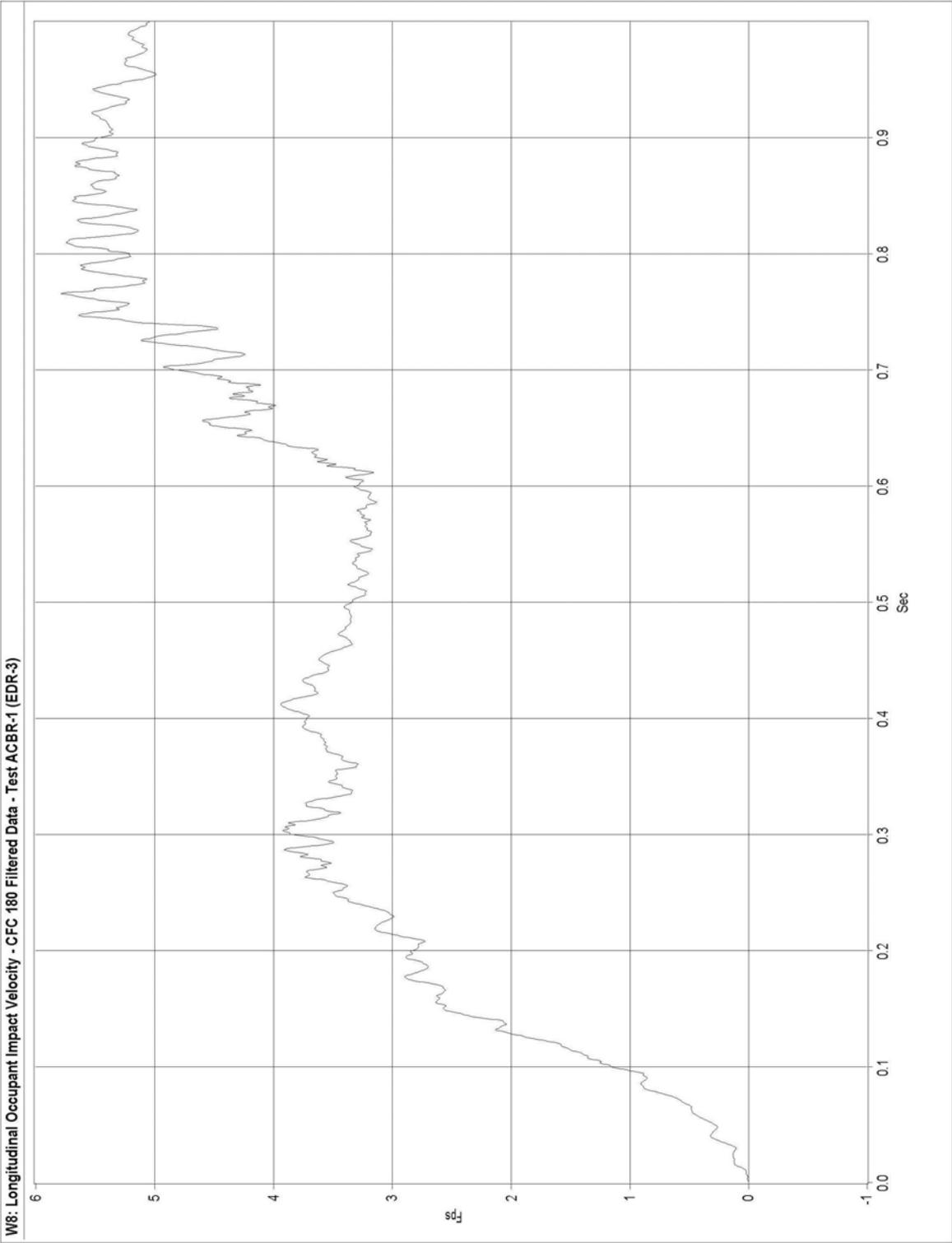
Figure D-13. Graph of Longitudinal Occupant Impact Velocity (CFC 180 Filtered) of the Trailer, Test ACBR-1
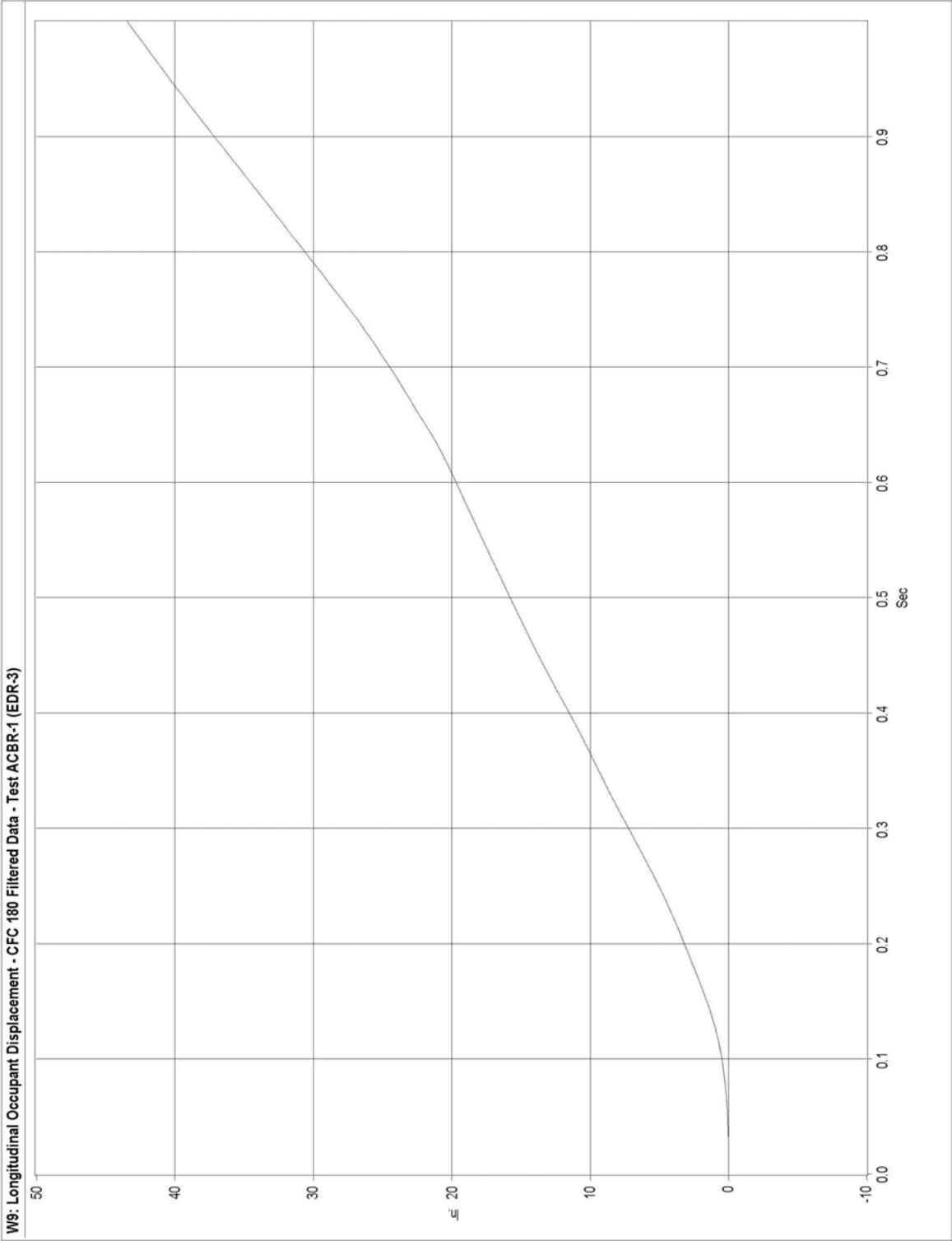
Figure D-14. Graph of Longitudinal Occupant Displacement (CFC 180 Filtered) of the Trailer, Test ACBR-1
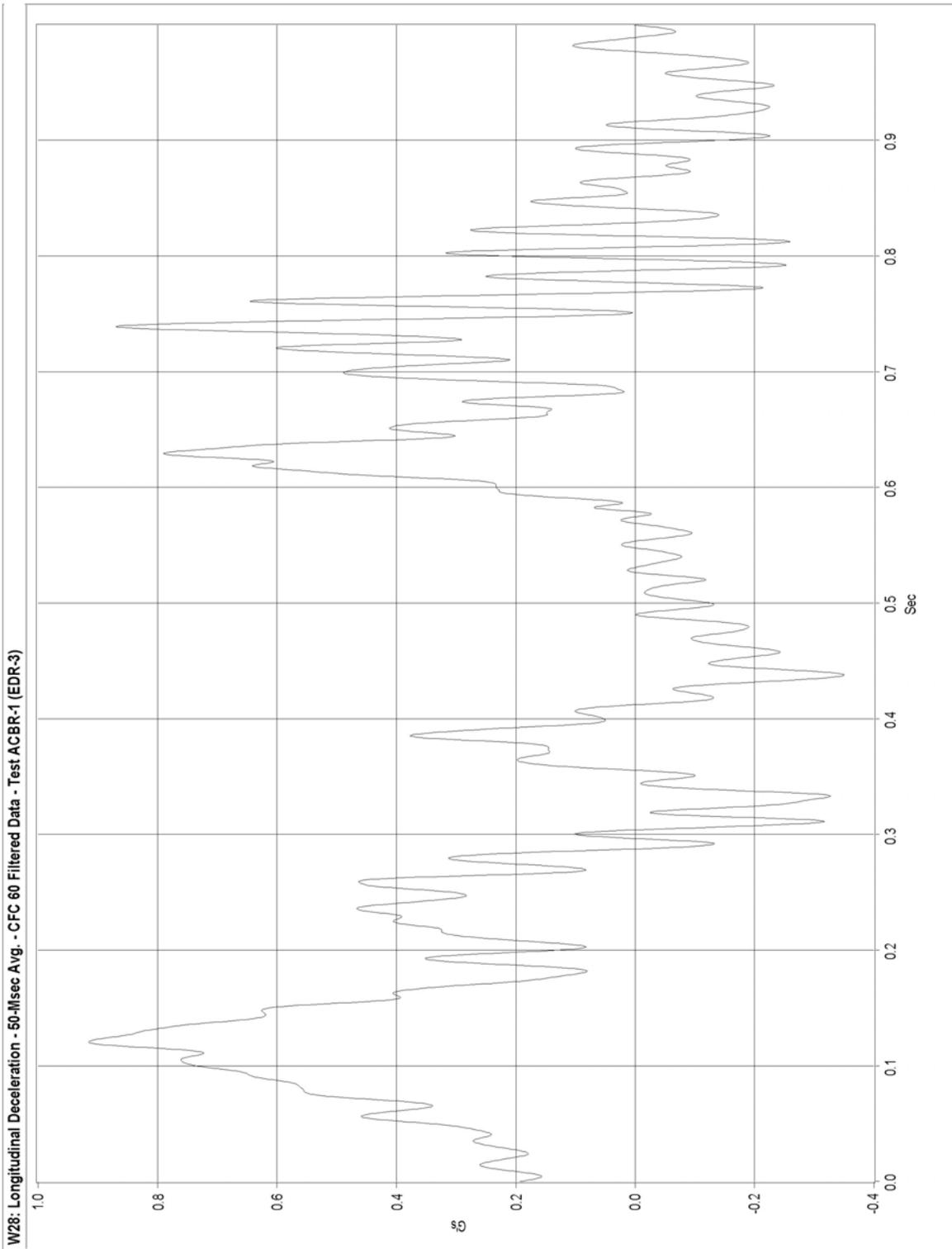
Figure D-15. Graph of 50-ms Average Longitudinal Deceleration (CFC 60 Filtered) of the Trailer, Test ACBR-1

147
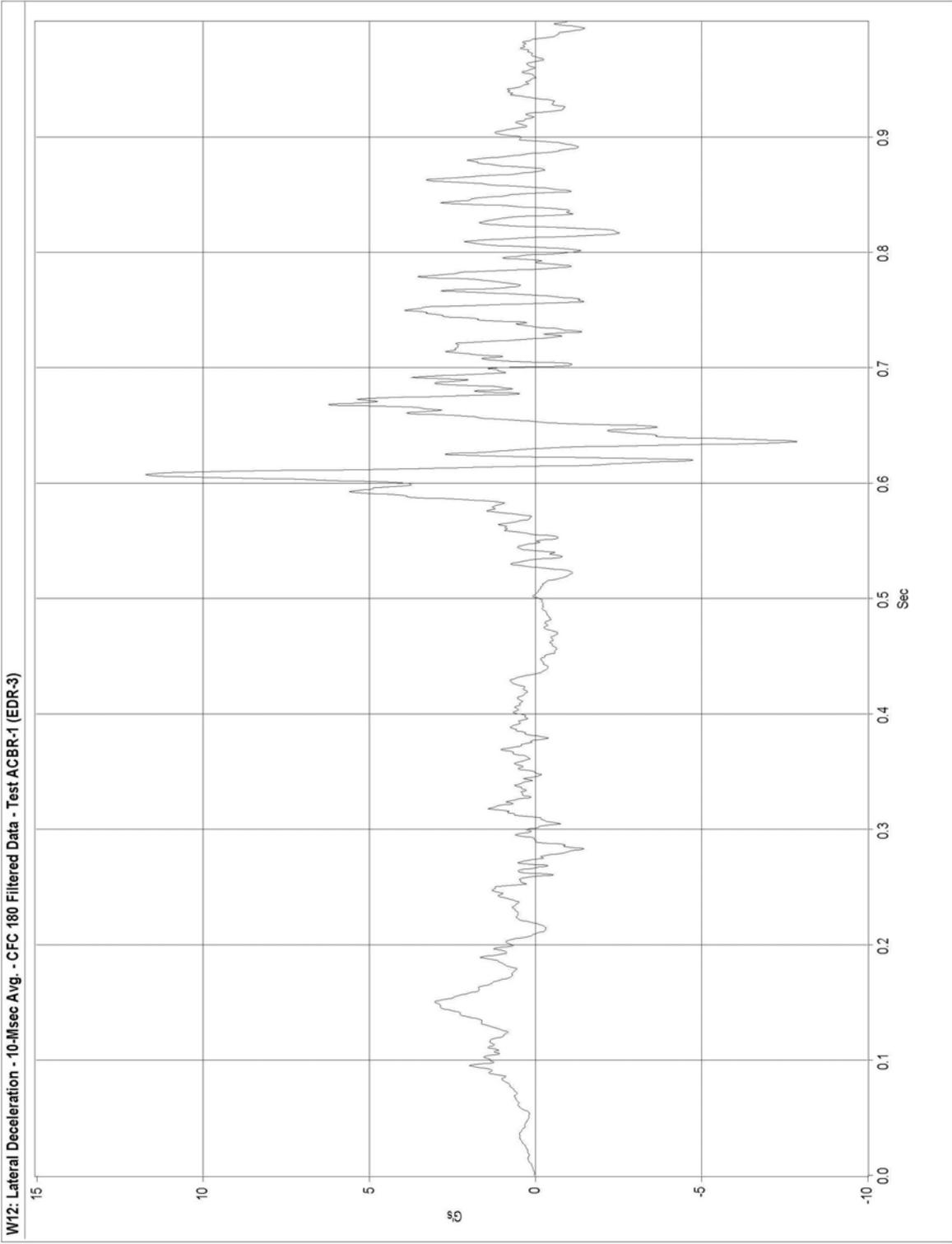
Figure D-16. Graph of 10-ms Average Lateral Deceleration (CFC 180 Filtered) of the Trailer, Test ACBR-1

148
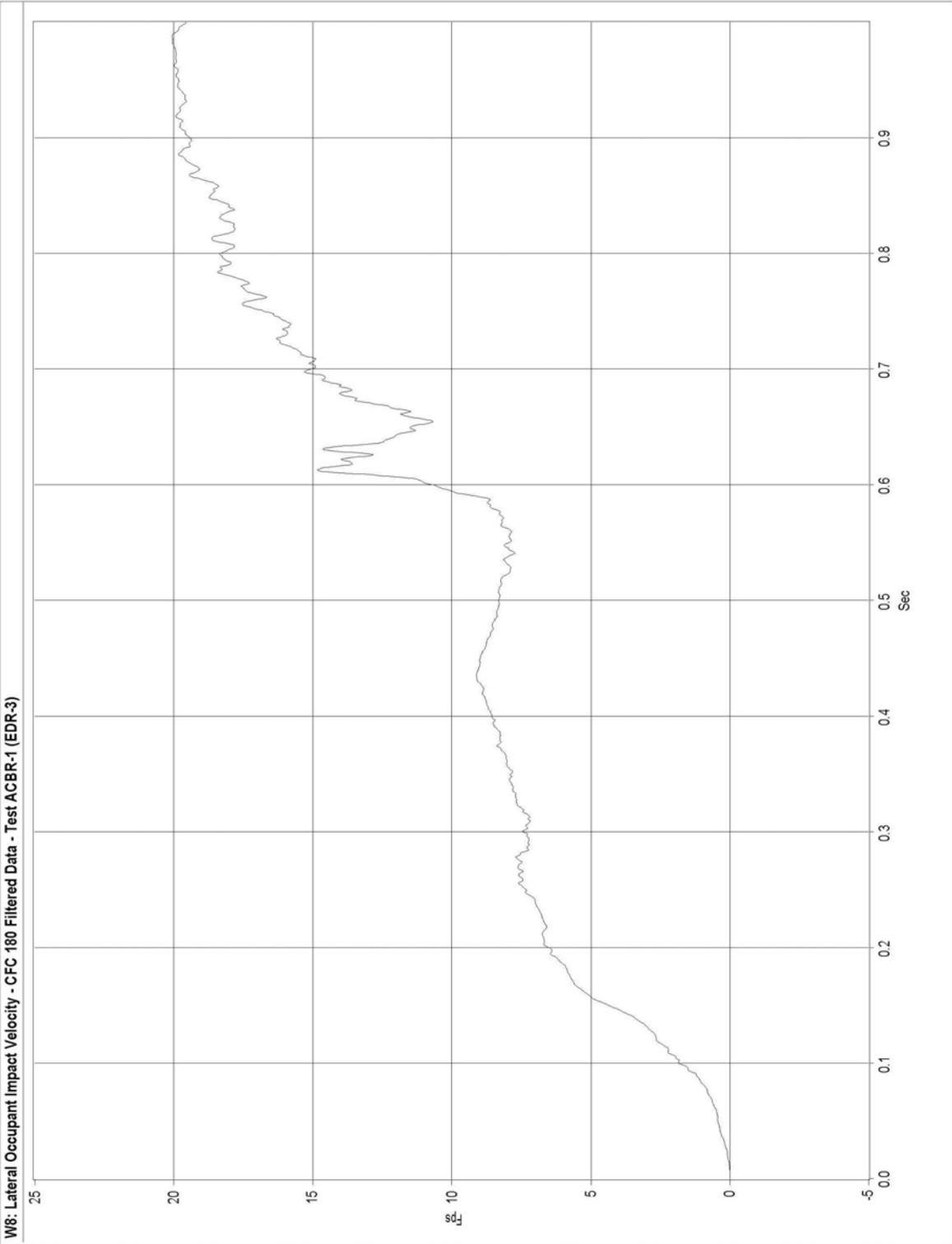
Figure D-17. Graph of Lateral Occupant Impact Velocity (CFC 180 Filtered) of the Trailer, Test ACBR-1
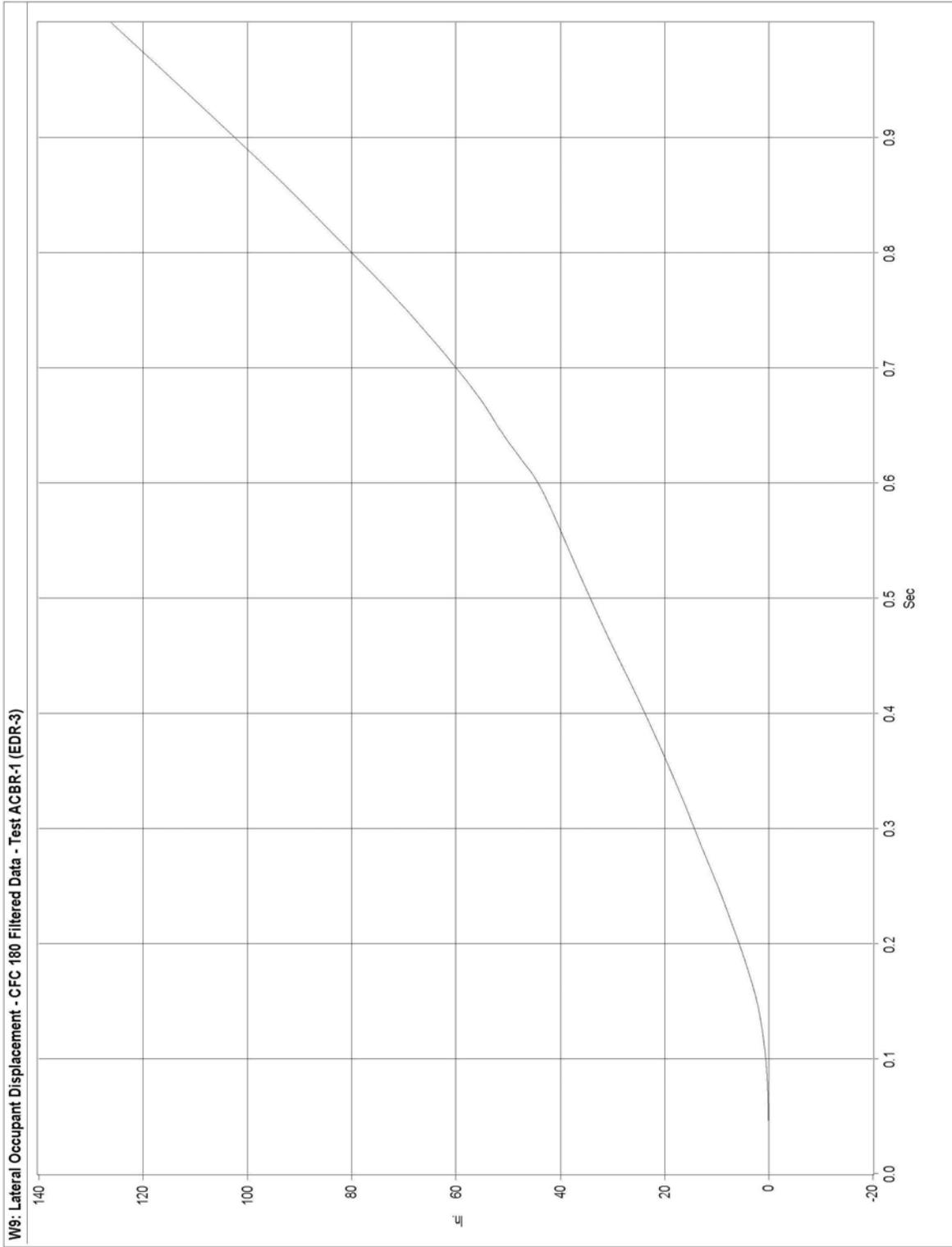
Figure D-18. Graph of Lateral Occupant Displacement (CFC 180 Filtered) of the Trailer, Test ACBR-1
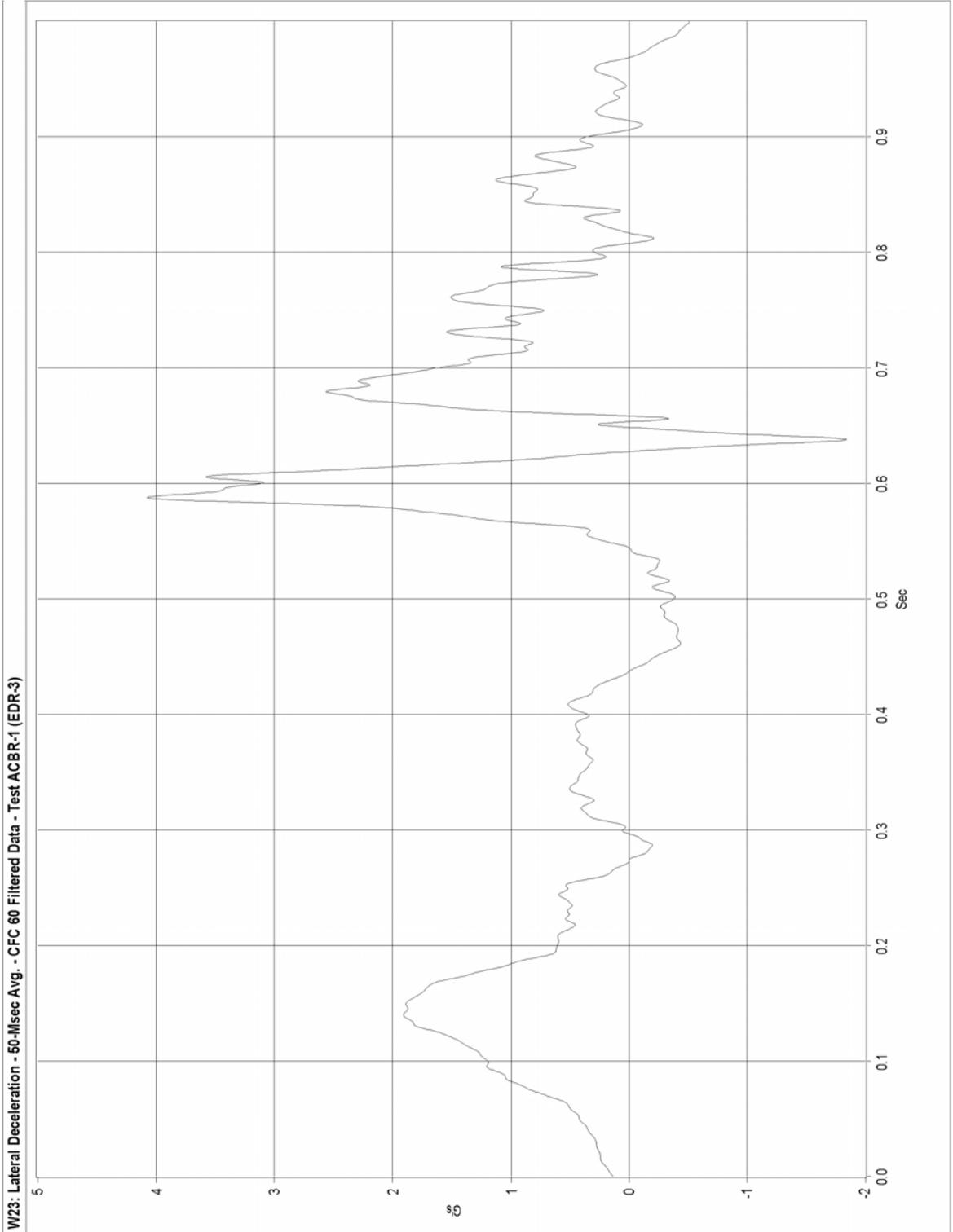
Figure D-19. Graph of 50-ms Average Lateral Deceleration (CFC 60 Filtered) of the Trailer, Test ACBR-1

151

Figure D-20. Comparison Graph of Vehicle Accelerations (CFC 60 Filtered) of the Trailer, Test ACBR-1

Figure D-21. Comparison Graph of 50-ms Average Vehicle Accelerations (CFC 60 Filtered) of the Trailer, Test ACBR-1

Test No. ACBR-1 Vehicle Delta V
CFC 180 (300 Hz) [EDR-3]
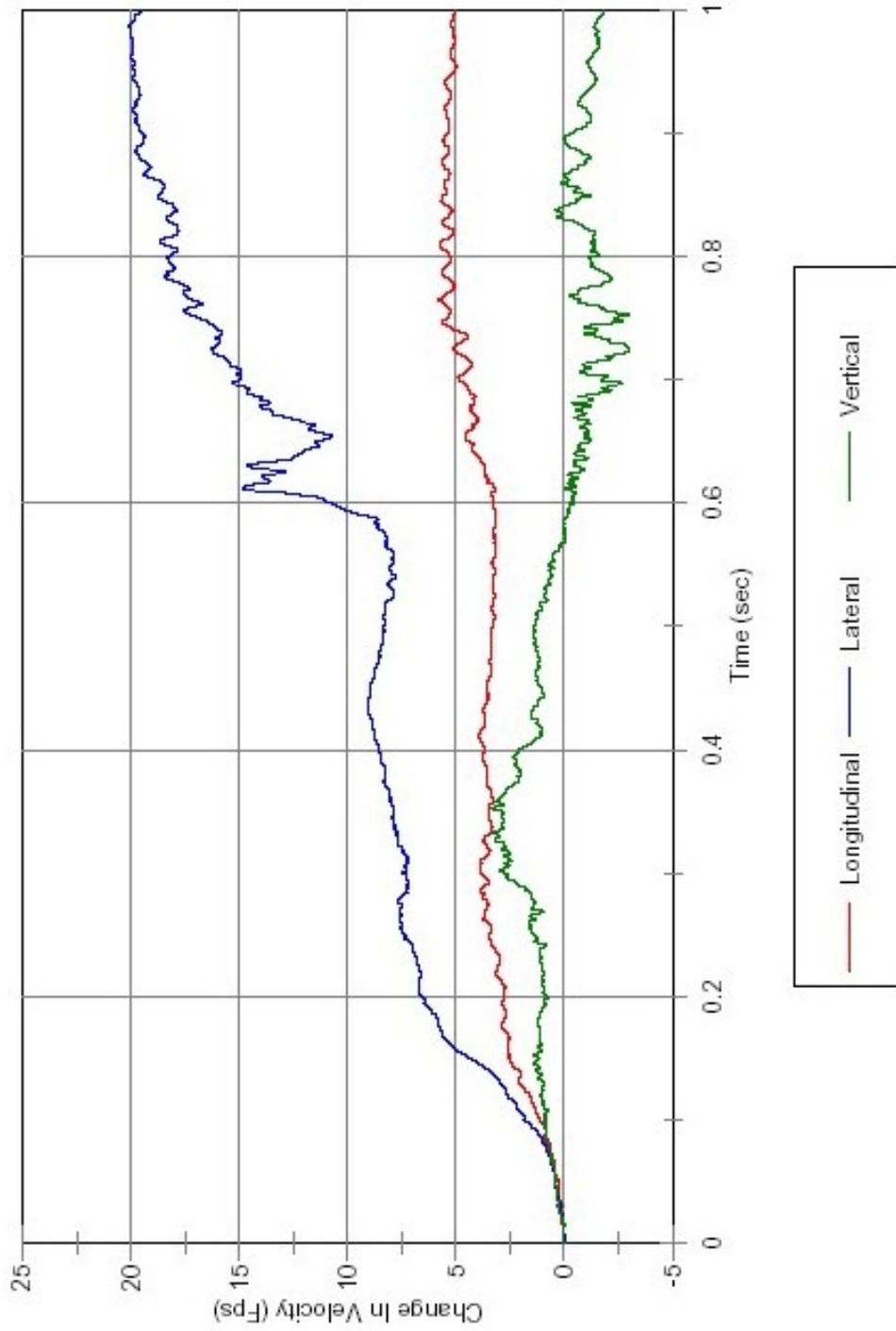
Figure D-22. Comparison Graph of Vehicle Velocity Change (CFC 180 Filtered) of the Trailer, Test ACBR-1

154